

2010

## Enhancing the maturation of dendritic cells and TRACKING THEIR SUBSEQUENT IN VIVO MIGRATION USING CELLULAR MAGNETIC RESONANCE IMAGING

Sonali N. de Chickera  
*Western University*

Follow this and additional works at: <https://ir.lib.uwo.ca/digitizedtheses>

---

### Recommended Citation

de Chickera, Sonali N., "Enhancing the maturation of dendritic cells and TRACKING THEIR SUBSEQUENT IN VIVO MIGRATION USING CELLULAR MAGNETIC RESONANCE IMAGING" (2010). *Digitized Theses*. 3880.

<https://ir.lib.uwo.ca/digitizedtheses/3880>

This Thesis is brought to you for free and open access by the Digitized Special Collections at Scholarship@Western. It has been accepted for inclusion in Digitized Theses by an authorized administrator of Scholarship@Western. For more information, please contact [wlsadmin@uwo.ca](mailto:wlsadmin@uwo.ca).

ENHANCING THE MATURATION OF DENDRITIC CELLS AND  
TRACKING THEIR SUBSEQUENT *IN VIVO* MIGRATION USING  
CELLULAR MAGNETIC RESONANCE IMAGING

(Spine title: Tracking Dendritic Cell Migration Using MRI)

(Thesis format: Integrated-Article)

by

Sonali N. de Chickera

Graduate Program in Anatomy and Cell Biology

A thesis submitted in partial fulfillment  
of the requirements for the degree of  
Master of Science

The School of Graduate and Postdoctoral Studies  
The University of Western Ontario  
London, Ontario, Canada

© Sonali N. de Chickera 2010

THE UNIVERSITY OF WESTERN ONTARIO  
SCHOOL OF GRADUATE AND POSTDOCTORAL STUDIES

CERTIFICATE OF EXAMINATION

Supervisor

\_\_\_\_\_  
Dr. Gregory A. Dekaban

Supervisory Committee

\_\_\_\_\_  
Dr. Lique Coolen

\_\_\_\_\_  
Dr. Martin Sandig

Examiners

\_\_\_\_\_  
Dr. Lynne Postovit

\_\_\_\_\_  
Dr. Trevor Shepherd

\_\_\_\_\_  
Dr. Bosco Chan

The thesis by

Sonali Natasha de Chickera

entitled:

The application of cellular magnetic resonance imaging  
as a non-invasive imaging modality to track and quantify the  
*in vivo* migration of dendritic cells

is accepted in partial fulfillment  
of the requirements for the degree of  
Master of Science

Date \_\_\_\_\_

\_\_\_\_\_  
Chair of the Thesis Examination Board

## Abstract

Dendritic cell (DC)-based cancer vaccines in clinical trials are promising, but their overall efficacy requires improvement. It is uncertain which DC subset, state of DC maturation/activation, and route of administration allow for optimum DC migration to lymph nodes (LNs) *in vivo*, thereby improving vaccine efficacy. A non-invasive imaging modality capable of tracking DC-based vaccine migration in patients would provide clinicians valuable information regarding these variables. A superparamagnetic iron oxide (SPIO) magnetic resonance imaging (MRI) contrast agent was used to label bone marrow-derived DCs (BMDCs) for tracking their subsequent migration using cellular MRI in a mouse model. Data indicate SPIO mechanically impedes migration of labelled-BMDCs *in vivo* compared to control cells. Data also demonstrate MRI is a sensitive modality capable of detecting differences in BMDC migration to LNs. These studies provide important information regarding the application cellular MRI as a means to assess parameters of DC-based immunotherapeutics for improving their efficacy.

**Keywords:** *dendritic cell, in vivo migration, cellular magnetic resonance imaging, non-invasive imaging, superparamagnetic iron oxide nanoparticle, active immunotherapy, cell-based cancer vaccine*

## **Co-authorships**

This thesis contains data from two manuscripts that have been prepared by Sonali de Chickera. The experimental design, methods, and data analysis were completed by Sonali de Chickera in Chapters 2 and 3, with technical assistance from Christy Willert. MRI scans presented in Chapter 2 were performed by Jonathan Snir and Roja Rohani. MRI scans in Chapter 3 were performed by Jenny Noad and Christiane Mallett. MRI analysis from Chapters 2 and 3 was performed by Sonali de Chickera.

## Acknowledgements

First and foremost, I offer my sincere gratitude to my supervisor, Dr. Greg Dekaban, who has supported me throughout my graduate career. I attribute my current laboratory skills and the level of my Master's thesis to your encouragement and expertise in the field. I am very grateful for having had such an approachable and supportive supervisor.

Thank you also to the members of my supervisory committee, Dr. Lique Coolen and Dr. Martin Sandig. Your added support and guidance throughout my Masters Degree was appreciated. Thank you also to Dr. Paula Foster and members of her, who provided me with additional guidance and technical support.

I would also like to thank the staff and faculty members of the Department of Anatomy and Cell Biology. This department has definitely helped to make my graduate school experience unforgettable.

To the members of the Dekaban lab (my surrogate lab family): Christy, Mia, Ryan (not to be confused with Bryan), Bryan, Lauren, Kemi, Sakina, and the other members (past and present)... I don't even know where to start. If I had more pages I would thank you in detail, but this will have to do: thank you for **everything!** You made the lab (in)sane (insane in a good way, though).

Next, thank you to my amazing friends. Again, I wish I had more pages, but hopefully you know how much I love all of you. I wouldn't be the person I am today without any of you. Sonja, Fiona, Tina, Colleen, and Christin – for the visits, phone calls, and emails – thank you. Also, thanks to the ACB 510 class of

2007/08 – you helped me survive grad school (with a little help from the Grad Club). We paddled our hearts out and we made it around that bend in the river, guys!

Finally, I would like end by thanking my family. Thank you for your guidance, thank you for letting me make mistakes, and thank for your continuous love and support. Without you none of this would have been possible.

## Table of Contents

<b>Certificate of Examination</b>	<b>ii</b>
<b>Abstract and Keywords</b>	<b>iii</b>
<b>Co-authorship</b>	<b>iv</b>
<b>Acknowledgements</b>	<b>v</b>
<b>Table of Contents</b>	<b>vii</b>
<b>List of Figures</b>	<b>xiii</b>
<b>List of Appendices</b>	<b>xvi</b>
<b>List of Abbreviations</b>	<b>xvii</b>
<b>CHAPTER 1: INTRODUCTION</b>	<b>1</b>
<b>1.1 Cancer Overview</b>	<b>1</b>
<b>1.2 Conventional Breast Cancer Therapies</b>	<b>2</b>
1.2.1 Surgery	3
1.2.2 Radiation Therapy	3
1.2.3 Chemotherapy	3
1.2.4 Hormone Therapy	4
1.2.5 Monoclonal Antibodies	5
<b>1.3 Metastatic Breast Cancer</b>	<b>5</b>
<b>1.4 Emerging Breast Cancer Therapies</b>	<b>6</b>
1.4.1 Active Immunotherapy	7
<b>1.5 Overview of the Immune System</b>	<b>7</b>
1.5.1 Innate Immunity	8



1.5.2 Adaptive Immunity	9
<b>1.6 Cancer Vaccine Development</b>	<b>12</b>
1.6.1 Tumour Associated Antigens	13
1.6.2 Platform of TAA Delivery and Adjuvants	14
<i>First Generation Breast Cancer Vaccines</i>	14
<i>Second Generation Cancer Vaccines</i>	15
<b>1.7 Dendritic Cell Biology</b>	<b>16</b>
1.7.1 Dendritic Cell Subsets	16
1.7.2 Dendritic Cell Life Cycle	17
1.7.3 Dendritic Cell Migration	20
<b>1.8 Challenges and efficacy of DC-based cancer vaccines</b>	<b>23</b>
<b>1.9 <i>In vivo</i> tracking of DC migration</b>	<b>24</b>
1.9.1 Cellular Magnetic Resonance Imaging	28
<i>Cellular MRI contrast agents</i>	31
<b>1.10 Rationale of Study</b>	<b>33</b>
<b>1.11 Hypothesis</b>	<b>35</b>
<b>1.12 Objectives</b>	<b>35</b>
<b>1.13 References</b>	<b>37</b>
<b>CHAPTER 2</b>	<b>LABELLING DENDRITIC CELLS WITH SPIO HAS IMPLICATIONS FOR SUBSEQUENT <i>IN VIVO</i> MIGRATION AS ASSESSED WITH CELLULAR MRI</b>
<b>2.1 Introduction</b>	<b>52</b>
<b>2.2 Methods</b>	<b>55</b>

2.2.1	Animal Care	55
2.2.2	Reagents	55
2.2.3	Generation of murine bone marrow-derived DCs and MRI contrast agent labelling	56
2.2.4	Magnetic separation of SPIO <sup>+</sup> DCs from SPIO <sup>-</sup> DCs	57
2.2.5	Detection of surface antigens	57
2.2.6	Luminex <sup>®</sup> cytokine assays	58
2.2.7	Labelling DCs with PKH	58
2.2.8	Adoptive transfer of DCs	59
2.2.9	Magnetic resonance imaging of DC migration and analysis	59
2.2.10	LN removal and cryostat sectioning	60
2.2.11	Histological analysis and quantification	60
2.2.12	<i>In vitro</i> migration assays	61
2.2.13	Preparation and administration of SIINFEKL-loaded DCs	62
2.2.14	Preparation of single cell suspensions from LNs	62
2.2.15	Tetramer and intracellular cytokine staining	63
2.2.16	Statistical analysis	64
<b>2.3</b>	<b>Results</b>	<b>65</b>
2.3.1	SPIO labelling does not affect DC viability	65
2.3.2	DC phenotype and cytokine profiles remain largely unaffected following <i>in vitro</i> labelling with SPIO	65
2.3.3	Magnetic separation of SPIO <sup>+</sup> from SPIO <sup>-</sup> DCs exposes differences	

in phenotypic surface marker expression and functional cytokine secretion	71
2.3.4 UT DCs migrate preferentially to popliteal LNs compared to SPIO <sup>+</sup> DCs <i>in vivo</i>	77
2.3.5 SPIO <sup>+</sup> DCs migrate more efficiently compared to SPIO <sup>mix</sup> DCs	82
2.3.6 Labelling DCs with SPIO mechanically impedes their subsequent migration <i>in vitro</i>	87
2.3.7 SPIO labelling does not physically slow the kinetics of <i>in vivo</i> DC migration	88
2.3.8 Differences between UT, SPIO <sup>mix</sup> , and SPIO <sup>+</sup> DCs migration correspond with <i>in vivo</i> antigen-specific T cells responses	95
<b>2.4 Discussion</b>	<b>104</b>
<b>2.5 References</b>	<b>112</b>
<b>CHAPTER 3</b>	<b>CELLULAR MRI AS A SENSITIVE, NON-INVASIVE MODALITY SUITABLE FOR DETECTING DIFFERENCES BETWEEN THE MIGRATORY EFFICIENCIES OF DIFFERENT DENDRITIC CELL POPULATIONS <i>IN VIVO</i></b>
<b>3.1 Introduction</b>	<b>114</b>
<b>3.2 Methods</b>	<b>117</b>
3.2.1 Animal Care	117
3.2.2 Reagents	117
3.2.3 Generation of murine bone marrow-derived DCs	118
3.2.4 DC Maturation Cocktail	118
3.2.5 SPIO Labelling	119

3.2.6	Magnetic separation of SPIO <sup>+</sup> DCs from SPIO <sup>-</sup> DCs	119
3.2.7	Detection of surface antigens	119
3.2.8	Luminex <sup>®</sup> cytokine assays	120
3.2.9	Labelling DCs with PKH	120
3.2.10	Adoptive transfer of DCs	121
3.2.11	Magnetic resonance imaging of DC migration	121
3.2.12	LN removal and cryostat sectioning	121
3.2.13	Histological analysis and quantification	122
3.2.14	Statistical analysis	122
<b>3.3</b>	<b>Results</b>	
3.3.1	CpG and cytokine cocktail (CpG-CC) stimulation leads to a DC population with a mature and migratory competent phenotype	123
3.3.2	SPIO has no significant effects on <i>in vitro</i> CpG-CC stimulation of DCs	128
3.3.3	CpG-CC-DCs secrete cytokines necessary for Th1 type responses	134
3.3.4	CpG-CC stimulation enhances DC migration to target LNs <i>in vivo</i> , as assessed with cellular MRI	137
<b>3.4</b>	<b>Discussion</b>	<b>143</b>
<b>3.5</b>	<b>References</b>	<b>152</b>
<b>CHAPTER 4</b>	<b>SUMMARY</b>	
<b>4.1</b>	<b>Discussion</b>	<b>158</b>
4.1.1	Labelling DCs with SPIO	157

4.1.2 Detection Threshold Using MRI	158
4.1.3 Quantification of SPIO-labelled DCs	160
4.1.4. Limitations of Cellular MRI	162
<b>4.2 Conclusion</b>	<b>164</b>
<b>4.3 References</b>	<b>165</b>
<b>APPENDIX</b>	<b>168</b>
<b>CURRICULUM VITAE</b>	<b>174</b>

## List of Figures

### CHAPTER 1

**Figure 1.1** The maturation and activation status of DCs can mediate different T cell responses *in vivo*.

**Figure 1.2** The basic principle of MRI and the concepts of T1 and T2 relaxation.

### CHAPTER 2

**Figure 2.1** SPIO has no significant effect on DC viability, nor does it induce premature cell death.

**Figure 2.2** SPIO does not significantly affect the phenotypic characteristics of DCs *in vitro*.

**Figure 2.3** SPIO does not significantly affect cytokine secretion of DCs *in vitro*.

**Figure 2.4.** Magnetic separation of DCs reveals the presence of two phenotypically distinct subpopulations within the SPIO<sup>mix</sup> DC population.

**Figure 2.5.** The cytokine profile of SPIO<sup>-</sup> DCs is different than that of UT, SPIO<sup>mix</sup>, and SPIO<sup>+</sup> DCs.

**Figure 2.6.** *In vivo* migration suggests unlabelled DCs migrate to LNs preferentially compared to SPIO<sup>+</sup> DCs.

**Figure 2.7.** *In vivo* migration assays of DC migration demonstrate SPIO<sup>+</sup> DC migration is more efficient than SPIO<sup>mix</sup> DCs.

**Figure 2.8.** Histological analysis of *in vivo* DC migration correlates with MRI data.

**Figure 2.9.** *In vitro* migration assays show SPIO<sup>+</sup> DCs migrate more efficiently than MPIO<sup>+</sup> DCs.

**Figure 2.10.** *In vivo* migration of SPIO<sup>+</sup> DCs to popliteal LNs peaks at day 2.

**Figure 2.11.** Histological analysis of DC migration kinetics to popliteal LNs correlates with MRI analysis.

**Figure 2.12.** MHC I-SIINFEKL complexes are present on mature DCs.

**Figure 2.13.** ICS for IFN- $\gamma$  indicates the presence of more CD8<sup>+</sup>IFN<sup>+</sup> T cells following adoptive transfer of either UT or SPIO<sup>+</sup> DCs.

**Figure 2.14.** Tetramer staining indicates the presence of more CD8<sup>+</sup> SIINFEKL-specific T cells following adoptive transfer of either UT or SPIO<sup>+</sup> DCs.

### CHAPTER 3

**Figure 3.1.** Mouse BMDCs express intracellular TLR9.

**Figure 3.2.** *In vitro* CpG-CC stimulation produces a mature and active population of DCs.

**Figure 3.3.** SPIO labelling does not affect CpG-CC-induced phenotypic maturation and activation of DCs.

**Figure 3.4.** SPIO labelling does not affect CpG-CC-induced surface expression of DC migration markers.

**Figure 3.5.** CpG-CC stimulation induces DCs to secrete Th 1 type cytokines *in vitro*.

**Figure 3.6.** MRI can detect differences between migration of SPIO<sup>+</sup> and CpG-CC-SPIO<sup>+</sup> DCs *in vivo*.

**Figure 3.7.** Histological analysis of *in vivo* migration correlates with MRI data and indicates SPIO has no effect on CpG-CC-enhanced *in vivo* migration.



## List of Appendices

<b>Appendix 1</b>	Proof of ethics approval for animal use.	169
<b>Appendix 2</b>	Labelling efficiency of DCs achieved following overnight incubation with SPIO.	171
<b>Appendix 3</b>	Magnetically labelling DCs <i>in vitro</i> on magnetic plates increases the amount of iron taken up per cell.	173

<b>FSL</b>	fractional signal loss
<b>GM-CSF</b>	granulocyte/macrophage-colony stimulating factor
<b>H</b>	proton
<b>HA</b>	hemagglutinin
<b>HBSS</b>	Hank's Balanced Salt Solution
<b>HER2/neu</b>	human epidermal growth factor receptor 2
<b>hTERT</b>	human telomerase reverse transcriptase
<b>i.v.</b>	intravenous
<b>iDC</b>	immature dendritic cell
<b>IFN</b>	interferon
<b>IL</b>	interleukin
<b>LN</b>	lymph node
<b>mAb</b>	monoclonal antibody
<b>MAP</b>	mitogen-activated phosphatase
<b>mDC</b>	mature dendritic cell
<b>MHC</b>	major histocompatibility complex
<b>MHC I</b>	major histocompatibility complex class I
<b>MHC II</b>	major histocompatibility complex class II
<b>MMP9</b>	matrix metalloproteinase 9
<b>MPIO</b>	micrón-sized iron oxide
<b>MPIO<sup>-</sup></b>	MPIO-unlabelled
<b>MPIO<sup>+</sup></b>	MPIO-labelled
<b>MRI</b>	magnetic resonance imaging

<b>MUC-1</b>	mucin-1
<b>NGS</b>	normal goat serum
<b>OCT</b>	optimum cutting temperature
<b>PAMP</b>	pathogen-associated molecular pattern
<b>pDC</b>	plasmacytoid dendritic cell
<b>PEI</b>	polyethylenimine
<b>PET</b>	positron emission tomography
<b>PFA</b>	paraformaldehyde
<b>PLL</b>	poly-L-lysine
<b>SA</b>	streptavidin
<b>SPIO</b>	superparamagnetic iron oxide
<b>SPIO<sup>mix</sup></b>	unseparated SPIO-treated dendritic cells
<b>SPIO<sup>-</sup></b>	SPIO-unlabelled
<b>SPIO<sup>+</sup></b>	SPIO-labelled
<b>T</b>	Tesla
<b>TAA</b>	tumour-associated antigen
<b>TCR</b>	T cell receptor
<b>Th</b>	helper T
<b>TLR</b>	toll-like receptor
<b>TLR-CC</b>	toll-like receptor ligand and cytokine cocktail
<b>TNF</b>	tumour necrosis factor
<b>USPIO</b>	ultra small paramagnetic iron oxide
<b>UT</b>	untreated

## **CHAPTER 1: INTRODUCTION**

### **1.1 Cancer Overview**

In Canada alone, an estimated 40% of Canadian women and 45% of men will develop cancer in their lifetime [1]. According to the Canadian Cancer Society, 1 in 4 people are expected to die from cancer, making it the leading cause of premature death in Canada.

Medically termed a malignant neoplasm, cancer is a class of diseases in which a group of cells display three major characteristics: i) uncontrolled cell division, ii) invasion of adjacent tissues, and iii) metastasis via the vasculature or lymphatic system [2]. It is these three defining features of cancer that differentiate it from benign tumours, which are defined as abnormal tissue masses that are self-contained, non-invasive, and unable to metastasize. Nevertheless benign tumours can be either symptomatic or asymptomatic and can possess the potential to become malignant.

Of all forms of cancer today, breast cancer remains one of the most prevalent forms in Canada and worldwide [1]. In fact, an estimated 1 in 9 Canadian women will be diagnosed with this disease in their lifetime, and 1 in 28 is expected to die from it. As a result, breast cancer is a significant cause of cancer-related morbidity, specifically when it comes to Canadian women. While breast cancer is more prevalent amongst women, it is important to realize that men are also prone to developing this disease, with 180 Canadian men expected to be diagnosed with breast cancer in 2009. Of those, 50 are expected to

succumb to this disease, making the death rate amongst men due to breast cancer comparable to that for Canadian women [1].

Clinically, breast cancer is a highly heterogeneous disease [3, 4]. Traditional means of diagnosis includes determination of tumour size, lymph node (LN) infiltration status, estrogen receptor (ER) status, and human epidermal growth factor receptor 2 (HER2/*neu*) status [5]. These diagnostic determinants allow clinicians to define treatment regimens and predict survival outcomes for patients with early stage breast cancer [6-8].

Within the past ten years, morbidity and mortality rates for breast cancer in Canada have declined [1]. Specifically, there has been an overall improvement in the 5-year survival rates with breast cancer largely due to improvements made in screening, diagnosis, and conventional treatments [1, 2, 6].

## **1.2 Conventional Breast Cancer Therapies**

Breast cancer treatments routinely used in clinics can be classified as either local or systemic [9]. Local treatments are generally focused to the site of disease and applied to a specific area of the body, which include surgery and radiation therapy. Alternatively, systemic treatments, namely chemotherapy, hormone therapy, and passive immunotherapy, are administered via intravenous (i.v.) or oral routes, resulting in their widespread distribution throughout the body [10]. Generally, conventional breast cancer therapies are used in combination with one or more treatments [8, 9], depending on the stage and typing of the breast cancer [11-13], as well as patient statistics [14]. A brief overview of the current conventional breast cancer therapies is provided below.

### **1.2.1 Surgery**

Surgery remains the most common therapy for breast cancer, and it is used to remove the primary breast tumour [15]. In general, surgical interventions for breast cancer can be breast conserving (lumpectomy) or invasive (mastectomy). In the case of lumpectomies, only the breast lump and immediate surrounding margin of normal breast tissue is removed. For most women with early-stage breast cancer, breast-conserving surgery is effective [16]. However, in cases of highly invasive or late-stage breast cancer, an invasive mastectomy is required [17, 18]. In this surgery, all breast tissue is removed, sometimes including surrounding tissues and nearby LNs (modified radical mastectomy). As with other surgical procedures, pain, swelling, bleeding, and infection are possible side effects of this therapy.

### **1.2.2 Radiation Therapy**

In the case of radiation therapy, high-energy waves (for instance, X-rays) are used to kill cancer cells or shrink breast tumours [19]. Radiation therapy can be administered in two ways: via internal beam radiation or external beam radiation [20]. For internal beam radiation, radioactive pellets are implanted next to cancerous tissue in the breast. External beam radiation is the more common form of radiation therapy, and side effects can include swelling of the treated area, irritation, and fatigue [19].

### **1.2.3 Chemotherapy**

Chemotherapy involves the use of anticancer drugs to treat the patient and can

be administered orally, intravenously, intramuscularly, or as a topical cream [21]. Neoadjuvant therapy can be used to treat patients with chemotherapeutics to shrink large tumours before surgery [22] while adjuvant therapy can be used after surgery [23-25] in order to reduce the risk of recurrence. Chemotherapeutics commonly act by interfering with the proliferation of rapidly dividing cells, a major characteristic of malignant cancer cells. However, host cells which proliferate rapidly under normal conditions can also be affected by chemotherapeutics – cells in hair follicles, bone marrow, and the digestive tract. This non-specific targeting of healthy, rapidly dividing cells by chemotherapeutics leads to most of their toxic side effects, including hair loss (alopecia), inflammation of the digestive tract (colitis), and decreased blood cell production (myelosuppression), as well as nausea and fatigue [23, 26, 27].

#### **1.2.4 Hormone Therapy**

Hormone therapy, another form of systemic therapy, is oftentimes used to help reduce the risk of breast cancer recurrence. For patients whose breast cancer has been classed as positive for the estrogen receptor (ER), blocking ER signalling can be useful in treating these patients. Commonly used drugs for blocking ER function are Tamoxifen [28, 29] and anastrozole [30, 31]. Fulvestrant, rather, is a drug that functions by actually damaging the ER [32, 33], and it is oftentimes recommended to patients no longer responding to Tamoxifen. Conversely, aromatase inhibitors are drugs designed to directly inhibit the production of estrogen [34]. Both fulvestrant and aromatase inhibitors are only given to post-menopausal women generally [35, 36]. Side effects of hormone

therapy include tiredness, hot flashes, and mood swings.

### **1.2.5 Monoclonal Antibodies**

The presence of HER2/*neu* surface over-expression in breast cancer cells predicts the patients who will be more responsive to HER2/*neu* specific therapies. HER2/*neu* is a membrane-bound receptor tyrosine kinase that is encoded by a proto-oncogene [37, 38]. Specifically, HER2/*neu* is associated with increased cell motility, decreased apoptosis, proliferation, and regulation of cellular adhesion [39]. Trastuzumab (Herceptin) is a monoclonal antibody (mAb) that specifically blocks HER2/*neu* signalling [40]. Although mAbs are considered to be targeted therapy for breast cancer, their efficacy is far less than expected. As breast tumours are highly heterogeneous with respect to cell phenotype, they have the ability to selectively up-regulate the function of those tumour cells which lack or express lower amounts of the specific surface molecule(s) being targeted by an antibody treatment. This, in turn, will allow the tumour to evade therapeutic treatment [41, 42]. While side effects of mAbs are relatively mild, they can still include diarrhea, nausea, numbness, and vomiting.

## **1.3 Metastatic Breast Cancer**

Optimization of conventional breast cancer treatment techniques and regimens has led to an overall decrease in morbidity and mortality of primary breast cancer. Despite this overall positive outlook for primary breast cancer, up to 40% of all breast cancers recur and metastasize [1].



In spite of advances in conventional therapeutics, patients with metastatic breast cancer have a 5-year survival index of less than 20%, compared to 87% for patients with primary breast cancer [1]. Commonly used conventional therapies are more effective in improving quality of life and are largely less effective at improving survival when it comes to metastatic breast cancers [10, 43, 44]. Furthermore, conventional cancer regimens are generally non-selective and can induce cytotoxic effects in both normal and malignant cells. This makes conventional treatments less tolerable at the doses required to effectively treat metastatic breast cancer [44]. Therefore, there is a necessity for safe, targeted therapies in order to effectively treat metastatic breast cancers.

#### **1.4 Emerging Breast Cancer Therapies**

Scientific advances and greater understanding of tumour biology have allowed for the emergence of therapies which target tumour-specific molecules [45]. These targeted therapies, designed to interfere with cancer cells' growth, signalling, or target the inherent immunogenicity of the tumour itself, include enzyme inhibitors, gene therapy, and cancer vaccines (active immunotherapy).

Breast cancer, like other forms of cancer, is a polygenic disease involving mutations of tumour suppressor genes, oncogenes, and other tumour-promoting genes [46-49]. As such, targeting the altered gene expression via gene therapy or over-active enzymatic pathways prominent in breast cancer through the use of enzyme inhibitors could provide alternatives to the conventional treatments available for breast cancer. Alternatively, metabolic enzyme pathways are known to be important for function, metabolism, and survival of breast cancer cells, such

as the cyclooxygenase (COX)-2 [50-54] and estrone sulphatase [55-58] pathways. New treatments for breast cancer which target these enzymatically-driven metabolic pathways are being investigated. The following reviews provide a comprehensive discussion of the application of gene therapy and enzyme inhibitors to treat breast cancer: [59], [60], [61], [62], [63], [64], and [65].

#### **1.4.1 Active Immunotherapy**

Immunotherapy refers to a type of therapy that uses components or cells of the body's immune system in order to treat a disease [66]. There are two forms of immunotherapy: passive and active. Passive immunotherapeutics, which include the mAb Herceptin, simply aim to block cancer cell signalling with the intention of inhibiting cell processes such as cell proliferation and survival. It is important to note that some studies have demonstrated the elicitation of some immune responses in patients given passive immunotherapies, but these responses are weak and occur in only a few individuals [67-69]. Alternatively, active immunotherapeutics, such as cancer vaccines, are designed to actively engage the body's own immune system to a level capable of actively eradicating the disease. This strategy, if successful, offers the advantage eliciting long-lasting immunological memory that can protect against tumour recurrence [70].

### **1.5 Overview of the Immune System**

The immune response contains innate and adaptive components, which differ based on speed and specificity. The innate immune system acts immediately (0 – 4 hours) following infection, trauma, or the presence of tumour cells, providing

broad-scale host defence. Conversely, the adaptive immune response is slow to develop, but consists of antigen-specific reactions mediated by B and T lymphocytes. Adaptive immunity also has memory, so subsequent exposure to the same antigen leads to a faster and stronger effector response [71].

### **1.5.1 Innate Immunity**

The epithelial layers of the body provide the primary innate defence for the host [72]. If a pathogen is able to traverse the epithelial barrier, they are, in most cases, recognized by phagocytes that reside in tissues [72]. Macrophages, dendritic cells (DCs), and neutrophils are the major types of phagocytes involved in the innate immune system defences [73]. Phagocytes can discriminate between pathogens or tumour cells and normal host cells by their pathogen-associated molecular patterns (PAMPs), as in the case of pathogens, or by detecting a mutated or abnormally expressed proteins, as in the case of tumour cells. Ligation of many of the cell-surface receptors that recognize pathogens leads to phagocytosis of the pathogen, followed by its death inside the phagocyte [74]. Neutrophils are short-lived cells, dying soon after they have accomplished a round of phagocytosis [75]. However, macrophages and DCs, which are also antigen presenting cells (APCs), have the ability to release pro-inflammatory cytokines and other mediators important for inflammation [76]. Natural killer (NK) cells are also involved in innate immunity, which are small lymphocytes that play a major role in host-rejection of both tumours [77] and virally infected cells [78]. By releasing granules which contain perforin and granzymes (proteases), NK cells can induce cell apoptosis [79-82]. The primary innate mechanisms for host

defence often succeed in preventing an infection or disease from becoming established. If not, the APCs which are activated in the early innate responses can help to initiate the development of an antigen-specific adaptive immune response.

Inflammation helps to enhance the innate defence against infection or a tumour by increasing the local infiltration of the infected tissue by phagocytes [83]. Cytokines are small factors secreted by one cell to alter the behaviour of it or another cell, therefore acting as autocrine or paracrine messengers [84]. They act by binding to their specific surface receptors on target cells. Cytokines are also critical to the development and normal functioning of innate and adaptive immunity, although their effects are not limited to just cells of the immune system. Cytokines produced by leukocytes and having effects mainly on other white cells are termed interleukins (ILs) [85]. Cytokines that have chemoattractant activity are called chemokines and have a key role in regulating the activation and migration of leukocytes [86]. Those that cause differentiation and proliferation of hematopoietic stem cells are generally called colony-stimulating factors (CSFs) [87]. Those that interfere with viral replication are called type I interferons (IFNs) [88]. IFN- $\gamma$ , a type II interferon, in particular, is only produced by cells of the immune system [71] and acts to increase local inflammation and phagocytosis.

### **1.5.2 Adaptive Immunity**

The hallmark of adaptive immunity is its memory and antigen-specificity, which is mediated by B and T lymphocytes. These lymphocytes reside in secondary lymphoid organs, (lymph nodes [LNs], spleen, and mucosal-associated lymphoid

tissue), as naïve cells until they encounter their specific antigen. These secondary lymphoid tissues provide cytokines necessary to maintain naïve lymphocyte populations and they provide a site for antigen presentation to occur. In the first stage of adaptive immunity, antigen is presented to antigen-specific receptors on B and T cells by APCs. This antigen presentation leads to subsequent lymphocyte priming, activation, differentiation, and proliferation.

B cells recognize their specific antigens through their specific receptors (B cell receptors (BCRs), which are capable of binding to free antigen [93]. B cells direct humoral immunity, and their effector function is the secretion of antigen-specific antibodies [94]. Antibodies can act to neutralize toxins or viral infectivity, prevent pathogens from adhering to mucosal surfaces, sensitize pathogens for phagocytosis by APCs, or indirectly kill pathogen-infected or tumour cells via antibody dependent complement-mediated cell lysis. Complement is a group of 20 proteins associated with the innate immune system [95]. Thus antibody can enhance elements of the innate immune response.

T cells, conversely, are only capable of recognizing antigen bound to major histocompatibility complexes (MHCs) on the surface of APCs via their antigen-specific T cell receptor (TCR) [96]. TCRs are associated with CD3, which upon antigen binding to the TCR, mediates signal transduction to the nucleus, resulting in gene transcription and T cell proliferation [97, 98]. In order for T cells to become activated, co-receptor (CD28) stimulation is required by co-stimulatory molecules (CD80, CD86) found on the surface of APCs [99, 100]. As a result,

antigen presentation to T cells without these co-stimulatory signals can lead to T cell anergy (non-responsiveness) or programmed cell death [101, 102].

The second stage of adaptive immunity involves the effector response, which differs for B and T cells [71, 89]. Upon activation of B and T lymphocytes, some become plasma memory cells and effector memory cells, respectively. These cells provide the memory aspect of the adaptive immune response, capable of surviving for up to 10 years and react faster to subsequent exposure to the same antigen [90-92].

Two major types of effector T cells have been identified: helper T cells (Th) and cytotoxic T cells, which are differentiated by their CD4 or CD8 surface molecules, respectively [96]. Endogenous antigens loaded onto MHC class I (MHC I) molecules activate CD8<sup>+</sup> cytotoxic T cells. Because all nucleated cells express MHC I, any such cell that is infected with a virus or other intracellular pathogen, or is producing abnormal tumour antigens can present these antigens to CD8<sup>+</sup> T cells for cytotoxic removal [103]. CD8<sup>+</sup> T cells mediate effector responses through the production of cytokines such as IFN- $\gamma$  and TNF $\alpha$  and/or direct cytolytic mechanisms involving perforin and granzyme B [89].

The differentiation of naïve CD4<sup>+</sup> T cells into effector T helper cells is initiated by engagement of their TCR by the peptide-MHC II complex and co-stimulatory molecules in the presence of specific cytokines produced by the innate immune system. IFN- $\gamma$  and IL-12 initiate the differentiation of Th 1 cells, which are characterized by their production of IFN- $\gamma$ . This IFN- $\gamma$  produced by Th 1-type cells activates macrophages, which go on to clear intracellular pathogens

by engulfing and killing infected cells. In contrast, IL-4 triggers the differentiation of Th 2 cells, which are key mediators in defending against extracellular pathogens such and in helping B cells to produce antibodies. [104]. The effector cytokines that are subsequently produced by Th 1 and Th 2 cells (i.e., IFN- $\gamma$  and IL-4) can potentially feed back to amplify Th 1 and Th 2 cells and further enhance differentiation of the respective T cell subset. Recently, the Th 1/Th 2 paradigm has been expanded following the discovery of a third subset of effector Th cells, the Th 17 cells, which produce IL-17 and exhibit effector functions distinct from Th 1 and Th 2 cells [105, 106]. The primary function of Th 17 cells, which are potent inducers of tissue inflammation, appears to be the clearance of pathogens that are not adequately handled by Th 1 or Th 2 cells. In addition, IL-2 stimulates CD8<sup>+</sup> T cell division and cytotoxicity by decreasing activation thresholds [107]. IL-10 and TGF- $\beta$ , on the other hand, are cytokines capable of stimulating T regulatory (T<sub>reg</sub>) cell production [108-110], which is a type of T lymphocyte that functions to suppress immune responses, thereby maintaining homeostasis and tolerance to self-antigens [111, 112].

## **1.6 Cancer Vaccine Development**

Due to the immune system's ability to distinguish between normal and abnormal tissue with great specificity, it has become a major target for development of treatment strategies [41, 84, 113, 114]. Specifically, the development of cancer vaccines to elicit an active anti-tumour immune response in patients has become an attractive form of emerging therapy, particularly for the treatment of cancers of the prostate [115, 116], skin [117-119], and breast [120-122]. Generation of a

successful breast cancer vaccine requires the following components: 1) a tumour-associated antigen (TAA) to target, 2) a platform to present the TAA to the adaptive immune system, and 3) an adjuvant to enhance immune stimulation.

### **1.6.1 Tumour Associated Antigens**

In order to distinguish tumour cells from normal, healthy cells, a relatively specific TAA must be identified [123]. It is important to note that most cancer antigens are self antigens and are normally only expressed during embryogenesis or early development [124]. They may also be relatively tissue specific and expressed to varying degrees by the normal host tissue. In the event of cancer, these antigens are generally over-expressed or expressed in a mutated form [125-129]. As a result, TAAs on their own confer weak immune responses at best in most cancer patients. This is because patient immune systems are usually already tolerant to the normal expression of TAAs, therefore protecting them from being effectively targeted by the immune system. Cancer vaccines, therefore, must be designed to introduce TAA(s) to the patient's immune system in a way that is capable of breaking tolerance to the antigen(s) present on tumour cells without inducing a serious autoimmune reaction directed against healthy cells which normally express the same antigen [130].

Potentially useful breast TAAs include mucin-1 (MUC-1) [131], carcinoembryonic antigen (CEA) [132], human telomerase reverse transcriptase (hTERT) [129], and p53 [133]. Perhaps the most investigated and attractive breast TAA is HER2/*neu* [134-138]. It has been determined that roughly 20-30% of all metastatic breast cancers over-express HER2/*neu*, and studies have



demonstrated that tumours over-expressing this receptor tend to be more aggressive and are associated with shorter patient survival rates [136]. Importantly, studies have indicated spontaneous T and B cell responses have developed in response to HER2/*neu*-positive tumours, confirming the immunogenicity of this TAA [139-145].

### **1.6.2 Platform of TAA Delivery and Adjuvants**

Breast cancer-related TAAs can be delivered to the adaptive immune system in one of two ways: 1) via direct injection (first generation vaccines), oftentimes in conjunction with immunostimulatory adjuvants, or 2) used for *ex vivo* or *in vivo* loading of antigen presenting cells (APCs), usually DCs (second generation vaccines).

#### *First Generation Breast Cancer Vaccines*

First generation vaccines encompass the earliest forms of breast cancer vaccines in clinical trials. While the following vaccines provide a proof of principle, these approaches have been largely abandoned due to a lack of clinical efficacy [70]. The earliest vaccine approaches investigated the use of whole killed autologous tumour cells [146, 147]. Tumour cells can be killed by heat, chemicals, or UV irradiation to create an attenuated cancer cell that is still capable of eliciting an immune response through its antigens. An alternative but similar approach is the use of tumour cell fragments. Because cancer cells are highly heterogeneous in terms of their antigen expression even within the same tumour, these vaccine strategies allows patients to be immunized with a large number of putative TAAs. Unfortunately, there is no way to standardize multiple

preparations. Furthermore, this method relies on the patient's innate immune cells to be capable processing these TAAs and efficiently presenting them to the adaptive immune system. Incorrect processing and presentation could result in immune tolerance to these antigens rather than immune reactivity [148].

Synthetic or naturally purified peptides have also been used in first generation breast cancer vaccines [149-151]. Peptides provide the advantages of being relatively easy to produce in large quantities and standardize compared to whole tumour cells or tumour cell fragments. A major disadvantage of using peptides is that they have less stability *in vivo* [152]. Furthermore, administration of recombinant TAAs alone allows for the possibility of conferring tolerance rather than anti-tumour responses [137]. As a result, peptides have been used in conjunction with immune adjuvants, which are agents capable of stimulating a stronger immune response without having any specific antigenic effect itself [153]. In the case of peptide-based breast cancer vaccines, the immunomodulatory cytokines granulocyte/macrophage-colony stimulating factor (GM-CSF) [135], IFN- $\gamma$ , and IL-2 [154] have been used.

#### *Second Generation Cancer Vaccines*

The generation or enhancement of tolerance to TAAs by patients administered first generation vaccines is a distinct possibility. Therefore, second generation vaccines were developed, which use cellular adjuvants to deliver TAAs to naïve B and T lymphocytes *in vivo* in order to effectively stimulate potent anti-tumour immune responses [155]. In fact, studies have shown that second generation cancer vaccines are a more effective form of active cancer immunotherapy [156,

157]. Specifically, DC-based cancer vaccines show the most promise in the context of cell-based cancer vaccines [156, 158]. DCs are the most potent APCs of the immune system, capable of acting as a key mediator between the innate and adaptive immune systems. In particular, DCs have the ability to directly activate naïve T cells to mediate antigen-specific immune responses, making them attractive candidates for use in cell-based immunotherapeutics. The discovery that monocyte-derived DCs can be generated from bone marrow cell precursors in culture in the presence of GM-CSF and IL-4 [159, 160] has provided an invaluable tool for developing a greater understanding of DC biology, thereby advancing the field of DC-based cancer vaccines.

## **1.7 Dendritic Cell Biology**

Two distinct DC subsets, myeloid and lymphoid, have been identified in the mouse [161-164] and human [165-167] based on surface phenotype, cytokine requirements, and immunologic function. In general, many of the major DC markers which characterize these two DC subsets are conserved between species [168], although expression patterns sometimes differ.

### **1.7.1 Dendritic Cell Subsets**

Lymphoid-derived DCs include the plasmacytoid DCs (pDCs), which have morphological features similar to plasma cells [169]. These cells are primarily located in the blood and enter LNs through the high endothelial venules (HEVs). Mouse pDCs are conventionally characterized as CD11c<sup>low</sup>PDCA1<sup>+</sup>B220<sup>+</sup> [170, 171]. pDCs are known to produce high amounts of IFN- $\alpha$  [172-174]. For this

reason, pDCs are effective at inducing adaptive immune responses against viruses, such as influenza [175, 176]. This type of DC has been largely unexplored as an adjuvant for use in cancer vaccines because they are difficult to obtain in sufficient numbers to be therapeutically useful [177].

Myeloid-derived DCs are CD11c<sup>+</sup> and include DCs found in peripheral tissues (i.e. epidermis and respiratory mucosa), Langerhans cells of the skin, and those found in LNs [178]. Myeloid-derived DCs are commonly used in human immunotherapeutic approaches [179, 180], as CD14<sup>+</sup> monocytes are plentiful in the blood [181, 182]. Alternatively, under appropriate conditions, sufficient numbers of CD34<sup>+</sup> precursor cells can be easily obtained and purified [183-185].

### **1.7.2 Dendritic Cell Life Cycle**

In general, DCs are derived from hematopoietic stem cell precursors in the bone marrow and reside in peripheral tissues in their immature state [186]. These immature DCs (iDCs) have a high capacity for non-specific (macropinocytosis) and receptor-specific (endocytosis) antigen uptake mechanisms during steady state conditions [187]. Some surface receptors present on iDCs important for antigen uptake include Fc and lectin receptors. Fc receptors are important in mediating immune complex uptake [188], which is an antigen bound to its antibody. Lectin receptors recognize microbial carbohydrates [189]. Also, uptake of apoptotic material occurs continuously by iDCs and requires accessory molecules such as CD36 [190, 191].

DC Maturation is a process in which iDCs down-regulate their endocytic abilities and transform into mature DCs (mDCs), which express high levels of

MHC-peptide complexes and co-stimulatory molecules (CD86, CD80). Following antigen uptake and in the presence of appropriate maturation signals, iDCs mature and activate to become mature DCs (mDCs) [192]. DCs are capable of processing both exogenous and endogenous antigens and present peptide in the context of either MHC class I or II molecules [193]. Maturation signals can include pro-inflammatory cytokines (TNF- $\alpha$ , IL-1 $\beta$ , IL-6), pathogen-associated molecular patterns (PAMPs), or host-derived inflammatory molecules (CD40 ligand [CD40L]) [192]. PAMPs are expressed by microbes, and are recognized by DCs via toll-like receptors (TLRs), which are transmembrane receptors. There are 10 characterized TLRs, and they are differentially expressed by mouse and human DC subsets, each of which recognizes a different set of PAMPs [194]. For instance, TLR 9, which is found in the endoplasmic reticulum (ER) in resting DCs [195], is transferred to lysosomes upon agonist internalization. Agonists for TLR 9 are oligonucleotides containing un-methylated CpG (cytosine and guanine separated by a phosphate) residues. DC maturation is also characterized elongation of cytoplasmic extensions called dendrites needed for interactions with T lymphocytes and increased migratory capacity to draining LNs from peripheral tissues [192]. DCs interact with naïve T cells through the interaction of CD80 and CD86 with their ligand on naïve T cells, CD28. These molecules amplify T cell receptor (TCR) signalling and promote T cell activation and proliferation. Association of a naïve T cell's TCR with an MHC-peptide complex without co-stimulation (CD28-CD86/CD80 interaction) results in T cell anergy

[193]. A surface adhesion molecule which helps to strengthen the immunological synapse between a DC and T cell is CD54 (ICAM-1) [197].

Danger signals, which act to alert resting DCs to the presence of pathogens, inflammation, or tissue injury (cancer), include the heat shock proteins (hsp) 70 and gp96. These are released from necrotic cells and are able to activate DCs. Intracellular nucleotides released under conditions of hypoxia, ischemia, inflammation or mechanical stress can also activate DCs. TLRs link the recognition of danger signals to DC maturation by initiating intracellular signalling cascades, resulting in the activation of the transcription factor NF- $\kappa$ B and mitogen-activated protein (MAP) kinases. These cascades induce the transcription of genes like TNF- $\alpha$ , IL-1, and IL-6 [196]. The process of DC activation is a terminal process, in which mDCs become functionally capable of stimulating T cells. This involves the secretion of cytokines and the up-regulation of CD40, which binds to CD4<sup>+</sup>/CD8<sup>+</sup> T helper cells via interaction with CD154 (CD40L) [198]. The distinct cytokine patterns released by mature DCs ultimately determine their Th 1/Th 2 polarizing capacities. DCs which secrete IL-12 will typically induce Th 1 differentiation, whereas low levels or no IL-12 production will promote Th 2 differentiation. Fully mature and activated DCs produce large amounts of IL-12p70 [199, 200], as well as IL-2 [201], which is important for DC-mediated T cell stimulation and proliferation [202]. In addition to Th 1 and Th 2 responses, DCs are also capable of secreting IL-23 to promote Th 17 type cell production.

### 1.7.3 Dendritic Cell Migration

DC migration is a tightly regulated process that depends on a cascade of discrete events. This process is controlled by chemokine production and chemokine receptor (CCR) surface expression, as well as lipid and non-lipid mediators.

It is generally believed that DC precursors differentiate into immature DCs and migrate via the blood into peripheral tissues. Immature DCs express a unique repertoire of inflammatory CCRs (CCR1, CCR2, CCR5, and CCR6) [203, 204]. These receptors bind a pattern of inflammatory chemokines, including CCL2, CCL3, CCL4, CCL5 and CCL20 [204]. In addition, immature DCs also express functional CXCR4 [205], the receptor for CXCL12, a chemokine that is constitutively expressed in many lymphoid and non-lymphoid tissues [206].

Little is known about the mechanisms that regulate the homing of DCs or their precursors, in steady-state conditions. However, it is conceivable that the same classes of molecules that regulate DC migration under inflammatory conditions also direct the migration of these cells under normal conditions [207]. Under inflammatory conditions, TNF- $\alpha$  and IL-1 $\beta$  produced by tissue macrophages can induce the expression of inflammatory chemokines by resident cells [208].

The proper localization of mature DCs to secondary lymphoid organs and their recruitment at sites of inflammation in response to chemotactic stimuli is vital for generating T and B cell-mediated immune responses [209, 210]. It is important to note, however, that although migration is often associated with mDCs, it is not restricted to these cells only. Under steady state conditions, iDCs

have been found to migrate to LNs [204], but this occurrence is relatively rare in healthy conditions. Migration of mDCs to LNs occurs through a series of steps, including 1) a change in CCR surface expression, 2) interstitial migration, 3) entry into afferent lymphatics, and 4) transit via the lymphatics.

IL-1 $\beta$  or TNF- $\alpha$  is not only required but also sufficient for mDC mobilization, resulting in altered adhesion molecule and CCR expression [211, 212]. Concurrent down-regulation of inflammatory CCRs associated with tissue retention and CCR7 up-regulation by mDCs allows them to leave peripheral tissues and migrate to draining LNs in response to CCL19 and CCL21 in a concentration-dependent manner [192, 213]. Once a signal has triggered DC mobilization, the cells must migrate through tissues rich in extracellular matrix (ECM) proteins, such as collagen types I–IV, fibronectin, and laminin. DCs must also traverse a basement membrane before gaining access into afferent lymphatics [214, 215]. Interstitial DC migration is controlled, in part, by a balance between tissue inhibitors of metalloproteinases (TIMPs) and matrix metalloproteinases (MMPs) 2 and 9. TIMPs function as endogenous regulators of MMP activity and block DC emigration from skin explants [216]. As DCs mature, they down-regulate TIMP expression while up-regulating the membrane-bound and secreted forms of MMPs 2 and 9 [215, 217, 218], tipping the balance of MMP:TIMP activity in favour of ECM degradation. Migration of mDCs also requires the adhesion to endothelial cells, basement membranes, and collagen via integrins (CD11b, CD11c) [219, 220].



Studies have shown that CCR7 surface expression is crucial for migration of mDCs to LNs [207, 221]. While CCR7 surface expression is necessary for DC migration towards its chemokine ligands (CCLs) 19 and 21, studies have shown that it is not sufficient to trigger migration under inflammatory conditions [222-224]. It has been shown that synthesis and secretion of lipid mediators, such as prostaglandin E<sub>2</sub> (PGE<sub>2</sub>), are involved in sensitizing CCR7 to its ligands CCL19 and CCL21 [225, 226]. PGE<sub>2</sub> is secreted by monocytes, macrophages, and fibroblasts in response to inflammatory stimuli. The effect of PGE<sub>2</sub> on maturing DCs is mediated by PGE receptor 2 (EP2) and EP4 surface receptors and the cyclic adenosine monophosphate (cAMP) pathways [199, 227, 228].

CD38 is an ectoenzyme that catalyses the synthesis of cyclic ADP ribose (a potent second messenger for calcium release). CD38 is also a receptor that initiates transmembrane signalling upon engagement with its counter-receptor, CD31 [229, 230]. CD38 was found to be up-regulated during DC maturation and to promote a migratory DC phenotype *in vitro*. CD38 apparently controls DC migration, since mice lacking CD38 have a defect in both the recruitment of DC precursors to peripheral tissues and in mobilization of mDCs to the draining LNs [231].

DCs enter the afferent lymphatics by squeezing through overlapping junctions between reticulo-endothelial cells. These cells are connected to each other through several molecules, including the junctional adhesion molecules (JAMs), that form tight and adherens junctions [232, 233]. JAM A-deficient mice

show an increase in DC trafficking within the afferent lymphatics [234], suggesting that resting lymphatic endothelium normally restricts DC access.

The migration of DCs within the lymphatics to LNs depends on factors such as interstitial, hydrostatic, and oncotic pressure gradients, contraction of skeletal muscles, and the contractions of larger collecting lymphatics. Once in the LN, DCs are believed to migrate to the paracortex (T cell-rich area) by following a gradient of CCL19. It is speculated that the gradual loss of DC motility after arrival in the LN might be caused by progressive attenuation of CCR7 signalling as a result of desensitization or down-regulation of the receptor [207].

## **1.8 Challenges and efficacy of DC-based cancer vaccines**

DCs are the most potent APCs of the immune system, capable of directly stimulating naïve T cells in the LN [89, 193]. For this reason, these cells are attractive candidates for use as cellular adjuvants [156, 235]. DCs being used in early-phase clinical trials investigating cancer vaccines are usually generated *ex vivo* using CD34<sup>+</sup> precursors or CD14<sup>+</sup> monocytes [165, 236]. While early-phase clinical trials in cancer patients provide proof-of-principle, the efficacy of DC-based vaccines still needs to be improved [235, 237, 238]. Pre-clinical studies in small animal models and early-phase clinical trials in humans have demonstrated the importance of targeted migration of *ex vivo*-generated DCs to LNs in order to generate potent T cell-mediated anti-tumour responses *in vivo* [209]. Furthermore, a study by de Vries *et al.* has demonstrated the importance of the maturation state of DCs before administration, as insufficiently mature and activated DCs can cause tolerance rather than immunogenicity against the TAA

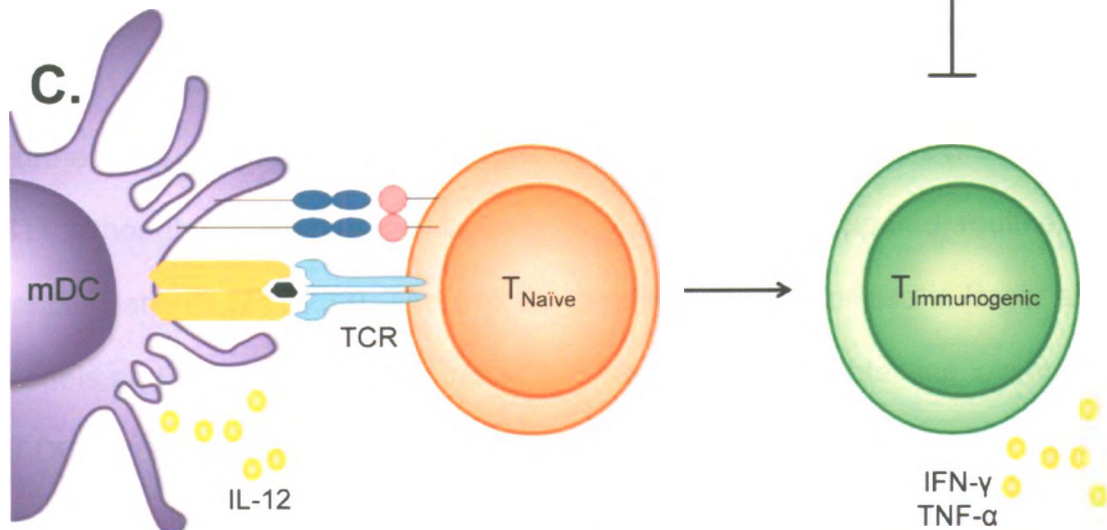
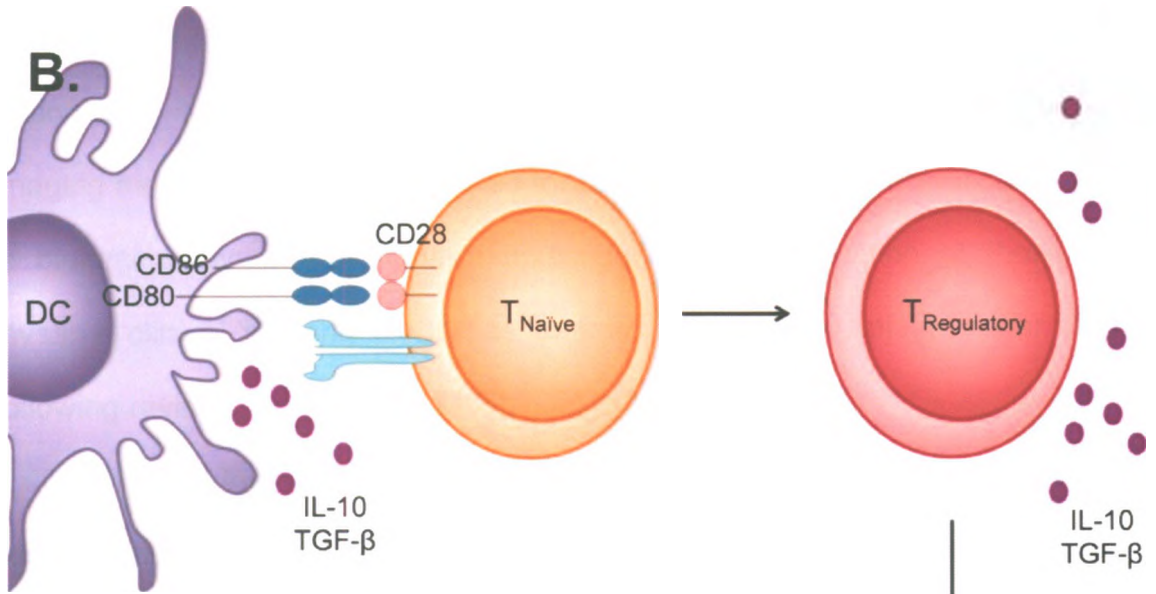
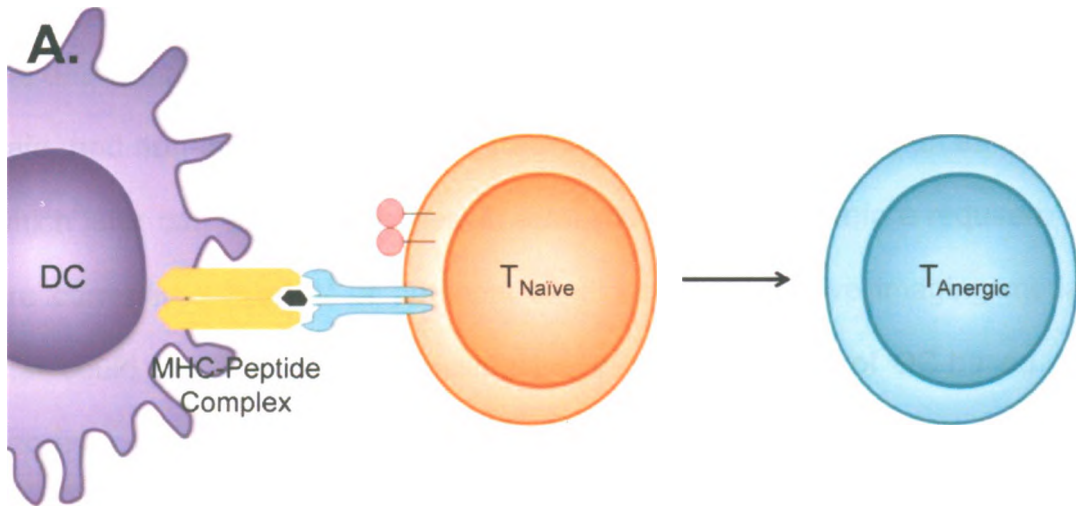
being presented [239]. As a result, recent focus on improving efficacy of DC-based cancer vaccines have focused on optimizing and standardizing protocols to improve *in vivo* migration and/or DC maturation state of *ex vivo*-generated DCs. Aspects of vaccine production and administration which require evaluation include DC culture protocols, DC maturation state, route of administration, and the optimal dose and frequency of vaccination [70, 126].

A study investigating the *in vivo* migration of In-111 labelled DCs in cancer patients revealed that fewer than 5% of DCs were migrating to target LNs [240], numbers that may be insufficient to stimulate a sufficient immune response. As a result, determining the optimal route of DC administration is important, as the targeted migration of clinically sufficient numbers of DCs to LNs is crucial to generate strong T cell-mediated anti-tumour responses [209]. In most clinical studies to date, *ex vivo*-generated DCs have been injected either intravenously (i.v.) [241, 242], subcutaneously (s.c.) [243], intradermally (i.d.) [244, 245], intranodally [246-248], or intralymphatically [249, 250]. As of yet, the optimal route of administration of the DC vaccine to which achieves the maximal immune response against tumours has yet to be defined [251].

## **1.9 *In vivo* tracking of DC migration**

Because of the efficient migration of mature DCs to target LNs is crucial for generating T cell-mediated immune responses, tracking DC migration following their administration in patients would provide clinicians with important feedback regarding their vaccination protocols. Current, conventional methods to track cell migration *in vivo* are highly invasive, and usually involve either partial or full LN

**Figure 1.1. The maturation and activation status of DCs can mediate different T cell responses *in vivo*.** (A) Semi-mature DCs capable of presenting antigen but not expressing co-receptors or secreting cytokines can induce T cell anergy. (B) DCs expressing appropriate co-stimulatory molecules but secreting IL-10 or TGF- $\beta$  can lead to the production of regulatory T cells, which are capable of suppressing the function of immunogenic T cells. (C) Fully mature DCs (mDCs) expressing appropriate antigen presenting molecules (MHC) and co-stimulatory receptors (CD80, CD86) also secreting appropriate pro-inflammatory cytokines (IL-12) can induce naïve T cells to become antigen-specific immunogenic T cells.



biopsy [252]. In general, LN biopsy is highly invasive and it is believed to affect the delicate architecture of the LN and the function of its resident cells. A reliable, safe, and non-invasive method for tracking these DCs *in vivo* in an animal model which later can be used routinely in a clinical setting is therefore required. There are currently a number of potential candidate non-invasive imaging modalities that could prove useful for tracking the *in vivo* migration of DC-based cancer vaccines in patients [253]. Clinically conventional imaging modalities that have been adapted to track DC migration *in vivo* include magnetic resonance imaging (MRI), positron emission tomography (PET), single-photon emission computed tomography (SPECT), and X-ray computed tomography (CT). An additional imaging modality that has been used for cell tracking in small animal studies only is bioluminescence. For reviews investigating the application of these non-invasive clinical imaging modalities to track DCs *in vivo*, please refer to the following reviews: [253], [254], [255], [256], [257], and [258].

Due to the lack of 3-dimensional (3-D) spatial resolution seen with scintigraphy [259] and PET [260], these imaging modalities are not able to provide accurate cell-localization. Ideally, 3-D imaging techniques are required to provide a more detailed analysis of DC migration patterns and behaviour. Furthermore, the use of radio-nuclides as labelling agents for DCs (PET, SPECT, CT), although not harmful to cells, may not be optimal for repeated, routine use in cancer patients [261-263]. The overall sensitivity of PET for use in larger animal models and even in humans is not at the level capable of detecting low numbers of DCs [260, 262, 264]. CT images provide poor image contrast of the LN [262].

Bioluminescence, although very sensitive, is restricted for use in small-animal applications due to the immunogenicity of luciferase and the toxicity of luciferin [265]. In contrast, MRI provides several advantages for tracking cell migration, as it is (1) non-invasive, (2) generates high-resolution 3-D images, (3) does not rely on radioactive isotopes, and (4) can be used for longitudinal studies. In order to track cells *in vivo*, cellular MRI, an application of MRI, is used. Cellular MRI combines the advantageous features of MRI with suitable contrast agents that specifically label cells of interest, allowing them to be distinguished above the signal of the surrounding tissue.

### 1.9.1 Cellular Magnetic Resonance Imaging

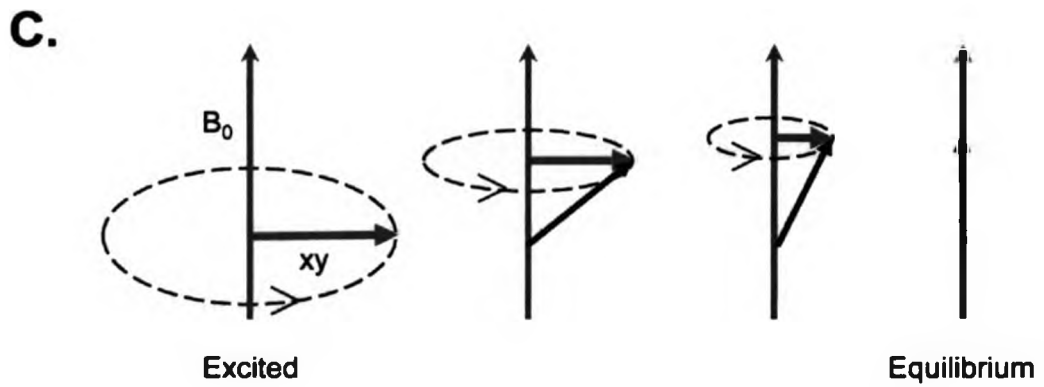
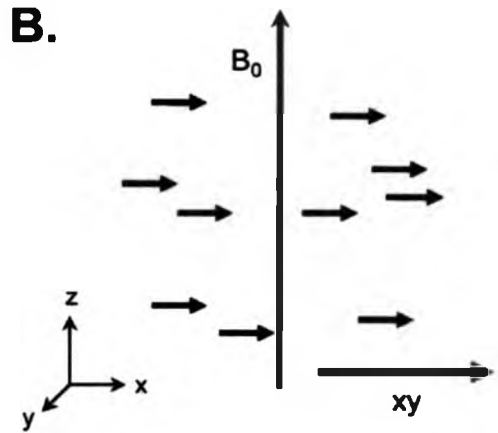
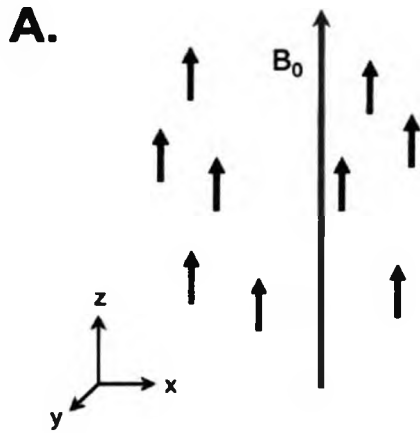
Conventional MRI uses signal generated from hydrogen protons ( $^1\text{H}$ ) of water in tissues to generate an image, as recently reviewed in [266]. Essentially, a strong magnetic field ( $B_0$ ) is first used (up to 2 Tesla [T] in current clinical procedures) to align  $^1\text{H}$  along the Z axis (Fig. 1.2A). A pulse of radiowave energy is subsequently applied (5-100 mega Hertz (MHz), which causes the  $^1\text{H}$  to flip  $90^\circ$  from the direction of the applied magnetic field ( $B_0$ ) into an excited state. Following the radiowave excitation,  $^1\text{H}$  rotate in the xy-plane and produce transverse magnetization (Fig 1.2B). It is this rotating transverse magnetization which provides the MR signal. Transverse magnetization decays and the MR signal fades proportionally as the  $^1\text{H}$  rotation gradually returns to equilibrium and re-aligns with the z axis of the  $B_0$ . This phenomenon is known as relaxation, and there are two independent forms of relaxation: T1 (Fig. 1.2C) and T2 (Fig. 1.2D) that act to return  $^1\text{H}$  back to equilibrium. Due to the inherent T1 and T2 relaxation

**Figure 1.2. The basic principle of MRI and the concepts of T1 and T2 relaxation. (A) Following application of a strong external magnetic field ( $B_0$ ,**

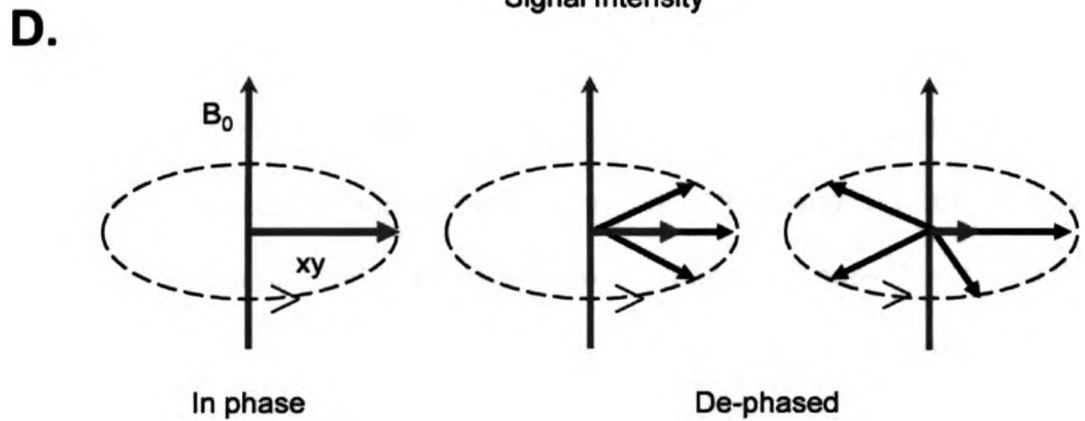


), free water protons ( $^1\text{H}$ ,





Signal Intensity



Signal Intensity

properties of various tissues in the body, differentiation between tissue types is possible without the use of a contrast agent. Cellular MRI combines the properties associated with anatomical MRI with the properties of contrast agents employed to label cells, providing dynamic assessment of cell detection in target tissues.

### *Cellular MRI contrast agents*

In order to distinguish cells of interest from surrounding tissues in an MR image, a contrast agent is required to label the cells for detection by cellular MRI. MRI contrast agents ranging from nanomolar to micromolar concentrations can alter the relaxation rates (T1 or T2) of many nearby tissue water  $^1\text{H}$ , thereby making them distinguishable [267]. MR contrast agents can be divided into two groups: 1) those which provide positive contrast and 2) those which produce negative contrast [267]. Positive contrast agents, such as paramagnetic contrast agents (gadolinium chelates) and perfluorocarbons ( $^{19}\text{F}$ ), produce hyperintense (bright) areas in MR images. Gadolinium chelates show a T1 shortening effect through interactions between the electron spins of the paramagnetic center and the nearby proton nuclei, thereby enhancing the signal intensity in the region immediately adjacent to the contrast material.  $^{19}\text{F}$  signalling relies on the spectroscopy of fluorine, and because there is no endogenous  $^{19}\text{F}$  in the body, it produces a very specific area of signal intensity [260]. Although the signal generated by positive contrast agents is readily quantifiable, MRI sensitivity for positive contrast agents is lower (10-100 fold less) compared that for negative contrast agents [260, 267, 268].

The major types of negative contrast agents contain iron oxide particles and can be divided into groups based on their particle size and sometimes based on their coating [267]. In terms of particle diameter, micron-sized iron oxide (MPIO) particles are the largest (0.9  $\mu\text{m}$ ), followed by superparamagnetic iron oxide (SPIO) nanoparticles (50-150 nm), and then ultra-small paramagnetic iron oxide (USPIO) particles. Essentially, these contrast agents act by shortening T2 relaxation, thereby producing hypointense (dark) regions in MR images. The T2 shortening effect of SPIO disrupts the signal in its immediate vicinity, creating a signal void that extends well outside the volume of the cell which contains it, thereby enhancing SPIO's level of detection and increases the amount of signal generated. However, the linear range of negative contrast agent signal is very small and therefore makes direct quantification of negative contrast signal severely limited [268]. At best, semi-quantitative techniques that measure signal void volume or fractional signal loss can be employed. Nevertheless, in terms of overall sensitivity, MRI cell tracking with iron oxide particles can actually be more sensitive than nuclear techniques, which have a sensitivity of only a few hundred cells [268, 269]. Heyn *et al.* showed that single cells labelled with SPIO could be imaged with a 1.5 T clinical scanner [270]. Furthermore, no other modality can simultaneously image the whole body in 3-D with high spatial resolution and concurrently detect a single cell *in vivo*. Accordingly, because of these advantages cellular MRI provides, the studies performed for this thesis employ it as the imaging modality to track the migration of SPIO-labelled DCs in a mouse model.

The detection of DCs labelled with SPIO nanoparticles has been accomplished by using various types imaging sequences. The imaging sequence used for these studies is called fast imaging employing steady state acquisition (FIESTA). FIESTA provides high sensitivity to SPIO-labelled cells but is relatively insensitive to background magnetic field inhomogeneities caused by free iron found in other tissues [270]. It is also important to note that FIESTA is a T2-based imaging modality. Therefore tissues such as fat, which possess short T2 relaxivities, will produce high (bright) signals in images while SPIO will produce local signal voids (hypointense regions).

### **1.10 Rationale of Study**

To date, the use of DCs as natural adjuvants in cell-based cancer vaccines has shown promise in terms of safety and feasibility. However, the overall efficacy of DC-based cancer vaccines must be enhanced. Furthermore, vaccine preparation protocols have yet to be optimized and standardized before they can be used routinely in the clinics. In order for DC-based cancer vaccines to reach their therapeutic potential, it is necessary to develop non-invasive techniques to safely track clinical grade DCs *in vivo* in patients to provide clinicians with useful feedback regarding proper DC function in terms of migration to target LNs. Furthermore, sensitive imaging techniques to detect improvements in migration may also prove useful, especially when refining methods to achieve *ex vivo* DC maturation and activation. This information can be used, in turn, to discern possible problems with current vaccination protocols and develop strategies to improve DC-based cancer vaccine therapy.

Our laboratory has previously demonstrated that using cellular MRI to track SPIO-labelled dendritic cells (SPIO DCs) is feasible in a mouse model and that the amount of migration detected can be semi-quantitatively analyzed [271]. However, there were problems encountered regarding SPIO's effect on *in vivo* migration of DCs to LNs compared to control cells. This raises an issue regarding the reliability of using cellular MRI to track labelled cells *in vivo*, as well as the use of MR data obtained to accurately quantify the *in vivo* migration of DC-based vaccines. In order for cellular MRI to be useful as an imaging modality in clinical settings, the use of contrast agents and their effect on cellular functions must be carefully and fully elucidated. Because *in vivo* migration of DCs is crucial for their effective function, the first part of this study will attempt to elucidate the reason as to why there is a discrepancy between SPIO DC and untreated DC migration *in vivo*.

Recent evidence suggests important factors which play a role regarding the DC-based vaccine efficacy are the maturity and activation state of the DCs being used [246], as well as their ability to migrate to targeted LNs. DCs develop the capacity for efficient LN-directed migration following maturation. Following analysis of the results of DC-based vaccine clinical trials, it was determined that very few *ex vivo*-generated DCs were migrating to target LNs, numbers possibly insufficient to generate strong anti-tumour responses. As a result, efforts have been made to develop stimulation cocktails using approved agents in order to sufficiently mature DCs *ex vivo* in hopes of improving their migratory abilities *in vivo*. In order to determine which cocktails are useful in enhancing this *in vivo*

migration in patients, a non-invasive, quantifiable imaging modality would be useful. As a result, the second part of this study a stimulation cocktail will be used in order to mature DCs *in vitro*, and their subsequent *in vivo* migration will be tracked and quantified using cellular MRI to demonstrate this technique is capable of detecting differences in the amount of DC migration.

### **1.11 Hypothesis**

The following was hypothesized:

1. SPIO mechanically affects the migration of DCs.
2. Cellular MRI is a sensitive, non-invasive imaging modality capable of detecting enhancements in DC migration to target LNs following their *ex vivo* stimulation.

### **1.12 Objectives**

These studies were designed to test the above hypotheses using the following objectives:

1. Elucidate the mechanism by which SPIO is affecting *in vivo* migration of DCs by:
  - a. Demonstrating SPIO has no significant effect on DC viability, maturation state, activation state, or functionality *in vitro*
  - b. Determining the reason as to why SPIO is affecting *in vivo* migration
  - c. Demonstrating a correlation between *in vivo* DC migration and antigen-specific T cell-mediated responses generated.

2. Determine if cellular MRI has the sensitivity required to detect differences in migration of matured DCs *in vivo* by:
  - a. Developing a DC stimulation cocktail to enhance *in vivo* migration
  - b. Confirming the labelling of DCs with SPIO has no effect on *in vitro* DC maturation induced by the stimulation cocktail
  - c. Demonstrating that cellular MRI can be used to detect enhancements in DC migration to target LNs following *ex vivo* stimulation.

## 1.13 References

1. Canadian Cancer Society's Steering Committee: *Canadian Cancer Statistics 2009*. 2009: April 2009, Toronto, ON.
2. Hennessy, B., et al., *Early Detection of Cancer: Molecular Screening*, in *The Molecular Basis of Cancer (Third Edition)*. 2008, W.B. Saunders: Philadelphia. p. 335-347.
3. Kinzler, K.W.V., Bert *The genetic basis of human cancer*. 2002.
4. Hatsell, S., et al., *Molecular, Cellular, and Developmental Biology of Breast Cancer*, in *Breast Cancer (Second Edition)*. 2005, Churchill Livingstone: Philadelphia. p. 27-41.
5. Sunami, E., et al., *Estrogen receptor and HER2/neu status affect epigenetic differences of tumor-related genes in primary breast tumors*. *Breast Cancer Research*, 2008. **10**(3): p. R46.
6. Tabár, L., et al., *Detection, Diagnosis, and Treatment of Early Breast Cancer Requires Creative Interdisciplinary Teamwork*. *Seminars in Breast Disease*, 2005. **8**(1): p. 4-9.
7. Tabar, L., et al., *Breast cancer treatment and natural history: new insights from results of screening*. *Lancet*, 1992. **339**(8790): p. 412-4.
8. Chow, L.W., et al., *The future perspectives of breast cancer therapy*. *Biomed Pharmacother*, 2006. **60**(6): p. 259-62.
9. Niederhuber, J.E., F.R. Daniel, and Md, *Multimodality Treatment of Breast Cancer*, in *Breast Cancer (Second Edition)*. 2005, Churchill Livingstone: Philadelphia. p. 355-382.
10. Rayson, D., et al., *Metaplastic breast cancer: prognosis and response to systemic therapy*. *Ann Oncol*, 1999. **10**(4): p. 413-9.
11. Colleoni, M., et al., *Preoperative systemic treatment: prediction of responsiveness*. *Breast*, 2003. **12**(6): p. 538-42.
12. Hayes, D.F., *Prognostic and predictive factors revisited*. *Breast*, 2005. **14**(6): p. 493-9.
13. Sonoo, H. and J. Kurebayashi, *Predictive factors for response to endocrine therapy in patients with recurrent breast cancer*. *Breast Cancer*, 2000. **7**(4): p. 297-301.
14. Mansell, J., et al., *Patterns and predictors of early recurrence in postmenopausal women with estrogen receptor-positive early breast cancer*. *Breast Cancer Res Treat*, 2009. **117**(1): p. 91-8.
15. Roses, D.F., et al., *Surgery for Breast Cancer*, in *Breast Cancer (Second Edition)*. 2005, Churchill Livingstone: Philadelphia. p. 401-459.
16. Benda, R.K., et al., *Breast-conserving therapy (BCT) for early-stage breast cancer*. *J Surg Oncol*, 2004. **85**(1): p. 14-27.
17. Jones, H.A., et al., *Impact of pathological characteristics on local relapse after breast-conserving therapy: a subgroup analysis of the EORTC boost versus no boost trial*. *J Clin Oncol*, 2009. **27**(30): p. 4939-47.
18. Millar, E.K., et al., *Prediction of local recurrence, distant metastases, and death after breast-conserving therapy in early-stage invasive breast cancer using a five-biomarker panel*. *J Clin Oncol*, 2009. **27**(28): p. 4701-8.
19. Doyle, J.J., et al., *Radiation Therapy, Cardiac Risk Factors, and Cardiac Toxicity in Early-Stage Breast Cancer Patients*. *International Journal of Radiation Oncology\*Biophysics\*Physics*, 2007. **68**(1): p. 82-93.



20. Stevens, R.E., F.R. Daniel, and Md, *Radiotherapy for In Situ, Stage I, and Stage II Breast Cancer*, in *Breast Cancer (Second Edition)*. 2005, Churchill Livingstone: Philadelphia. p. 499-536.
21. Cancer, *Chemotherapy: A guide for people with cancer*. . 2004.
22. Kuerer, H.M., et al., *Surgical conservation planning after neoadjuvant chemotherapy for stage II and operable stage III breast carcinoma*. *Am J Surg*, 2001. **182**(6): p. 601-8.
23. Jenkins, P. and R. Wallis, *Dose-rounding of adjuvant chemotherapy for breast cancer: an audit of toxicity*. *J Oncol Pharm Pract*, 2009.
24. Lohrisch, C., et al., *Impact on survival of time from definitive surgery to initiation of adjuvant chemotherapy for early-stage breast cancer*. *J Clin Oncol*, 2006. **24**(30): p. 4888-94.
25. Gomez-Iturriaga, A., et al., *Early breast cancer treated with conservative surgery, adjuvant chemotherapy, and delayed accelerated partial breast irradiation with high-dose-rate brachytherapy*. *Brachytherapy*, 2008. **7**(4): p. 310-5.
26. Heijer, A.D.-d., *Representative information on side-effects of chemotherapy*. *European Journal of Cancer*, 1999. **35**(Supplement 4): p. S8-S9.
27. Sjøvall, K., et al., *Adjuvant radiotherapy of women with breast cancer - Information, support and side-effects*. *Eur J Oncol Nurs*, 2009.
28. Brauch, H. and V.C. Jordan, *Targeting of tamoxifen to enhance antitumour action for the treatment and prevention of breast cancer: the 'personalised' approach?* *Eur J Cancer*, 2009. **45**(13): p. 2274-83.
29. Schafer, J.M., et al., *A mechanism of drug resistance to tamoxifen in breast cancer*. *The Journal of Steroid Biochemistry and Molecular Biology*, 2002. **83**(1-5): p. 75-83.
30. Boccardo, F., et al., *Switching to anastrozole versus continued tamoxifen treatment of early breast cancer: preliminary results of the Italian Tamoxifen Anastrozole Trial*. *J Clin Oncol*, 2005. **23**(22): p. 5138-47.
31. Baum, M., et al., *Anastrozole alone or in combination with tamoxifen versus tamoxifen alone for adjuvant treatment of postmenopausal women with early-stage breast cancer: results of the ATAC (Arimidex, Tamoxifen Alone or in Combination) trial efficacy and safety update analyses*. *Cancer*, 2003. **98**(9): p. 1802-10.
32. Lynn, J., *Fulvestrant ([<sup>3</sup>H]Faslodex)--a new hormonal treatment for advanced breast cancer*. *European Journal of Oncology Nursing*, 2004. **8**(Supplement 2): p. S83-S88.
33. Come, S.E. and V.F. Borges, *Role of fulvestrant in sequential hormonal therapy for advanced, hormone receptor-positive breast cancer in postmenopausal women*. *Clin Breast Cancer*, 2005. **6 Suppl 1**: p. S15-22.
34. Goss, P. and M. Wu, *Application of aromatase inhibitors in endocrine responsive breast cancers*. *Breast*, 2007. **16 Suppl 2**: p. S114-9.
35. Dodwell, D. and I. Vergote, *A comparison of fulvestrant and the third-generation aromatase inhibitors in the second-line treatment of postmenopausal women with advanced breast cancer*. *Cancer Treatment Reviews*, 2005. **31**(4): p. 274-282.
36. Gonnelli, S. and R. Petrioli, *Aromatase inhibitors, efficacy and metabolic risk in the treatment of postmenopausal women with early breast cancer*. *Clin Interv Aging*, 2008. **3**(4): p. 647-57.
37. Yen, L., et al., *Loss of Nrdp1 enhances ErbB2/ErbB3-dependent breast tumor cell growth*. *Cancer Res*, 2006. **66**(23): p. 11279-86.

38. Zhou, B.P. and M.C. Hung, *Dysregulation of cellular signaling by HER2/neu in breast cancer*. *Semin Oncol*, 2003. **30**(5 Suppl 16): p. 38-48.
39. Cabodi, S., et al., *p130Cas as a new regulator of mammary epithelial cell proliferation, survival, and HER2-neu oncogene-dependent breast tumorigenesis*. *Cancer Res*, 2006. **66**(9): p. 4672-80.
40. Nielsen, D.L., M. Andersson, and C. Kamby, *HER2-targeted therapy in breast cancer. Monoclonal antibodies and tyrosine kinase inhibitors*. *Cancer Treatment Reviews*, 2009. **35**(2): p. 121-136.
41. Rescigno, M., F. Avogadri, and G. Curigliano, *Challenges and prospects of immunotherapy as cancer treatment*. *Biochimica et Biophysica Acta (BBA) - Reviews on Cancer*, 2007. **1776**(1): p. 108-123.
42. Park, B.H. and N.E. Davidson, *PI3 kinase activation and response to Trastuzumab Therapy: what's neu with herceptin resistance?* *Cancer Cell*, 2007. **12**(4): p. 297-9.
43. Moore, S. and M.A. Cobleigh, *Targeting metastatic and advanced breast cancer*. *Semin Oncol Nurs*, 2007. **23**(1): p. 37-45.
44. Buchholz, T.A., et al., *Importance of radiation therapy for breast cancer patients treated with high-dose chemotherapy and stem cell transplant*. *Int J Radiat Oncol Biol Phys*, 2000. **46**(2): p. 337-43.
45. Riley, L.B. and D.C. Desai, *The molecular basis of cancer and the development of targeted therapy*. *Surg Clin North Am*, 2009. **89**(1): p. 1-15, vii.
46. Gould, M.N., *The utility of comparative genetics to inform breast cancer prevention strategies*. *Genetics*, 2009. **183**(2): p. 409-12.
47. Hamilton, R., *Genetics: breast cancer as an exemplar*. *Nurs Clin North Am*, 2009. **44**(3): p. 327-38.
48. Somers, T.J., et al., *Cancer genetics service interest in women with a limited family history of breast cancer*. *J Genet Couns*, 2009. **18**(4): p. 339-49.
49. Eccles, D.M., *Identification of personal risk of breast cancer: genetics*. *Breast Cancer Res*, 2008. **10 Suppl 4**: p. S12.
50. Yu, K.D., et al., *Current evidence on the relationship between polymorphisms in the COX-2 gene and breast cancer risk: a meta-analysis*. *Breast Cancer Res Treat*, 2009.
51. Valsecchi, M.E., et al., *Reduced risk of bone metastasis for patients with breast cancer who use COX-2 inhibitors*. *Clin Breast Cancer*, 2009. **9**(4): p. 225-30.
52. Su, B. and S. Chen, *Lead optimization of COX-2 inhibitor nimesulide analogs to overcome aromatase inhibitor resistance in breast cancer cells*. *Bioorg Med Chem Lett*, 2009. **19**(23): p. 6733-5.
53. Peralta, E.A., et al., *American Ginseng inhibits induced COX-2 and NFKB activation in breast cancer cells*. *J Surg Res*, 2009. **157**(2): p. 261-7.
54. Chen, B., B. Su, and S. Chen, *A COX-2 inhibitor nimesulide analog selectively induces apoptosis in Her2 overexpressing breast cancer cells via cytochrome c dependent mechanisms*. *Biochem Pharmacol*, 2009. **77**(12): p. 1787-94.
55. Ahmed, S., et al., *Review of estrone sulfatase and its inhibitors--an important new target against hormone dependent breast cancer*. *Curr Med Chem*, 2002. **9**(2): p. 263-73.
56. Pasqualini, J.R. and G.S. Chetrite, *Estrone sulfatase versus estrone sulfotransferase in human breast cancer: potential clinical applications*. *J Steroid Biochem Mol Biol*, 1999. **69**(1-6): p. 287-92.

57. Selcer, K.W., P.V. Hegde, and P.K. Li, *Inhibition of estrone sulfatase and proliferation of human breast cancer cells by nonsteroidal (p-O-sulfamoyl)-N-alkanoyl tyramines*. *Cancer Res*, 1997. **57**(4): p. 702-7.
58. Pasqualini, J.R., *Role, control and expression of estrone sulfatase and 17 beta-hydroxysteroid dehydrogenase activities in human breast cancer*. *Zentralbl Gynakol*, 1997. **119 Suppl 2**: p. 48-53.
59. Wilson, D.R., *Viral-mediated gene transfer for cancer treatment*. *Curr Pharm Biotechnol*, 2002. **3**(2): p. 151-64.
60. Day, J.M., et al., *The development of steroid sulfatase inhibitors for hormone-dependent cancer therapy*. *Ann N Y Acad Sci*, 2009. **1155**: p. 80-7.
61. Stanway, S.J., et al., *Steroid sulfatase: a new target for the endocrine therapy of breast cancer*. *Oncologist*, 2007. **12**(4): p. 370-4.
62. Harris, R.E., *Cyclooxygenase-2 (cox-2) blockade in the chemoprevention of cancers of the colon, breast, prostate, and lung*. *Inflammopharmacology*, 2009. **17**(2): p. 55-67.
63. Arun, B. and P. Goss, *The role of COX-2 inhibition in breast cancer treatment and prevention*. *Semin Oncol*, 2004. **31**(2 Suppl 7): p. 22-9.
64. Wu, Q., T. Moyana, and J. Xiang, *Cancer gene therapy by adenovirus-mediated gene transfer*. *Curr Gene Ther*, 2001. **1**(1): p. 101-22.
65. Collins, S.A., et al., *Viral vectors in cancer immunotherapy: which vector for which strategy?* *Curr Gene Ther*, 2008. **8**(2): p. 66-78.
66. Chaudhuri, D., et al., *Targeting the immune system in cancer*. *Curr Pharm Biotechnol*, 2009. **10**(2): p. 166-84.
67. Kokowski, K., et al., *Quantification of the CD8+ T cell response against a mucin epitope in patients with breast cancer*. *Arch Immunol Ther Exp (Warsz)*, 2008. **56**(2): p. 141-5.
68. Rentzsch, C., et al., *Evaluation of pre-existent immunity in patients with primary breast cancer: molecular and cellular assays to quantify antigen-specific T lymphocytes in peripheral blood mononuclear cells*. *Clin Cancer Res*, 2003. **9**(12): p. 4376-86.
69. Nagorsen, D., et al., *Differences in T-cell immunity toward tumor-associated antigens in colorectal cancer and breast cancer patients*. *Int J Cancer*, 2003. **105**(2): p. 221-5.
70. Baxevanis, C.N., S.A. Perez, and M. Papamichail, *Cancer immunotherapy*. *Crit Rev Clin Lab Sci*, 2009. **46**(4): p. 167-89.
71. Mak, T.W. and M.E. Saunders, *Introduction to the Immune Response*, in *The Immune Response*. 2006, Academic Press: Burlington. p. 17-33.
72. Whitby, J.L. and D. Rowley, *The role of macrophages in the elimination of bacteria from the mouse peritoneum*. *Br J Exp Pathol*, 1959. **40**: p. 358-70.
73. Oren, R., et al., *Metabolic patterns in three types of phagocytizing cells*. *J Cell Biol*, 1963. **17**: p. 487-501.
74. Hertzog, A.J., *The phagocytic activity of human leukocytes with special reference to their type and maturity*. *Am J Pathol*, 1938. **14**(5): p. 595-604 1.
75. Hancock, B.W., L. Bruce, and J. Richmond, *Neutrophil function in lymphoreticular malignancy*. *Br J Cancer*, 1976. **33**(5): p. 496-500.
76. Cohen, S. and S. Winkler, *Cellular immunity and the inflammatory response*. *J Periodontol*, 1974. **45**(5): p. 348-50.
77. Purdy, A.K. and K.S. Campbell, *Natural killer cells and cancer: Regulation by the killer cell Ig-like receptors (KIR)*. *Cancer Biol Ther*, 2009. **8**(23).

78. Luci, C. and E. Tomasello, *Natural killer cells: Detectors of stress*. The International Journal of Biochem. & Cell Bio., 2008. **40**(11): p. 2335-2340.
79. Nishihori, Y., et al., *Interleukin-2 gene transfer potentiates the alpha-galactosylceramide-stimulated antitumor effect by the induction of TRAIL in NKT and NK cells in mouse models of subcutaneous and metastatic carcinoma*. Cancer Biol Ther, 2009. **8**(18): p. 1763-70.
80. Kim, H.R., et al., *Anti-cancer activity and mechanistic features of a NK cell activating molecule*. Cancer Immunol Immunother, 2009. **58**(10): p. 1691-700.
81. Sutton, V.R., et al., *Measuring cell death mediated by cytotoxic lymphocytes or their granule effector molecules*. Methods, 2008. **44**(3): p. 241-9.
82. Veugelers, K., et al., *Granule-mediated killing by granzyme B and perforin requires a mannose 6-phosphate receptor and is augmented by cell surface heparan sulfate*. Mol Biol Cell, 2006. **17**(2): p. 623-33.
83. Netea, M.G., B.J. Kullberg, and J.W. Van der Meer, *Proinflammatory cytokines in the treatment of bacterial and fungal infections*. BioDrugs, 2004. **18**(1): p. 9-22.
84. Lee, S.J., J. Chinen, and A. Kavanaugh, *28. Immunomodulator therapy: Monoclonal antibodies, fusion proteins, cytokines, and immunoglobulins*. J Allergy Clin Immunol, 2009.
85. Beller, D.I., A.G. Farr, and E.R. Unanue, *Regulation of lymphocyte proliferation and differentiation by macrophages*. Fed Proc, 1978. **37**(1): p. 91-6.
86. Taylor, J.R., Jr., et al., *Expression and function of chemokine receptors on human thymocytes: implications for infection by human immunodeficiency virus type 1*. J Virol, 2001. **75**(18): p. 8752-60.
87. Sheridan, J.W. and E.R. Stanley, *Tissue sources of bone marrow colony stimulating factor*. J Cell Physiol, 1971. **78**(3): p. 451-60.
88. Lindenmann, J., D.C. Burke, and A. Isaacs, *Studies on the production, mode of action and properties of interferon*. Br J Exp Pathol, 1957. **38**(5): p. 551-62.
89. Santana, M.A., F. EsquivelGuadarrama, and W.J. Kwang, *Cell Biology of T Cell Activation and Differentiation*, in *International Review of Cytology*. 2006, Academic Press. p. 217-274.
90. Burkett, P.R., et al., *Generation, maintenance, and function of memory T cells*. Adv Immunol, 2004. **83**: p. 191-231.
91. Sprent, J. and C.D. Surh, *Generation and maintenance of memory T cells*. Curr Opin Immunol, 2001. **13**(2): p. 248-54.
92. Dai, Z., B.T. Konieczny, and F.G. Lakkis, *The dual role of IL-2 in the generation and maintenance of CD8+ memory T cells*. J Immunol, 2000. **165**(6): p. 3031-6.
93. Gowans, J.L., *Differentiation of the cells which synthesize the immunoglobulins*. Ann Immunol (Paris), 1974. **125C**(1-2): p. 201-11.
94. Schoenberg, M.D., et al., *Cellular Sites of Synthesis of Rabbit Immunoglobulins during Primary Response to Diphtheria Toxoid-Freund's Adjuvant*. J Exp Med, 1965. **121**: p. 577-90.
95. van Furth, R., H.R. Schuit, and W. Hijmans, *The formation of immunoglobulins by human tissues in vitro. 3. Spleen, lymph nodes, bone marrow and thymus*. Immunology, 1966. **11**(1): p. 19-27.
96. Crone, M., C. Koch, and M. Simonsen, *The elusive T cell receptor*. Transplant Rev, 1972. **10**: p. 36-56.
97. Walker, C., et al., *Different effects of IL-2 addition or antibody crosslinking on T-cell subset stimulation by CD3 antibodies*. Cell Immunol, 1986. **101**(1): p. 195-203.

98. Yang, S.Y., S. Chouaib, and B. Dupont, *A common pathway for T lymphocyte activation involving both the CD3-Ti complex and CD2 sheep erythrocyte receptor determinants*. J Immunol, 1986. **137**(4): p. 1097-100.
99. Levine, B.L., et al., *CD28 ligands CD80 (B7-1) and CD86 (B7-2) induce long-term autocrine growth of CD4+ T cells and induce similar patterns of cytokine secretion in vitro*. Int Immunol, 1995. **7**(6): p. 891-904.
100. Thebeau, L.G., et al., *B7 costimulation molecules expressed from the herpes simplex virus 2 genome rescue immune induction in B7-deficient mice*. J Virol, 2007. **81**(22): p. 12200-9.
101. Wu, H.Y., A. Monsonogo, and H.L. Weiner, *The mechanism of nasal tolerance in lupus prone mice is T-cell anergy induced by immature B cells that lack B7 expression*. J Autoimmun, 2006. **26**(2): p. 116-26.
102. Ragazzo, J.L., et al., *Costimulation via lymphocyte function-associated antigen 1 in the absence of CD28 ligation promotes anergy of naive CD4+ T cells*. Proc Natl Acad Sci U S A, 2001. **98**(1): p. 241-6.
103. Fleischer, B., H. Schrezenmeier, and H. Wagner, *Function of the CD4 and CD8 molecules on human cytotoxic T lymphocytes: regulation of T cell triggering*. J Immunol, 1986. **136**(5): p. 1625-8.
104. Mosmann, T.R. and R.L. Coffman, *TH1 and TH2 cells: different patterns of lymphokine secretion lead to different functional properties*. Annu Rev Immunol, 1989. **7**: p. 145-73.
105. Bettelli, E., et al., *Reciprocal developmental pathways for the generation of pathogenic effector TH17 and regulatory T cells*. Nature, 2006. **441**(7090): p. 235-8.
106. Veldhoen, M., et al., *TGFbeta in the context of an inflammatory cytokine milieu supports de novo differentiation of IL-17-producing T cells*. Immunity, 2006. **24**(2): p. 179-89.
107. Jankovic, D., Z. Liu, and W.C. Gause, *Th1- and Th2-cell commitment during infectious disease: asymmetry in divergent pathways*. Trends Immunol, 2001. **22**(8): p. 450-7.
108. Bollyky, P.L., et al., *CD44 costimulation promotes FoxP3+ regulatory T cell persistence and function via production of IL-2, IL-10, and TGF-beta*. J Immunol, 2009. **183**(4): p. 2232-41.
109. Pyzik, M. and C.A. Piccirillo, *TGF-beta1 modulates Foxp3 expression and regulatory activity in distinct CD4+ T cell subsets*. J Leukoc Biol, 2007. **82**(2): p. 335-46.
110. Chen, W., et al., *Conversion of peripheral CD4+CD25- naive T cells to CD4+CD25+ regulatory T cells by TGF-beta induction of transcription factor Foxp3*. J Exp Med, 2003. **198**(12): p. 1875-86.
111. Klunker, S., et al., *Transcription factors RUNX1 and RUNX3 in the induction and suppressive function of Foxp3+ inducible regulatory T cells*. J Exp Med, 2009. **206**(12): p. 2701-15.
112. Ahangarani, R.R., et al., *In vivo induction of type 1-like regulatory T cells using genetically modified B cells confers long-term IL-10-dependent antigen-specific unresponsiveness*. J Immunol, 2009. **183**(12): p. 8232-43.
113. Kavanaugh, A., *An overview of immunomodulatory intervention in rheumatoid arthritis*. Drugs Today (Barc), 1999. **35**(4-5): p. 275-86.
114. Bosani, M., S. Ardizzone, and G.B. Porro, *Biologic targeting in the treatment of inflammatory bowel diseases*. Biologics, 2009. **3**: p. 77-97.
115. Chakraborty, N.G., et al., *Recognition of PSA-derived peptide antigens by T cells from prostate cancer patients without any prior stimulation*. Cancer Immunol Immunother, 2003. **52**(8): p. 497-505.

116. Elkord, E., et al., *Differential CTLs specific for prostate-specific antigen in healthy donors and patients with prostate cancer*. *Int Immunol*, 2005. **17**(10): p. 1315-25.
117. Perales, M.A., et al., *Phase I/II study of GM-CSF DNA as an adjuvant for a multi-peptide cancer vaccine in patients with advanced melanoma*. *Mol Ther*, 2008. **16**(12): p. 2022-9.
118. Markovic, S.N., et al., *Peptide vaccination of patients with metastatic melanoma: improved clinical outcome in patients demonstrating effective immunization*. *Am J Clin Oncol*, 2006. **29**(4): p. 352-60.
119. Weber, J., et al., *Phase 1 trial of intranodal injection of a Melan-A/MART-1 DNA plasmid vaccine in patients with stage IV melanoma*. *J Immunother*, 2008. **31**(2): p. 215-23.
120. Wiedermann, U., et al., *A virosomal formulated Her-2/neu multi-peptide vaccine induces Her-2/neu-specific immune responses in patients with metastatic breast cancer: a phase I study*. *Breast Cancer Res Treat*, 2009.
121. Disis, M.L., et al., *Generation of immunity to the HER-2/neu oncogenic protein in patients with breast and ovarian cancer using a peptide-based vaccine*. *Clin Cancer Res*, 1999. **5**(6): p. 1289-97.
122. Disis, M.L., et al., *Effect of dose on immune response in patients vaccinated with an her-2/neu intracellular domain protein--based vaccine*. *J Clin Oncol*, 2004. **22**(10): p. 1916-25.
123. Neller, M.A., J.A. López, and C.W. Schmidt, *Antigens for cancer immunotherapy*. *Seminars in Immunology*, 2008. **20**(5): p. 286-295.
124. Huebner, R.J., et al., *Group-specific antigen expression during embryogenesis of the genome of the C-type RNA tumor virus: implications for ontogenesis and oncogenesis*. *Proc Natl Acad Sci U S A*, 1970. **67**(1): p. 366-76.
125. Klein, O., et al., *An approach for high sensitivity detection of breast cancer by analysis of changes in structure of the cytoplasmic matrix of lymphocytes specifically induced by a specific breast tumour antigen (MUC-I/SEC)*. *The Breast*, 2002. **11**(2): p. 137-143.
126. Mocellin, S., C.R. Rossi, and D. Nitti, *Cancer vaccine development: on the way to break immune tolerance to malignant cells*. *Experimental Cell Research*, 2004. **299**(2): p. 267-278.
127. Atsuta, Y., et al., *Identification of metalloproteinase-1 as a member of a tumor associated antigen in patients with breast cancer*. *Cancer Letters*, 2002. **182**(1): p. 101-107.
128. Narita, D., A. Anghel, and M. Motoc, *Prostate-specific antigen may serve as a pathological predictor in breast cancer*. *Rom J Morphol Embryol*, 2008. **49**(2): p. 173-80.
129. Poremba, C., et al., *Telomerase as a prognostic marker in breast cancer: high-throughput tissue microarray analysis of hTERT and hTR*. *J Pathol*, 2002. **198**(2): p. 181-9.
130. Gritzapis, A.D., et al., *Vaccination with human HER-2/neu (435-443) CTL peptide induces effective antitumor immunity against HER-2/neu-expressing tumor cells in vivo*. *Cancer Res*, 2006. **66**(10): p. 5452-60.
131. Taylor-Papadimitriou, J., et al., *MUC1 and cancer*. *Biochimica et Biophysica Acta (BBA) - Molecular Basis of Disease*, 1999. **1455**(2-3): p. 301-313.
132. Jiang, X.P., et al., *Vaccination with a mixed vaccine of autogenous and allogeneic breast cancer cells and tumor associated antigens CA15-3, CEA and CA125--results in immune and clinical responses in breast cancer patients*. *Cancer Biother Radiopharm*, 2000. **15**(5): p. 495-505.
133. Curigliano, G., M. Rescigno, and A. Goldhirsch, *Immunology and breast cancer: Therapeutic cancer vaccines*. *The Breast*, 2007. **16**(Supplement 2): p. 20-26.

134. Peoples, G.E., et al., *Clinical trial results of a HER2/neu (E75) vaccine to prevent recurrence in high-risk breast cancer patients*. J Clin Oncol, 2005. **23**(30): p. 7536-45.
135. Dela Cruz, J.S., S.L. Morrison, and M.L. Penichet, *Insights into the mechanism of anti-tumor immunity in mice vaccinated with the human HER2/neu extracellular domain plus anti-HER2/neu IgG3-(IL-2) or anti-HER2/neu IgG3-(GM-CSF) fusion protein*. Vaccine, 2005. **23**(39): p. 4793-4803.
136. Freudenberg, J.A., et al., *The role of HER2 in early breast cancer metastasis and the origins of resistance to HER2-targeted therapies*. Experimental and Molecular Pathology, 2009. **87**(1): p. 1-11.
137. Hueman, M.T., et al., *Immunological monitoring of regulatory T cells by flow cytometry in a novel HLA Class II HER2/neu peptide vaccine clinical trial in breast cancer patients*. Journal of the American College of Surgeons, 2006. **203**(3, Supplement 1): p. S82-S83.
138. Borghaei, H., et al., *Induction of adaptive Anti-HER2/neu immune responses in a Phase 1B/2 trial of 2B1 bispecific murine monoclonal antibody in metastatic breast cancer (E3194): a trial coordinated by the Eastern Cooperative Oncology Group*. J Immunother, 2007. **30**(4): p. 455-67.
139. Disis, M.L., et al., *In vitro generation of human cytolytic T-cells specific for peptides derived from the HER-2/neu protooncogene protein*. Cancer Res, 1994. **54**(4): p. 1071-6.
140. Pavoni, E., et al., *A study of the humoral immune response of breast cancer patients to a panel of human tumor antigens identified by phage display*. Cancer Detection and Prevention, 2006. **30**(3): p. 248-256.
141. Fernandez Madrid, F., *Autoantibodies in breast cancer sera: candidate biomarkers and reporters of tumorigenesis*. Cancer Lett, 2005. **230**(2): p. 187-98.
142. Takeuchi, N., et al., *Anti-HER-2/neu immune responses are induced before the development of clinical tumors but declined following tumorigenesis in HER-2/neu transgenic mice*. Cancer Res, 2004. **64**(20): p. 7588-95.
143. Disis, M.L., et al., *Existent T-cell and antibody immunity to HER-2/neu protein in patients with breast cancer*. Cancer Res, 1994. **54**(1): p. 16-20.
144. Fisk, B., et al., *Existent proliferative responses of peripheral blood mononuclear cells from healthy donors and ovarian cancer patients to HER-2 peptides*. Anticancer Res, 1997. **17**(1A): p. 45-53.
145. Fisk, B., et al., *Identification of an immunodominant peptide of HER-2/neu protooncogene recognized by ovarian tumor-specific cytotoxic T lymphocyte lines*. J Exp Med, 1995. **181**(6): p. 2109-17.
146. Guckel, B., et al., *A CD80-transfected human breast cancer cell variant induces HER-2/neu-specific T cells in HLA-A\*02-matched situations in vitro and in vivo*. Cancer Immunol Immunother, 2005. **54**(2): p. 129-40.
147. Fifis, T., et al., *Vaccination with in vitro grown whole tumor cells induces strong immune responses and retards tumor growth in a murine model of colorectal liver metastases*. Vaccine, 2008. **26**(2): p. 241-9.
148. Sioud, M., *Does our current understanding of immune tolerance, autoimmunity, and immunosuppressive mechanisms facilitate the design of efficient cancer vaccines?* Scand J Immunol, 2009. **70**(6): p. 516-25.
149. Mittendorf, E.A., et al., *Evaluation of the HER2/neu-derived peptide GP2 for use in a peptide-based breast cancer vaccine trial*. Cancer, 2006. **106**(11): p. 2309-17.

150. Mittendorf, E.A., et al., *Vaccination with a HER2/neu peptide induces intra- and inter-antigenic epitope spreading in patients with early stage breast cancer*. *Surgery*, 2006. **139**(3): p. 407-18.
151. Disis, M.L., et al., *Generation of T-cell immunity to the HER-2/neu protein after active immunization with HER-2/neu peptide-based vaccines*. *J Clin Oncol*, 2002. **20**(11): p. 2624-32.
152. Knutson, K.L., et al., *Immunization of cancer patients with a HER-2/neu, HLA-A2 peptide, p369-377, results in short-lived peptide-specific immunity*. *Clin Cancer Res*, 2002. **8**(5): p. 1014-8.
153. Klein, E., et al., *Immunologic approaches to various types of cancer with the use of BCG and purified protein derivatives*. *Natl Cancer Inst Monogr*, 1973. **39**: p. 229-42.
154. Nguyen, C.L., et al., *Mechanisms of enhanced antigen-specific T cell response following vaccination with a novel peptide-based cancer vaccine and systemic interleukin-2 (IL-2)*. *Vaccine*, 2003. **21**(19-20): p. 2318-28.
155. Farkas, A., et al., *Current state and perspectives of dendritic cell vaccination in cancer immunotherapy*. *Skin Pharmacol Physiol*, 2006. **19**(3): p. 124-31.
156. Chan, T., et al., *HER-2/neu-gene engineered dendritic cell vaccine stimulates stronger HER-2/neu-specific immune responses compared to DNA vaccination*. *Gene Ther*, 2006. **13**(19): p. 1391-402.
157. Sakai, Y., et al., *Vaccination by genetically modified dendritic cells expressing a truncated neu oncogene prevents development of breast cancer in transgenic mice*. *Cancer Res*, 2004. **64**(21): p. 8022-8.
158. Wei, H., et al., *Targeted delivery of tumor antigens to activated dendritic cells via CD11c molecules induces potent antitumor immunity in mice*. *Clin Cancer Res*, 2009. **15**(14): p. 4612-21.
159. Chapuis, F., et al., *Differentiation of human dendritic cells from monocytes in vitro*. *Eur J Immunol*, 1997. **27**(2): p. 431-41.
160. Inaba, K., et al., *Generation of large numbers of dendritic cells from mouse bone marrow cultures supplemented with granulocyte/macrophage colony-stimulating factor*. *J Exp Med*, 1992. **176**(6): p. 1693-702.
161. Iyoda, T., et al., *The CD8+ dendritic cell subset selectively endocytoses dying cells in culture and in vivo*. *J Exp Med*, 2002. **195**(10): p. 1289-302.
162. Inaba, K., *Dendritic cells as antigen-presenting cells in vivo*. *Immunol Cell Biol*, 1997. **75**(2): p. 206-8.
163. Guimont-Desrochers, F., et al., *Cutting edge: genetic characterization of IFN-producing killer dendritic cells*. *J Immunol*, 2009. **182**(9): p. 5193-7.
164. Bedoui, S., et al., *Characterization of an immediate splenic precursor of CD8+ dendritic cells capable of inducing antiviral T cell responses*. *J Immunol*, 2009. **182**(7): p. 4200-7.
165. Szabolcs, P., et al., *Growth and differentiation of human dendritic cells from CD34+ progenitors*. *Adv Exp Med Biol*, 1997. **417**: p. 15-9.
166. Martin-Martin, L., et al., *Immunophenotypical, morphologic, and functional characterization of maturation-associated plasmacytoid dendritic cell subsets in normal adult human bone marrow*. *Transfusion*, 2009.
167. Masten, B.J., et al., *Characterization of myeloid and plasmacytoid dendritic cells in human lung*. *J Immunol*, 2006. **177**(11): p. 7784-93.



168. Robbins, S.H., et al., *Novel insights into the relationships between dendritic cell subsets in human and mouse revealed by genome-wide expression profiling*. *Genome Biol*, 2008. **9**(1): p. R17.
169. O'Keeffe, M., et al., *Mouse plasmacytoid cells: long-lived cells, heterogeneous in surface phenotype and function, that differentiate into CD8(+) dendritic cells only after microbial stimulus*. *J Exp Med*, 2002. **196**(10): p. 1307-19.
170. Ferrero, I., et al., *Mouse CD11c(+) B220(+) Gr1(+) plasmacytoid dendritic cells develop independently of T-cells*. *Blood*, 2002. **100**(8): p. 2852-7.
171. Nikolic, T., et al., *A subfraction of B220(+) cells in murine bone marrow and spleen does not belong to the B cell lineage but has dendritic cell characteristics*. *Eur J Immunol*, 2002. **32**(3): p. 686-92.
172. Petzke, M.M., et al., *Recognition of Borrelia burgdorferi, the Lyme disease spirochete, by TLR7 and TLR9 induces a type I IFN response by human immune cells*. *J Immunol*, 2009. **183**(8): p. 5279-92.
73. Asselin-Paturel, C., et al., *Mouse type I IFN- cells are immature APCs with plasmacytoid morphology*. *Nat Immunol*, 2001. **2**(12): p. 1144-50.
174. Demedts, I.K., et al., *Identification and characterization of human pulmonary DCs*. *Am J Respir Cell Mol Biol*, 2005. **32**(3): p. 177-84.
175. GeurtsvanKessel, C.H., et al., *Dendritic cells are crucial for maintenance of tertiary lymphoid structures in the lung of influenza virus-infected mice*. *J Exp Med*, 2009. **206**(11): p. 2339-49.
176. GeurtsvanKessel, C.H., et al., *Both conventional and interferon killer dendritic cells have antigen-presenting capacity during influenza virus infection*. *PLoS One*, 2009. **4**(9): p. e7187.
177. Gilliet, M., et al., *The development of murine plasmacytoid dendritic cell precursors is differentially regulated by FLT3-ligand and granulocyte/macrophage colony-stimulating factor*. *J Exp Med*, 2002. **195**(7): p. 953-8.
178. Manz, M.G., et al., *Dendritic cell development from common myeloid progenitors*. *Ann N Y Acad Sci*, 2001. **938**: p. 167-73; discussion 173-4.
179. Mytar, B., et al., *Biological activity of dendritic cells generated from cord blood CD34+ hematopoietic progenitors in IL-7- and IL-13-conditioned cultures*. *Arch Immunol Ther Exp (Warsz)*, 2009. **57**(1): p. 67-74.
180. Schuler, G. and N. Romani, *Generation of mature dendritic cells from human blood. An improved method with special regard to clinical applicability*. *Adv Exp Med Biol*, 1997. **417**: p. 7-13.
181. Almeida, J., et al., *Extensive characterization of the immunophenotype and pattern of cytokine production by distinct subpopulations of normal human peripheral blood MHC II+/lineage- cells*. *Clin Exp Immunol*, 1999. **118**(3): p. 392-401.
182. Almeida, J., et al., *Comparative analysis of the morphological, cytochemical, immunophenotypical, and functional characteristics of normal human peripheral blood lineage(-)/CD16(+)/HLA-DR(+)/CD14(-/lo) cells, CD14(+) monocytes, and CD16(-) dendritic cells*. *Clin Immunol*, 2001. **100**(3): p. 325-38.
183. Stephen, T.L., et al., *In vitro generation of murine myeloid dendritic cells from CD34-positive precursors*. *Cell Biol Int*, 2009. **33**(7): p. 778-84.

184. Basak, S.K., et al., *Increased dendritic cell number and function following continuous in vivo infusion of granulocyte macrophage-colony-stimulating factor and interleukin-4*. *Blood*, 2002. **99**(8): p. 2869-79.
185. Ratta, M., et al., *Generation and functional characterization of human dendritic cells derived from CD34 cells mobilized into peripheral blood: comparison with bone marrow CD34+ cells*. *Br J Haematol*, 1998. **101**(4): p. 756-65.
186. Ardavin, C., et al., *Origin and differentiation of dendritic cells*. *Trends in Immunology*, 2001. **22**(12): p. 691-700.
187. Andersson, L.I., P. Hellman, and H. Eriksson, *Receptor-mediated endocytosis of particles by peripheral dendritic cells*. *Hum Immunol*, 2008. **69**(10): p. 625-33.
188. Da Silva, D.M., et al., *Uptake of human papillomavirus virus-like particles by dendritic cells is mediated by Fcγ receptors and contributes to acquisition of T cell immunity*. *J Immunol*, 2007. **178**(12): p. 7587-97.
189. Weck, M.M., et al., *hDectin-1 is involved in uptake and cross-presentation of cellular antigens*. *Blood*, 2008. **111**(8): p. 4264-72.
190. Urban, B.C., N. Willcox, and D.J. Roberts, *A role for CD36 in the regulation of dendritic cell function*. *Proc Natl Acad Sci U S A*, 2001. **98**(15): p. 8750-5.
191. Rubartelli, A., A. Poggi, and M.R. Zocchi, *The selective engulfment of apoptotic bodies by dendritic cells is mediated by the α(v)β3 integrin and requires intracellular and extracellular calcium*. *Eur J Immunol*, 1997. **27**(8): p. 1893-900.
192. Banchereau, J., et al., *Immunobiology of dendritic cells*. *Annu Rev Immunol*, 2000. **18**: p. 767-811.
193. Guermonprez, P., et al., *Antigen presentation and T cell stimulation by dendritic cells*. *Annu Rev Immunol*, 2002. **20**: p. 621-67.
194. Loskog, A. and T.H. Totterman, *CD40L - a multipotent molecule for tumor therapy*. *Endocr Metab Immune Disord Drug Targets*, 2007. **7**(1): p. 23-8.
195. Vollmer, J. and A.M. Krieg, *Immunotherapeutic applications of CpG oligodeoxynucleotide agonists*. *Drug Deliv Rev*, 2009. **61**(3): p. 195-204.
196. Tsujimura, H., et al., *Toll-like receptor 9 signaling activates NF-κB through IFN regulatory factor-8/IFN consensus sequence binding protein in dendritic cells*. *J Immunol*, 2004. **172**(11): p. 6820-7.
197. Averbek, M., et al., *Early cytoskeletal rearrangement during dendritic cell maturation enhances synapse formation and Ca<sup>2+</sup> signaling in CD8(+) T cells*. *Eur J Immunol*, 2004. **34**(10): p. 2708-19.
198. Caux, C., et al., *Activation of human dendritic cells through CD40 cross-linking*. *J Exp Med*, 1994. **180**(4): p. 1263-72.
199. Boullart, A.C., et al., *Maturation of monocyte-derived dendritic cells with Toll-like receptor 3 and 7/8 ligands combined with prostaglandin E2 results in high interleukin-12 production and cell migration*. *Cancer Immunol Immunother*, 2008. **57**(11): p. 1589-97.
200. Czerniecki, B.J., et al., *Targeting HER-2/neu in early breast cancer development using dendritic cells with staged interleukin-12 burst secretion*. *Cancer Res*, 2007. **67**(4): p. 1842-52.
201. Granucci, F., et al., *Inducible IL-2 production by dendritic cells revealed by global gene expression analysis*. *Nat Immunol*, 2001. **2**(9): p. 882-8.
202. Langenkamp, A., et al., *Kinetics of dendritic cell activation: impact on priming of TH1, TH2 and nonpolarized T cells*. *Nat Immunol*, 2000. **1**(4): p. 311-6.

203. Allavena, P., et al., *The chemokine receptor switch paradigm and dendritic cell migration: significance in tumors*. Immunol Rev, 2000. **177**: p. 141-9.
204. Cavanagh, L.L. and U.H. Von Andrian, *Travellers in many guises: the origins and destinations of dendritic cells*. Immunol Cell Biol, 2002. **80**(5): p. 448-62.
205. Kabashima, K., et al., *CXCL12-CXCR4 engagement required for migration of cutaneous dendritic cells*. Am J Pathol, 2007. **171**(4): p. 1249-57.
206. Veldkamp, C.T., et al., *The monomer-dimer equilibrium of stromal cell-derived factor-1 (CXCL 12) is altered by pH, phosphate, sulfate, and heparin*. Protein Sci, 2005. **14**(4): p. 1071-81.
207. Sozzani, S., et al., *Differential regulation of chemokine receptors during dendritic cell maturation: a model for their trafficking properties*. J Immunol, 1998. **161**(3): p. 1083-6.
208. Chabaud, M., G. Page, and P. Miossec, *Enhancing effect of IL-1, IL-17, and TNF-alpha on macrophage inflammatory protein-3alpha production in rheumatoid arthritis: regulation by soluble receptors and Th2 cytokines*. J Immunol, 2001. **167**(10): p. 6015-20.
209. Kimber, I., et al., *Correlation between Lymphocyte Proliferative Responses and Dendritic Cell Migration in Regional Lymph Nodes following Skin Painting with Contact-Sensitizing Agents*. International Archives of Allergy and Immunology, 1990. **93**(1): p. 47-53.
210. MartIn-Fontecha, A., et al., *Regulation of dendritic cell migration to the draining lymph node: impact on T lymphocyte traffic and priming*. J Exp Med, 2003. **198**(4): p. 615-21.
211. Vecchi, A., et al., *Differential responsiveness to constitutive vs. inducible chemokines of immature and mature mouse dendritic cells*. J Leukoc Biol, 1999. **66**(3): p. 489-94.
212. Nishibu, A., et al., *Roles for IL-1 and TNFalpha in dynamic behavioral responses of Langerhans cells to topical hapten application*. J Dermatol Sci, 2007. **45**(1): p. 23-30.
213. Ardavin, C., S. Amigorena, C. Reis Sousa, *Dendritic cells: immunobiology and cancer immunotherapy*. Immunity, 2004. **20**(1): p. 17-23.
214. Faveeuw, C., G. Preece, and A. Ager, *Transendothelial migration of lymphocytes across high endothelial venules into lymph nodes is affected by metalloproteinases*. Blood, 2001. **98**(3): p. 688-95.
215. Ratzinger, G., et al., *Matrix metalloproteinases 9 and 2 are necessary for the migration of Langerhans cells and dermal dendritic cells from human and murine skin*. J Immunol, 2002. **168**(9): p. 4361-71.
216. Osman, M., et al., *Expression of matrix metalloproteinases and tissue inhibitors of metalloproteinases define migratory characteristics of human monocyte-derived dendritic cells*. Immunology, 2002. **105**(1): p. 73-82.
217. Jotwani, R., et al., *MMP-9/TIMP-1 imbalance induced in human dendritic cells by Porphyromonas gingivalis*. FEMS Immunol Med Microbiol, 2009.
218. Lackey, D.E., et al., *Retinoic acid decreases adherence of murine myeloid dendritic cells and increases production of matrix metalloproteinase-9*. J Nutr, 2008. **138**(8): p. 1512-9.
219. Price, A.A., et al., *Alpha 6 integrins are required for Langerhans cell migration from the epidermis*. J Exp Med, 1997. **186**(10): p. 1725-35.
220. Xu, H., et al., *Role of ICAM-1 molecule in migration of Langerhans cells in skin and regional lymph node*. Eur J Immunol, 2001. **31**(10): p. 3085-93.
221. Yanagihara, S., et al., *EBI1/CCR7 is a new member of dendritic cell chemokine receptor that is up-regulated upon maturation*. J Immunol, 1998. **161**(6): p. 3096-102.

222. Gunn, M.D., et al., *Mice lacking expression of secondary lymphoid organ chemokine have defects in lymphocyte homing and dendritic cell localization.* J Exp Med, 1999. **189**(3): p. 451-60.
223. Ogata, M., et al., *Chemotactic response toward chemokines and its regulation by transforming growth factor-beta1 of murine bone marrow hematopoietic progenitor cell-derived different subset of dendritic cells.* Blood, 1999. **93**(10): p. 3225-32.
224. Saeki, H., et al., *Cutting edge: secondary lymphoid-tissue chemokine (SLC) and CC chemokine receptor 7 (CCR7) participate in the emigration pathway of mature dendritic cells from the skin to regional lymph nodes.* J Immunol, 1999. **162**(5): p. 2472-5.
225. Scandella, E., et al., *Prostaglandin E2 is a key factor for CCR7 surface expression and migration of monocyte-derived dendritic cells.* Blood, 2002. **100**(4): p. 1354-61.
226. Scandella, E., et al., *CCL19/CCL21-triggered signal transduction and migration of dendritic cells requires prostaglandin E2.* Blood, 2004. **103**(5): p. 1595-601.
227. Brueggemeier, R.W. and E.S. Diaz-Cruz, *Relationship between aromatase and cyclooxygenases in breast cancer: potential for new therapeutic approaches.* Minerva Endocrinol, 2006. **31**(1): p. 13-26.
228. Robertson, F.M., et al., *Molecular and pharmacological blockade of EP4 receptor inhibits proliferation and invasion of human inflammatory breast cancer cells.* J Exp Ther Oncol, 2008. **7**(4): p. 299-312.
229. Frasca, L., et al., *CD38 orchestrates migration, survival, and Th1 immune response of human mature dendritic cells.* Blood, 2006. **107**(6): p. 2392-9.
230. Deaglio, S., et al., *CD38/CD31 interactions activate genetic pathways leading to proliferation and migration in chronic lymphocytic leukemia cells.* Mol Med, 2009.
231. Partida-Sanchez, S., et al., *Chemotaxis of mouse bone marrow neutrophils and dendritic cells is controlled by adp-ribose, the major product generated by the CD38 enzyme reaction.* J Immunol, 2007. **179**(11): p. 7827-39.
232. Moll, R., et al., *Endothelial and virgular cell formations in the mammalian lymph node sinus: endothelial differentiation morphotypes characterized by a special kind of junction (complexus adhaerens).* Cell Tissue Res, 2009. **335**(1): p. 109-41.
233. Aurrand-Lions, M., et al., *Heterogeneity of endothelial junctions is reflected by differential expression and specific subcellular localization of the three JAM family members.* Blood, 2001. **98**(13): p. 3699-707.
234. Cera, M.R., et al., *Increased DC trafficking to lymph nodes and contact hypersensitivity in junctional adhesion molecule-A-deficient mice.* J Clin Invest, 2004. **114**(5): p. 729-38.
235. Ovali, E., et al., *Active immunotherapy for cancer patients using tumor lysate pulsed dendritic cell vaccine: a safety study.* J Exp Clin Cancer Res, 2007. **26**(2): p. 209-14.
236. Santin, A.D., et al., *Expression of surface antigens during the differentiation of human dendritic cells vs macrophages from blood monocytes in vitro.* Immunobiology, 1999. **200**(2): p. 187-204.
237. Meidenbauer, N., R. Andreesen, and A. Mackensen, *Dendritic cells for specific cancer immunotherapy.* Biol Chem, 2001. **382**(4): p. 507-20.
238. Wierecky, J., et al., *Immunologic and clinical responses after vaccinations with peptide-pulsed dendritic cells in metastatic renal cancer patients.* Cancer Res, 2006. **66**(11): p. 5910-8.
239. de Vries, I.J., et al., *Maturation of dendritic cells is a prerequisite for inducing immune responses in advanced melanoma patients.* Clin Cancer Res, 2003. **9**(14): p. 5091-100.

240. Verdijk, P., et al., *Limited amounts of dendritic cells migrate into the T-cell area of lymph nodes but have high immune activating potential in melanoma patients*. Clin Cancer Res, 2009. **15**(7): p. 2531-40.
241. Kim, S., et al., *Vaccination with recombinant adenoviruses and dendritic cells expressing prostate-specific antigens is effective in eliciting CTL and suppresses tumor growth in the experimental prostate cancer*. Prostate, 2009. **69**(9): p. 938-48.
242. Palmer, D.H., et al., *A phase II study of adoptive immunotherapy using dendritic cells pulsed with tumor lysate in patients with hepatocellular carcinoma*. Hepatology, 2009. **49**(1): p. 124-32.
243. Curti, A., et al., *Phase I/II clinical trial of sequential subcutaneous and intravenous delivery of dendritic cell vaccination for refractory multiple myeloma using patient-specific tumour idiotype protein or idiotype (VDJ)-derived class I-restricted peptides*. Br J Haematol, 2007. **139**(3): p. 415-24.
244. Toh, H.C., et al., *Clinical Benefit of Allogeneic Melanoma Cell Lysate-Pulsed Autologous Dendritic Cell Vaccine in MAGE-Positive Colorectal Cancer Patients*. Clin Cancer Res, 2009. **15**(24): p. 7726-7736.
245. Van Driessche, A., et al., *Clinical-grade manufacturing of autologous mature mRNA-electroporated dendritic cells and safety testing in acute myeloid leukemia patients in a phase I dose-escalation clinical trial*. Cytotherapy, 2009. **11**(5): p. 653-68.
246. De Vries, I.J., et al., *Effective migration of antigen-pulsed dendritic cells to lymph nodes in melanoma patients is determined by their maturation state*. Cancer Res, 2003. **63**(1): p. 12-7.
247. Nestle, F.O., et al., *Vaccination of melanoma patients with peptide- or tumor lysate-pulsed dendritic cells*. Nat Med, 1998. **4**(3): p. 328-32.
248. Jonuleit, H., et al., *A comparison of two types of dendritic cell as adjuvants for the induction of melanoma-specific T-cell responses in humans following intranodal injection*. Int J Cancer, 2001. **93**(2): p. 243-51.
249. Lesimple, T., et al., *Immunologic and clinical effects of injecting mature peptide-loaded dendritic cells by intralymphatic and intranodal routes in metastatic melanoma patients*. Clin Cancer Res, 2006. **12**(24): p. 7380-8.
250. West, E., et al., *Clinical grade OK432-activated dendritic cells: in vitro characterization and tracking during intralymphatic delivery*. J Immunother, 2009. **32**(1): p. 66-78.
251. Adema, G.J., et al., *Migration of dendritic cell based cancer vaccines: in vivo veritas?* Curr Opin Immunol, 2005. **17**(2): p. 170-4.
252. Mhawech-Fauceglia, P., et al., *Submission of the entire lymph node dissection for histologic examination in gynecologic-oncologic specimens. Clinical and pathologic relevance*. Gynecol Oncol, 2009. **115**(3): p. 354-6.
253. Baumjohann, D. and M.B. Lutz, *Non-invasive imaging of dendritic cell migration in vivo*. Immunobiology, 2006. **211**(6-8): p. 587-597.
254. Francia, G., et al., *Long-term progression and therapeutic response of visceral metastatic disease non-invasively monitored in mouse urine using beta-human choriogonadotropin secreting tumor cell lines*. Mol Cancer Ther, 2008. **7**(10): p. 3452-9.
255. Long, C.M. and J.W. Bulte, *Tracking of cellular therapies using magnetic resonance imaging*. Expert Opin Biol Ther, 2009. **9**(3): p. 293-306.
256. Kiessling, F., *Noninvasive cell tracking*. Handb Exp Pharmacol, 2008(185 Pt 2): p. 305-21.

257. Hon, H. and J. Jacob, *Tracking dendritic cells in vivo: insights into DC biology and function*. Immunol Res, 2004. **29**(1-3): p. 69-80.
258. Bulte, J.W., *In vivo MRI cell tracking: clinical studies*. AJR Am J Roentgenol, 2009. **193**(2): p. 314-25.
259. de Vries, I.J., et al., *Magnetic resonance tracking of dendritic cells in melanoma patients for monitoring of cell therapy*. Nat Biotechnol, 2005. **23**(11): p. 1407-13.
260. Olasz, E.B., et al., *Fluorine-18 labeled mouse bone marrow-derived dendritic cells can be detected in vivo by high resolution projection imaging*. J Immunol Methods, 2002. **260**(1-2): p. 137-48.
261. Nair, S., et al., *Injection of immature dendritic cells in adjuvant-treated skin obviates need for ex vivo maturation*. J Immunol. **171**(11): p. 6275-82.
262. Awasthi, S., et al., *Efficacy of antigen 2/proline-rich antigen cDNA-transfected dendritic cells in immunization of mice against Coccidioides posadasii*. J Immunol, 2005. **175**(6): p. 3900-6.
263. Eggert, A.A., et al., *Analysis of dendritic cell trafficking using EGFP-transgenic mice*. Immunol Lett, 2003. **89**(1): p. 17-24.
264. Viehl, C.T., et al., *A tat fusion protein-based tumor vaccine for breast cancer*. Ann Surg Oncol, 2005. **12**(7): p. 517-25.
265. Troy, T., et al., *Quantitative comparison of the sensitivity of detection of fluorescent and bioluminescent reporters in animal models*. Mol Imaging, 2004. **3**(1): p. 9-23.
266. Jackson, G.D., et al., *Principles of Magnetic Resonance Imaging*, in *Magnetic Resonance in Epilepsy (Second Edition)*. 2005, Academic Press: Burlington. p. 17-28.
267. Bulte, J.W.M., *Magnetic nanoparticles as markers for cellular MR imaging*. Journal of Magnetism and Magnetic Materials, 2005. **289**: p. 423-427.
268. Liu, W. and J.A. Frank, *Detection and quantification of magnetically labeled cells by cellular MRI*. Euro Jour of Rad., 2009. **70**(2): p. 258-264.
269. Herschman, H.R., *PET reporter genes for noninvasive imaging of gene therapy, cell tracking and transgenic analysis*. Critical Reviews in Oncology/Hematology, 2004. **51**(3): p. 191-204.
270. Heyn, C., et al., *Detection threshold of single SPIO-labeled cells with FIESTA*. Magn Reson Med, 2005. **53**(2): p. 312-20.
271. Dekaban, G.A., et al., *Semiquantitation of mouse dendritic cell migration in vivo using cellular MRI*. J Immunother, 2009. **32**(3): p. 240-51.

## CHAPTER 2 LABELLING DENDRITIC CELLS WITH SPIO HAS IMPLICATIONS FOR SUBSEQUENT *IN VIVO* MIGRATION AS ASSESSED WITH CELLULAR MRI

### 2.1 Introduction

Dendritic cells (DCs) serve as important mobile sentinels for the immune system, acting as a link between the innate and adaptive immune responses [1]. Specifically, DCs are capable of directly activating NK cells [2, 3] and naïve T and B lymphocytes cells in secondary lymphoid tissues [1, 4-6], leading to the generation of antigen-independent and antigen-specific immune responses, respectively. Due to their ability to directly mediate immune responses, clinical application of DCs has focused on cell-based immunotherapies, one such being the DC-based cancer vaccine [1, 7-9].

Most commonly, antigen-loaded DCs are generated *ex vivo* and administered to the patient in order to generate an *in vivo*, antigen-specific T cell-mediated immune response [9]. While early phase clinical trials have proven the safety and feasibility of DC-based cancer vaccines, the quality and efficacy of the immune responses generated by these vaccines have yet to reach their full potential [7]. In order for DCs to carry out their function, migration of clinically relevant numbers of these cells to T cell-rich areas of the lymph node (LN) is crucial [4]. For this reason, the efficacy of DC-based cancer vaccines depends largely on the migration of *ex vivo*-generated DCs to target LNs. Therefore, an important step in improving vaccine efficacy is to determine the region(s) to

which the *ex vivo*-generated DCs are migrating to once they are administered to the patient.

So as to safely and non-invasively track DC migration in clinical patients, an alternative to the conventional, highly-invasive histological analysis is required. While there are several modalities capable of non-invasively tracking cells *in vivo* [10], cellular magnetic resonance imaging (MRI) is a modality that is non-toxic, non-invasive, and sensitive enough to detect low numbers of cells in humans [11, 12]. Furthermore, cellular MRI provides the advantage of producing 3-dimensional (3-D) high-resolution images with excellent soft-tissue contrast. For these reasons, this pre-clinical study employed cellular MRI as the method to track the *in vivo* migration of *ex vivo*-generated bone marrow-derived DCs in a mouse model. In addition to targeted migration, the amount of *in vivo* DC migration to LNs can generally be correlated with the strength of antigen-specific T cell responses generated [13-15]. As a result, quantification of MR signal was also carried out to determine if there was a correlation between *in vivo* migration and peptide-specific T cells generated following our adoptive transfer studies.

In order to distinguish cells of interest from surrounding tissues, Feridex<sup>®</sup> or FeREX<sup>®</sup>, both superparamagnetic iron oxide (SPIO) nanoparticles, have been used by our laboratory to label DCs *in vitro*. SPIO particles produce areas of hypointensity on T2-weighted MR images [16]. MRI has previously been shown to be sensitive enough to detect single cells labelled with SPIO [17]. While the use of SPIO has no effect on DC viability or phenotype, *in vivo* migration experiments from our laboratory [18] and one other have shown that DCs labelled with SPIO seem to migrate less efficiently to LNs compared to untreated



control DCs. This study aims to elucidate the reason as to why labelling DCs *in vitro* with SPIO is affecting their subsequent *in vivo* migration to target LNs. Since SPIO particles are 80-120 nm in diameter, it was initially hypothesized that labelling DCs with SPIO mechanically impedes DCs from crossing reticulo-endothelial cell junctions to effectively enter the lymphatics. In our initial published study [18], labelling efficiency of DCs with SPIO was not taken into consideration. Consequently, the efficiency of labelling DCs with SPIO was first determined. A more detailed examination of the phenotypic and functional properties of SPIO-labelled (SPIO<sup>+</sup>) DC specifically compared to those DCs which remained unlabelled (SPIO<sup>-</sup>) was carried out. Results from these studies outline important points to consider relevant for optimizing the use of MR contrast agents in combination with cellular MRI for accurately tracking and quantifying migration of clinical-grade DCs in cancer patients.

## **2.2 Methods**

### **2.2.1 Animal Care**

C57BL/6 male mice (6 – 12 weeks) were obtained from Charles River Laboratories Inc. (Kingston, NY) and housed in pathogen-free conditions in the Robarts Barrier Facility at the Robarts Research Institute (London, Ontario) until use. All experiments were undertaken in accordance with Animal Care guidelines with the approval from the Animal Use Subcommittee at the University of Western Ontario, London, Ontario (Appendix 1).

### **2.2.2 Reagents**

RPMI 1640 culture medium (Gibco, Burlington, ON) was supplemented with 10% FBS (Hyclone, Logan, USA), 5 mL penicillin-streptomycin, 5 mL L-glutamine, 5 mL MEM non-essential amino acids, 5 mL sodium pyruvate, 5 mL HEPES buffer solution, and 500 µL 2-mercaptoethanol (Invitrogen, Burlington, ON). Hanks buffered salt solution (HBSS) was from Invitrogen and bovine serum albumin (BSA) was purchased from Sigma-Aldrich (Oakville, ON). Mouse GM-CSF and IL-4 were gifts from Dr. Peta O'Connell (Robarts Research Institute, London, ON) originally provided by Schering-Plough (Kenilworth, NJ). Feridex<sup>®</sup> I.V. was obtained from Berlex Laboratories (Wayne, NJ) and FeREX<sup>®</sup> was obtained from BioPAL (Worcester, MA). Bangs Beads<sup>®</sup>, which are the micron-sized paramagnetic iron oxide (MPIO) particles we used for transwell experiments (see below), were obtained from Bangs Laboratories Inc. (Fishers, IN). Anti-mouse CD11c, CD86, CD80, CD40, and I-A<sup>B</sup> fluorescence conjugated antibodies were purchased from Becton, Dickinson and Co. (BD, Mississauga, ON). Anti-mouse

CD3 $\epsilon$ , CD4, CD8 $\alpha$ , CD11b, CD54, CCR7, H2K<sup>b</sup>-SIINFEKL, IFN- $\gamma$ , and biotinylated CD36 and CD38 antibodies and secondary antibodies (SA-PE) were purchased from eBioscience (San Diego, CA). H2K<sup>b</sup>-SIINFEKL tetramer was purchased from BD. Respective isotype controls were purchased from the same companies. Normal goat serum (NGS) was purchased from Sigma-Aldrich.

### **2.2.3 Generation of murine bone marrow-derived DCs and MRI contrast agent labelling**

DCs used for these experiments were mouse bone marrow-derived DCs (BMDCs). DCs were prepared and enriched as previously described [18]. Briefly, bone marrow cells were collected from the femurs and tibias of C57BL/6 mice and red blood cells (RBCs) were lysed using ACK lysis buffer. B220 and MHC II positive cells were depleted using antibody-specific complement-mediated lysis (Cedarlane Laboratories, Burlington, ON). Cells were re-suspended at a concentration of  $3 \times 10^5$  cells/mL in complete RPMI 1640 medium and cultured for 4 days at 37°C in the presence of GM-CSF (4 ng/mL media) and IL-4 (1000 U/mL media). Enrichment of DCs was performed on day 4 using HistoDenz (13.5% w/v, Sigma-Aldrich) gradient centrifugation.

Feridex or FeREX labelling (both at 200  $\mu$ g Fe/mL) was carried out after enrichment during overnight incubation at 37°C for 20 hours. For those experiments requiring DCs labelled with MPIO (Bangs Beads), 12.5  $\mu$ M was added to each well of cell suspension and cells were cultured overnight, as above. Cells were left untreated to serve as a control in all cases.

#### **2.2.4 Magnetic separation of SPIO<sup>+</sup> DCs from SPIO<sup>-</sup> DCs**

On day 5, SPIO-treated DCs were collected and washed 3 times with cold HBSS + 0.1% bovine serum albumin (BSA) to remove any free iron nanoparticles. This SPIO-treated DC population contained DCs which were effectively labelled with SPIO nanoparticles (SPIO<sup>+</sup>) and DCs which remained unlabelled (SPIO<sup>-</sup>). Therefore the total SPIO-treated DC population which remains un-separated will be referred to as the mixed-SPIO (SPIO<sup>mix</sup>) DC population. SPIO<sup>mix</sup> DCs were transferred to a 12x75 mm tube and re-suspended in 2.5 mLs of cold HBSS + 0.1% BSA. This tube was put in an EasySep magnet (StemCell Technologies, Vancouver, BC) for 5 minutes. The supernatant was poured off into a second 12x75 mm tube, which was subsequently put into the EasySep magnet to collect any remaining SPIO-labelled DCs. The supernatant containing unlabelled (SPIO<sup>-</sup>) cells was poured off into another 12x75 mm tube. SPIO-labelled (SPIO<sup>+</sup>) cells were pooled together and both cell populations were counted to determine the efficiency of SPIO labelling. Magnetic separation of MPIO-labelled (MPIO<sup>+</sup>) from MPIO-unlabelled (MPIO<sup>-</sup>) DCs was performed using the same protocol.

#### **2.2.5 Detection of surface antigens**

Cells were collected from overnight cultures on day 5 and washed 3X with HBSS + 0.1% BSA to remove free SPIO nanoparticles. Cells were blocked in 1 mL of cold HBSS + 0.1% BSA using 5% v/v of normal goat serum (NGS) and washed 1X following a 20 minute incubation at 4°C (on ice). CCR7 staining was carried out first at 20°C (room temperature) for 20 minutes. Cells were washed 1X and stained with all other required antibodies at 4°C (on ice) in the dark. Flow

cytometry was performed using a FACSCalibur (BD) and analyzed with CellQuest Pro software (BD) or FloJo software (Tree Star Inc., Ashland, OR).

### **2.2.6 Luminex<sup>®</sup> cytokine assays**

The Luminex<sup>®</sup> Cytokine Mouse 10-plex Panel antibody detection kit, reagents, and buffers were obtained from Invitrogen. The Luminex<sup>®</sup> kit was used according to the manufacturer's protocol in order to analyze the cytokine profiles of supernatants collected from overnight cultures of DCs that received SPIO. Supernatants collected from untreated DCs served as controls. All incubations were carried out at room temperature in the dark. Briefly, test samples or serial dilutions of kit standards were incubated for 2 hours with the Luminex detection beads provided. After washing with assay wash buffer, biotinylated primary antibody was added and incubated for 1 hour. Following another wash step, SA-PE was added to wells and plates were incubated for an additional 30 minutes. After a final three washes, plates were analyzed using the Luminex 100 plate reader and IS 2.3 Software (both from Luminex Corporation, Austin, TX). A minimum of 400 events (beads) was collected for each cytokine per sample, and mean fluorescence intensities were obtained.

### **2.2.7 Labelling DCs with PKH**

DCs were collected from day 5 cultures and washed 1X in cold PBS. The membrane intercalating dyes, PKH26 (red) or PKH67 (green), were used to label DCs for histological detection as per manufacturer's instructions (Sigma-Aldrich). Briefly, DCs were re-suspended in Diluent C (Sigma Aldrich) and incubated with  $2 \times 10^{-6}$  M of PKH dye for no longer than 3 minutes. Excess dye was removed by

incubating cells with 2 mLs of FBS for 1 minute. Cells were washed 3X, first in complete RPMI 1640 media, then in HBSS + 0.1% BSA, and finally in PBS. Following the final wash, cells were re-counted and re-suspended accordingly in PBS for adoptive transfer.

### **2.2.8 Adoptive transfer of DCs**

PKH-labelled DCs were adoptively transferred via subcutaneous injection into the hind footpads of C57BL/6 mice. Briefly, either  $3 \times 10^5$  or  $1 \times 10^6$  PKH-labelled SPIO<sup>mix</sup> or SPIO<sup>+</sup> DCs were administered into the right hind footpads (n=4). Untreated DCs labelled with PKH were administered to the contralateral footpads of all mice at the appropriate dose to serve as a control.

### **2.2.9 Magnetic resonance imaging of DC migration and analysis**

Mice were imaged 1, 2, 3, 4, or 7 days post DC adoptive transfer. MRI was performed using a 1.5T clinical scanner (GE Medical Systems, Milwaukee, WI) with a custom gradient-coil insert as previously described [18]. Briefly, a 3-D FIESTA (GE Medical Systems) imaging pulse sequence was used, and scan times averaged 23 minutes. Spatial resolution was  $200 \mu\text{m}^3$  and slice thickness was 200  $\mu\text{m}$ . MR images were analyzed for LN volume, signal void volume, and fractional signal loss (FSL).

LN volumes and void volumes were determined using segmentation of MR images. First, areas of interest (popliteal LN or area of void) were manually selected. To accurately delineate the areas of interest, a threshold was manually set either at the interface of fat and LN tissue contrast or at the interface of LN

tissue and signal void contrast. The volume (in mm<sup>3</sup>) was then obtained based on selected segmentations and thresholds.

In order to calculate the FSL for each mouse, the mean signal intensity of the control popliteal node ( $\bar{S}_{control}$ ) was obtained and the lowest signal intensity was obtained from the contralateral node, which contained the negative SPIO signal ( $S_{void}$ ). The following calculation was used to derive the FSL:

$$FSL = \frac{\Delta S}{\bar{S}_{control}} = \frac{S_{void} - \bar{S}_{control}}{\bar{S}_{control}}$$

### 2.2.10 LN removal and cryostat sectioning

Following MR scans, mice were euthanized by CO<sub>2</sub> inhalation and popliteal LNs (behind the knee) were removed. LNs were fixed overnight in 4% v/v paraformaldehyde (PFA) at 4°C, LNs were cryo-protected by overnight incubations in increasing concentrations of sucrose (10%, 20%, and 30%) to prepare them for cryostat sectioning. For sectioning, LNs were embedded in optimal cutting temperature (OCT) compound (Sakura Finetek U.S.A. Inc., Torrance, CA) and serial sections were cut using a Leica CM3050S cryostat (Leica Microsystems, Wetzlar, Germany). Serial sections were cut and mounted onto sets of four alternating Plus Slides (VWR International, Westchester, PA). Slides were cover-slipped with PBS for histological analysis.

### 2.2.11 Histological analysis and quantification

To verify MR results of *in vivo* DC migration, conventional histological analysis of DC migration was performed. To determine the area of PKH26 (red) or PKH67 (green) fluorescence, digital images (10X) were collected using an Olympus

BX50 microscope (Olympus America Inc. Centre Valley, PA) equipped with an Olympus IX50 digital camera (Olympus America Inc.) and digital morphometry (Image Pro v4.0) was used to determine the area of fluorescence (DCs): area of interest (popliteal LN). Briefly, the area of interest was selected manually and a threshold for fluorescence intensity was set such that any PKH<sup>+</sup> fluorescence above this threshold was included in the area of fluorescence.

### **2.2.12 *In vitro* migration assays**

5x10<sup>5</sup> of untreated, SPIO<sup>mix</sup>, SPIO<sup>+</sup>, SPIO<sup>-</sup>, MPIO<sup>mix</sup> (Bangs Beads), MPIO<sup>+</sup>, or MPIO<sup>-</sup> DCs were added to the top chamber of 3.0 μM pore transwell inserts (BD Falcon) in a total volume of 250 μL of complete medium. 600 μL of complete medium was added to the bottom chambers. The bottom chambers of negative control wells received only complete media while positive control wells were supplemented with CCR7 ligands CCL19 and CCL21 (each at 100 ng/mL; PeproTech, Rocky Hill NJ). Chemokinetic control wells received 100 ng/mL of both CCL19 and CCL21 in the top and bottom chambers.. Each treatment was performed in triplicate. Plates were incubated for 2 hours at 37°C and cells were collected from top and bottom chambers. Surface staining for CD11c and CD86 was carried out. CountBrite Absolute Counting Beads (Invitrogen) were added to cells and flow cytometry was used to count 2000 bead events. CellQuest Software (BD) was used to determine the number of CD11c<sup>+</sup> cells based on the number of beads acquired. The number of DCs that migrated was determined by subtracting the number of CD11c<sup>+</sup> cells which migrated in negative control wells from the number of CD11c<sup>+</sup> cells which migrated in positive control wells.



### **2.2.13 Preparation and administration of SIINFEKL-loaded DCs**

DCs were prepared as above. On day 4 following HistoDenz enrichment, DCs were labelled with SPIO (200 µg of Fe/mL FeREX). Some DCs were left untreated (UT DC) to serve as appropriate control cells. On day 5, DCs were given 10 µg/mL of SIINFEKL (MHC I specific ovalbumin peptide, amino acids 257-265; Sigma-Aldrich) peptide for two hours prior to cell collection. UT DC and SPIO<sup>mix</sup> DCs not given SIINFEKL peptide served as flow cytometric controls. DCs given hemagglutinin (HA) peptide (Sigma-Aldrich) served as non-specific control cells for flow cytometry. Cells were collected and washed 2X using room temperature HBSS + 0.1% BSA, and finally washed 1X in room temperature PBS. Some SIINFEKL-SPIO<sup>mix</sup> DCs were magnetically separated to obtain SIINFEKL-SPIO<sup>+</sup> DCs. SPIO<sup>+</sup> DCs served as the corresponding flow cytometric control.

SIINFEKL-UT, SIINFEKL-SPIO<sup>mix</sup>, and SIINFEKL-SPIO<sup>+</sup> DCs were re-suspended in room temperature PBS at a concentration of  $25 \times 10^6$  cells/mL for adoptive transfer into C57BL/6 mice. Briefly, mice were subcutaneously administered SIINFEKL-SPIO<sup>mix</sup> DCs or SIINFEKL-SPIO<sup>+</sup> DCs to both hind footpads ( $10^6$  DCs per footpad, n=4). SIINFEKL-UT DCs served as the control and  $10^6$  were administered to both hind footpad of 4 mice.

### **2.2.14 Preparation of single cell suspensions from LNs**

Two weeks following the adoptive transfer of SIINFEKL-UT, SIINFEKL-SPIO<sup>mix</sup>, or SIINFEKL-SPIO<sup>+</sup> DCs, mice were euthanized (CO<sub>2</sub> inhalation) and both popliteal LNs were removed and pooled together for each mouse. LN pairs were

digested by incubation at 37°C for 45 minutes in DNase (0.5 µg/mL, Sigma-Aldrich) and collagenase type V (1 µg/mL, Sigma-Aldrich). Cells were washed 1X in cold HBSS + 0.1% BSA, counted, and re-suspended in complete medium at a concentration of  $10 \times 10^6$  cells/mL for use in intracellular cytokine staining (ICS) and T cell proliferation experiments.

### **2.2.15 Tetramer and intracellular cytokine staining**

$2 \times 10^6$  LN cells from each mouse were plated in 96 well plates. Cells were either given media (untreated control), hemagglutinin (HA) peptide (non-specific peptide control, Sigma-Aldrich), concanavalin (Con) A (positive control, 10 µg/mL, BD), or SIINFEKL peptide (10 µg/mL). Each treatment was repeated in triplicate.

For intracellular staining (ICS) of IFN- $\gamma$  positive cells, LN cells were incubated for 2 hours at 37°C. Brefeldin A (3 µg/mL, eBioscience) was then added to cells and plates were incubated for an additional 3 hours. Cells were collected and washed 2X with cold HBSS + 0.1% BSA. Surface antibody staining for CD3 $\epsilon$ , CD4, and CD8 $\alpha$  was carried out as per usual. Cells were then fixed for 20 minutes in fixative (eBioscience) and washed 2X in permeabilization buffer (eBioscience). Following a 30 minute room temperature staining incubation for IFN- $\gamma$  in 100 µL of permeabilization buffer, cells were washed, re-suspended in 300 µL of flow cytometry buffer (eBioscience), and analyzed using flow cytometry.

For analysis of SIINFEKL-specific T cells, medium was supplemented with recombinant mouse IL-2 (0.2 ng/mL; PeproTech) and cells were incubated for 2

days at 37°C. LN cells were collected and washed 2X with cold HBSS + 0.1% BSA. Subsequently, cells were stained for surface expression of CD3ε, CD4, and CD8α and MHC I-SIINFEKL specific tetramer as per usual. Analysis was carried out using flow cytometry.

#### **2.2.16 Statistical analysis**

All data were expressed as means and standard error means. Statistical significance was determined using a repeated measures ANOVA followed by a post-hoc Tukey's Test. Differences were considered significant if  $p < 0.05$ . Correlation between MRI and histological data was determined using a linear rank correlation.

## 2.3 Results

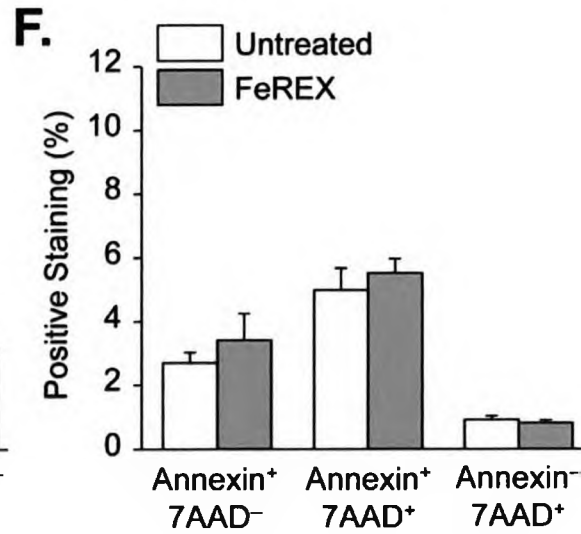
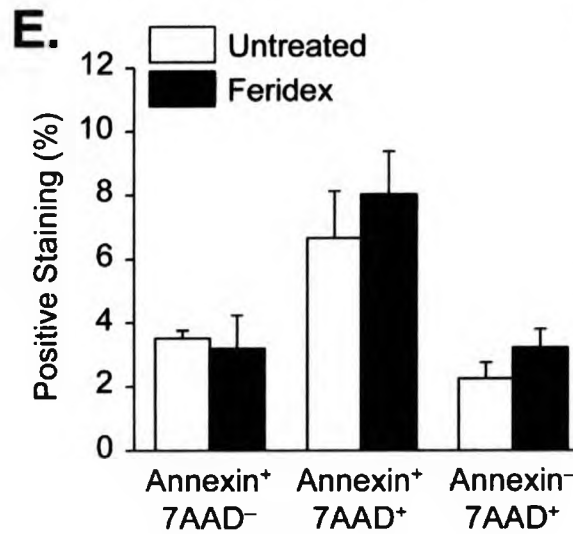
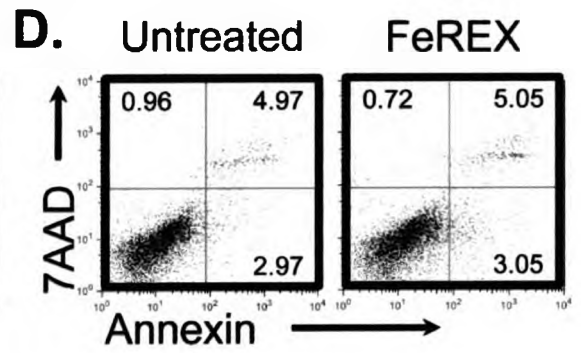
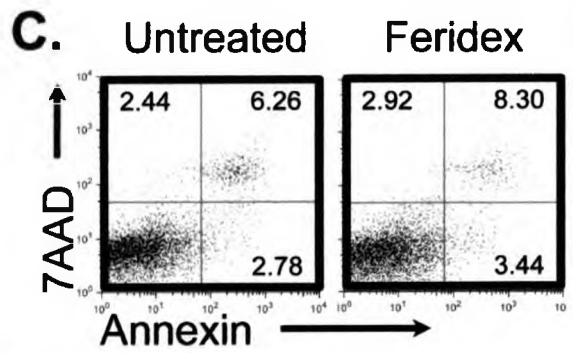
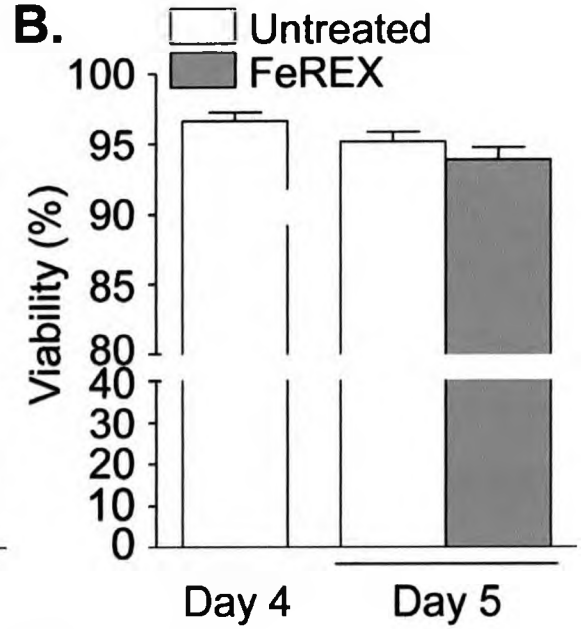
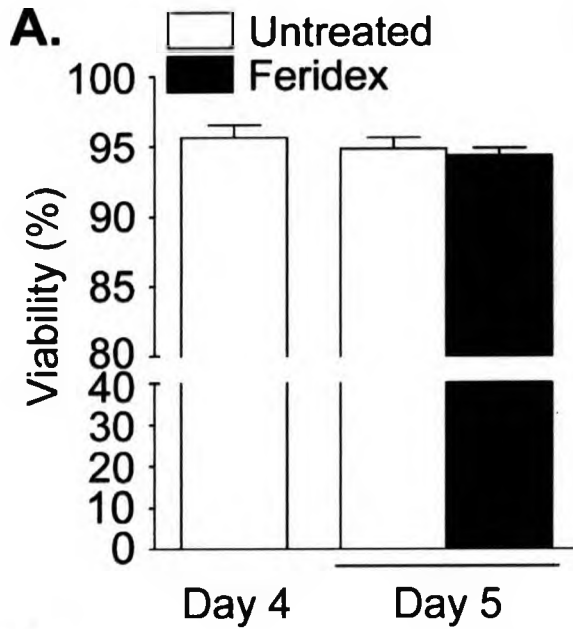
### 2.3.1 SPIO labelling does not affect DC viability




It was first necessary to confirm that SPIO labelling does not significantly affect DC viability *in vitro*, which could have accounted for the differences in subsequent *in vivo* migration between SPIO<sup>mix</sup> and untreated control DCs (UT DCs). The Trypan Blue exclusion assay and Annexin/7AAD staining were used as means to evaluate the viability of SPIO<sup>mix</sup> DCs. Trypan Blue exclusion assays indicated there was no significant cell loss due to overnight Feridex (Fig. 2.1A) or FeREX (Fig. 2.1B) labelling compared to UT DCs on day 5. Furthermore, neither Feridex (Fig. 2.1E) nor FeREX (Fig. 2.1F) induced additional cell death due to apoptosis (Annexin<sup>+</sup>7AAD<sup>-</sup> or Annexin<sup>+</sup>7AAD<sup>+</sup>) or necrosis (Annexin<sup>-</sup>7AAD<sup>+</sup>) ( $p > 0.05$ ).

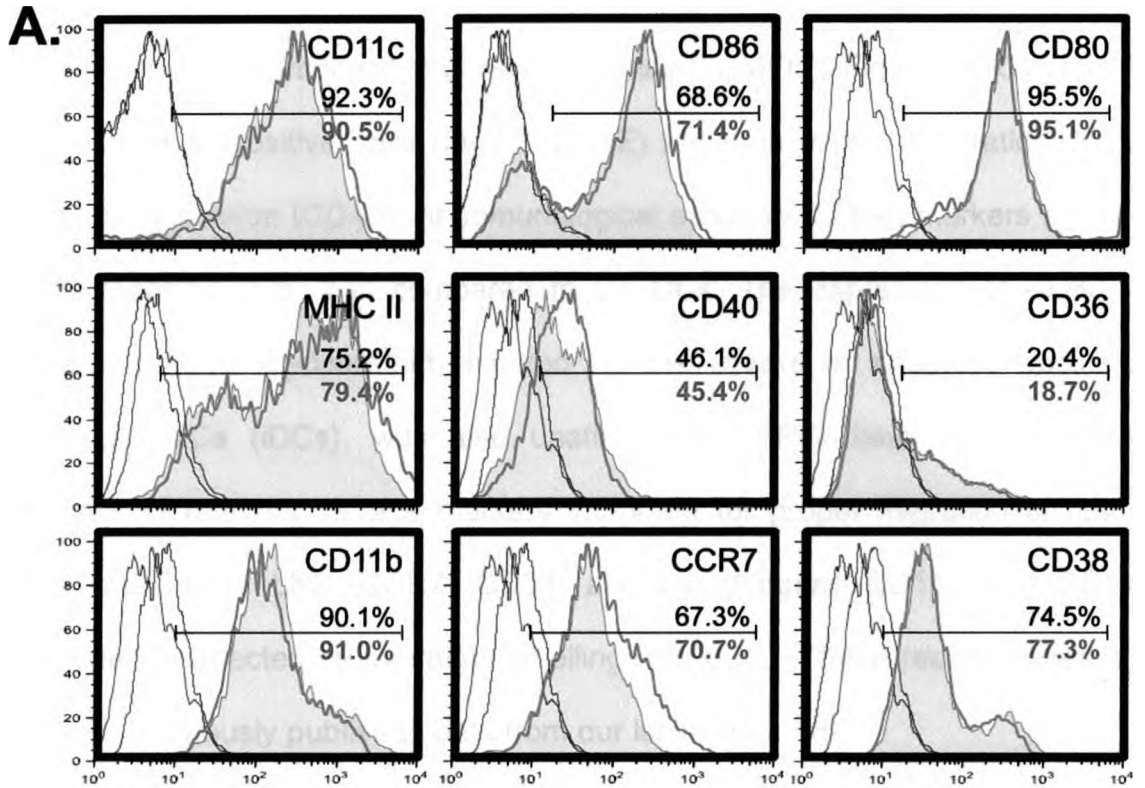
### 2.3.2 DC phenotype and cytokine profiles remain largely unaffected following *in vitro* labelling with SPIO

DC viability prior to injection did not provide an explanation for the effect SPIO has on *in vivo* migration. As a result, the next step taken was to analyze the surface expression of several DC markers known to be important for normal cell signalling and function, including migration, to ensure SPIO was not affecting their surface expression. Flow cytometry was used to determine the level of surface expression (mean fluorescence intensity [MFI]) and percentage of positive cells (Fig. 2.2). The expression of CD11c and CD86, important cluster of differentiation (CD) surface markers used to identify and characterize the maturation of mouse DCs, were not affected by either Feridex or FeREX.

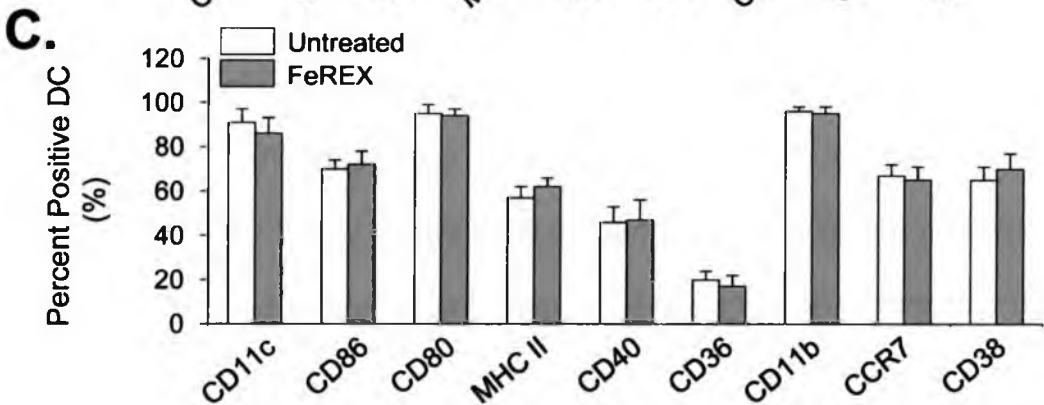
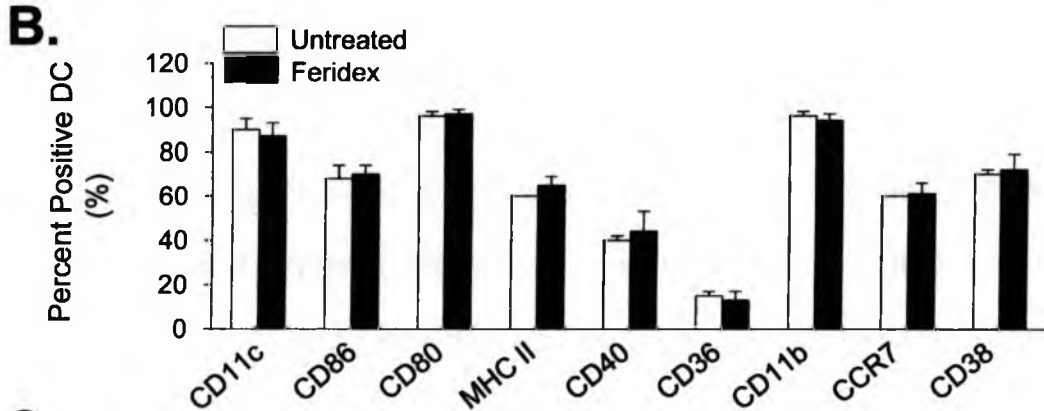
**Figure 2.1 SPIO has no significant effect on DC viability, nor does it induce premature cell death.** Trypan Blue exclusion assays were used to assess viability of DCs following overnight labelling with SPIO (either Feridex or FeREX, both at 200  $\mu$ M). (A, B) SPIO has no significant effect on DC viability according to results obtained on day 5 compared to untreated (UT) cells. (C, D) Annexin/7AAD staining of DCs labelled with SPIO was carried out in order to determine if labelling resulted in abnormal levels of cell death due to apoptosis (Annexin+) or necrosis (7AAD+). Representative flow cytometry figures of Annexin/7AAD staining are shown. According to the data, neither Feridex (E) nor FeREX (F) significantly increased the rate of apoptosis or necrosis. Data are means  $\pm$  SE and are representative of at least 3 independent experiments. Differences are not significant ( $p > 0.05$ ).



**Figure 2.2 SPIO does not significantly affect the phenotypic characteristics of DCs *in vitro*.** Following overnight culture in the presence of SPIO (200  $\mu$ M of Feridex or FeREX), cells were stained for relevant DC surface markers and analyzed using flow cytometry. (A) Representative histograms of either untreated (UT) DC (  ) and FeREX-labelled cells (  ). Isotype controls are shown as  . Numbers above gate are the mean fluorescence intensities (MFIs)  $\pm$  SE of the UT control cells. Bold numbers below the gate are the MFIs  $\pm$  SE of the cells treated with FeREX. CD11c histograms are gated on viable DC. All other histograms are gated on viable CD11c+ cells. Histograms are representative of 3 independent experiments. Neither (B) Feridex nor (C) FeREX labelling affected the percentage of positive cells for any of the DC surface markers examined compared to respective untreated (UT) control cells.



MFI →





Furthermore, the DCs did not exhibit any significant changes in the surface expression levels (mean fluorescence intensities [MFIs]; Fig. 2.2B, C) or in the percentage of positive cells (Figs. 2.2D, E) for each of the maturation (CD80, MHC II), activation (CD40), or immunological synapse (CD54) markers following SPIO labelling (Fig. 2.2) compared to UT DCs. The expression of CD36, an integral surface glycoprotein required for the uptake of apoptotic bodies by immature DCs (iDCs), was also unaffected by SPIO labelling. Importantly, analysis of relevant surface markers important for proper migration of mature DCs (mDCs) to LNs (CCR7, CD38, and the integrins CD11b and CD11c) remained unaffected by overnight labelling with SPIO. These results correspond with our previously published data from our laboratory [18].

Another important aspect of DC biology relevant to *in vivo* migration is the appropriate secretion of cytokines. As a result, we investigated if SPIO labelling had an effect on DC cytokine secretion *in vitro*. DC supernatants were collected following overnight incubation with SPIO nanoparticles (Feridex or FeREX) and Luminex assay analysis of mouse cytokines (IL-1 $\beta$ , IL-2, IL-4, IL-5, IL-6, IL-10, IL-12, IFN- $\gamma$ , TNF- $\alpha$ , and GM-CSF) was performed. Supernatants collected from overnight UT DCs were used as the control. As our DC culture protocol requires the addition of mouse IL-4 and GM-CSF, detected levels of these cytokines were not reflective of DC production and they were therefore excluded from our final analysis. Luminex assay analysis did not detect any significant differences in the levels of cytokines produced following Feridex (Fig. 2.3A) or FeREX (Fig. 2.3B) labelling compared to UT DCs. Importantly, all cytokines were secreted at picomolar amounts, much lower than those required for biological function by

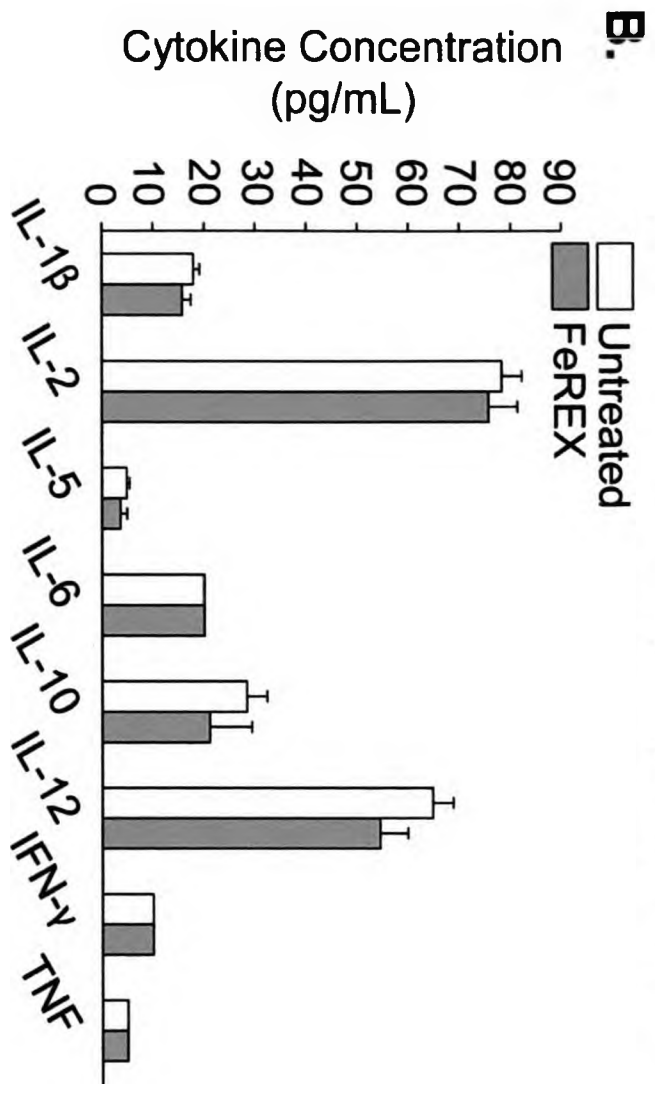
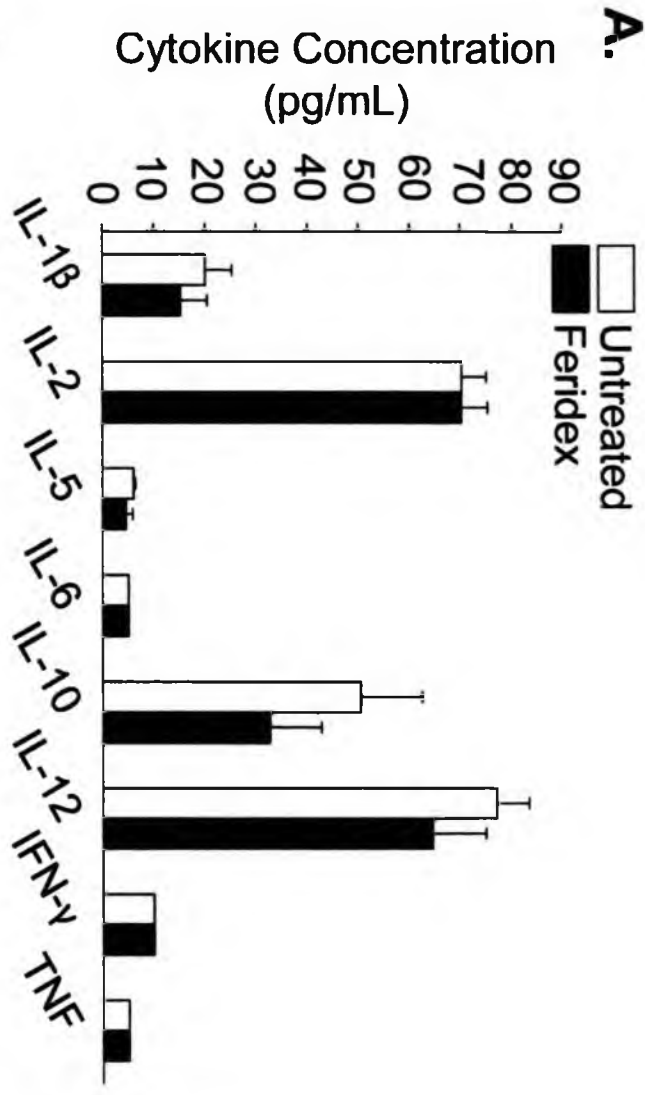
cells (i.e. nanomolar levels [19]). Therefore neither Feridex nor FeRex leads to inappropriate DC activation with respect to cytokine production.

### **2.3.3 Magnetic separation of SPIO<sup>+</sup> from SPIO<sup>-</sup> DCs exposes differences in phenotypic surface marker expression and functional cytokine secretion**

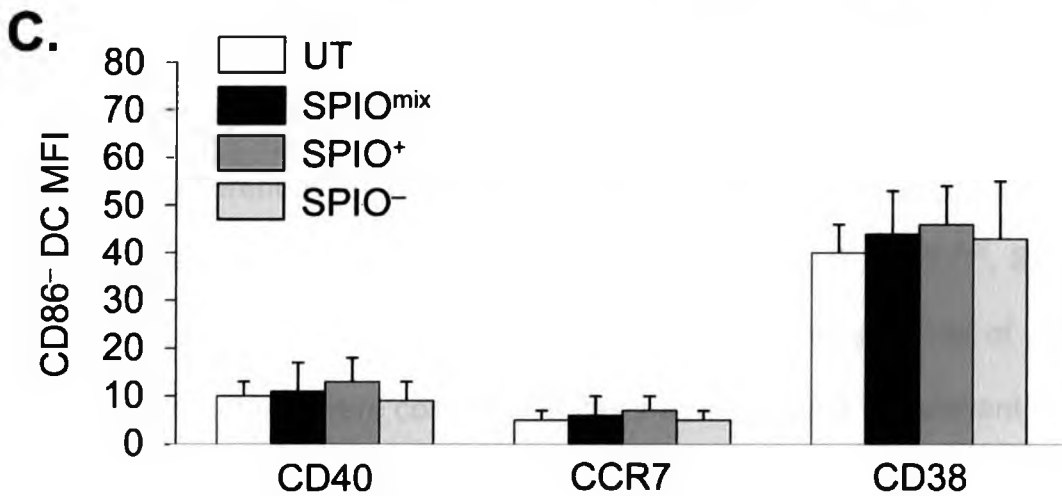
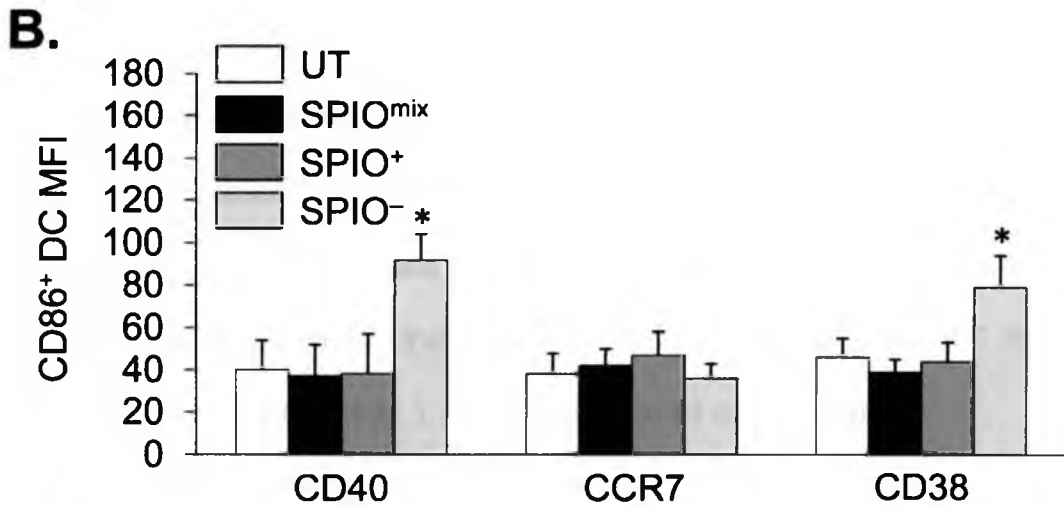
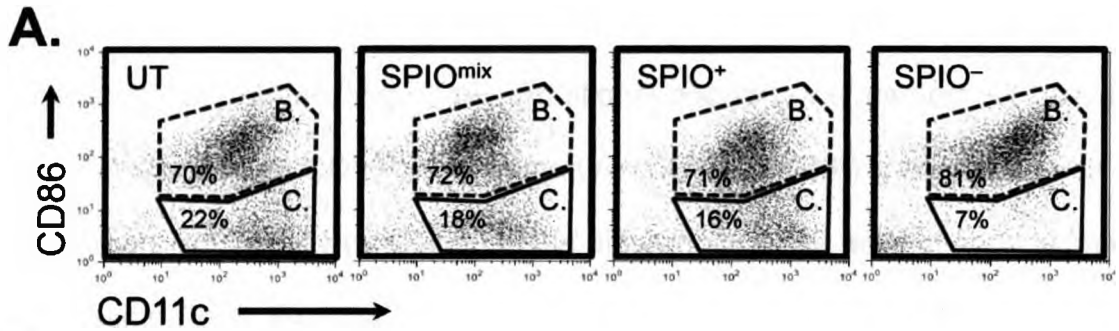
There were no detectable significant differences between our SPIO<sup>mix</sup> and UT DC populations, as described above. We were able to determine that SPIO labelling was not 100% efficient, as some DCs remained unlabelled after overnight culture. It was proposed that the presence of two subpopulations within the overall SPIO<sup>mix</sup> population (SPIO-labelled [SPIO<sup>+</sup>] and SPIO-unlabelled [SPIO<sup>-</sup>]) could have some biological significance, although it was unknown to what extent. In order to further investigate the biology of the two subpopulations, a method to separate the SPIO<sup>+</sup> from the SPIO<sup>-</sup> DCs was required. Magnetic separation of the SPIO<sup>mix</sup> DC population into SPIO<sup>+</sup> and SPIO<sup>-</sup> DCs was carried out using an EasySep magnetic column. First, the percentage of DCs that were taking up SPIO nanoparticles (Feridex or FeREX) following overnight culture was determined. After counting the number of cells in each subpopulation, the labelling efficiencies of DCs *in vitro* following overnight culturing with Feridex and FeREX were found to average 85.6±1.1% and 78.2±2.6% respectively (n=5; Appendix 2).

Due to the presence of SPIO<sup>+</sup> and SPIO<sup>-</sup> DCs in our *in vitro* cultures, it was relevant to determine if there were any phenotypic differences between these two cell populations. SPIO<sup>+</sup> and SPIO<sup>-</sup> DCs were analyzed using flow cytometry (Fig. 2.4) for the surface expression of several phenotypic markers

**Figure 2.3 SPIO does not significantly affect cytokine secretion of DCs *in vitro*.** Following overnight culture in the presence of SPIO (Feridex or FeREX, both at 200  $\mu$ M), supernatants from cultures were collected and secreted cytokines were analyzed using Luminex assays. Supernatants collected from UT DCs served as a control. Neither (A) Feridex nor (B) FeREX nanoparticles affect the cytokine secretion of DCs *in vitro* compared to UT controls. Data are means  $\pm$  SE and are representative of 3 independent experiments. Differences are not significant ( $p > 0.05$ ).



**Figure 2.4. Magnetic separation of DCs reveals the presence of two phenotypically distinct subpopulations within the SPIO<sup>mix</sup> DC population.** Following overnight culture with SPIO (FeREX), SPIO<sup>mix</sup> DCs were collected and magnetically separated in order to examine several surface markers of the labelled (SPIO<sup>+</sup>) and unlabelled (SPIO<sup>-</sup>) subpopulations. (A) Representative dot plots for untreated (UT), SPIO<sup>mix</sup>, SPIO<sup>+</sup>, and SPIO<sup>-</sup> DC populations are shown. Dot plots are gated on viable cells and mature CD11c<sup>+</sup>CD86<sup>+</sup> (dashed gate, B.) and immature CD11c<sup>+</sup>CD86<sup>-</sup> (solid gate, C.) DC populations are gated on. The data presented is representative of 4 independent experiments. Analysis for mean fluorescence intensities of (B) mature DC and (C) immature DC populations was carried out for several DC surface markers. Cell surface marker analysis determined that CD11c<sup>+</sup>CD86<sup>+</sup> (mature) SPIO<sup>-</sup> DCs express more CD40 (DC activation marker) and CD38 (required for DC migration) compared to other DC populations. Data are mean MFIs  $\pm$  SE from 4 independent experiments. Means are significantly different from mean control MFIs if  $p < 0.05$  (\*).



important for DC maturation (CD86), activation (CD40), and migration (CCR7, CD38). SPIO<sup>mix</sup> and UT DCs were used as the control populations. Analysis of the data indicates that, on average, 30% more SPIO<sup>-</sup> DCs express CD86 when compared to all other DC populations (UT, SPIO<sup>mix</sup>, and SPIO<sup>+</sup>), indicating SPIO<sup>-</sup> DCs are more mature (Fig. 2.4A). Additional analysis was carried out based on the mature (CD11c<sup>+</sup>CD86<sup>+</sup>) and immature (CD11c<sup>+</sup>CD86<sup>-</sup>) groups for each cell population, specifically by looking at the differences in the level of surface marker expression (MFI) for CD40, CD38, and CCR7 (Fig. 2.4B). It is first important to note that CCR7 and CD40, usually up-regulated following DC maturation and activation, respectively, were only detected on CD11c<sup>+</sup>CD86<sup>+</sup> mature DCs (mDCs) in all cases. The percentage of CCR7<sup>+</sup> cells did not change significantly between groups. The surface expression (MFI) of CD40 increased by 2.2X on the SPIO<sup>-</sup> mDCs. Finally, the level of CD38 expression on SPIO<sup>-</sup> mDCs was found to be up-regulated by 1.7X compared to all other groups.

Flow cytometric data indicate the existence of two phenotypically distinct sub-populations of DCs within the SPIO<sup>mix</sup> DC population. As a result, we assessed the cytokine profiles of the SPIO<sup>+</sup> and SPIO<sup>-</sup> DCs to determine if there were any differences in regards to their *in vitro* cytokine profiles. Following magnetic separation of SPIO<sup>+</sup> from SPIO<sup>-</sup> DCs, 2x10<sup>6</sup> UT, SPIO<sup>mix</sup>, SPIO<sup>+</sup> and SPIO<sup>-</sup> DCs were put back into overnight culture (in the absence of additional SPIO). Supernatants were collected on day 6 and analyzed for relevant cytokines using Luminex assays. Data show no significant differences in secretion of IL-1 $\beta$ , IL-2, IL-5, IL-6, IL-10, IL-12, or IFN- $\gamma$  (Fig. 2.5). Significantly less TNF was detected in the supernatant of SPIO<sup>-</sup> DCs compared to all other groups.

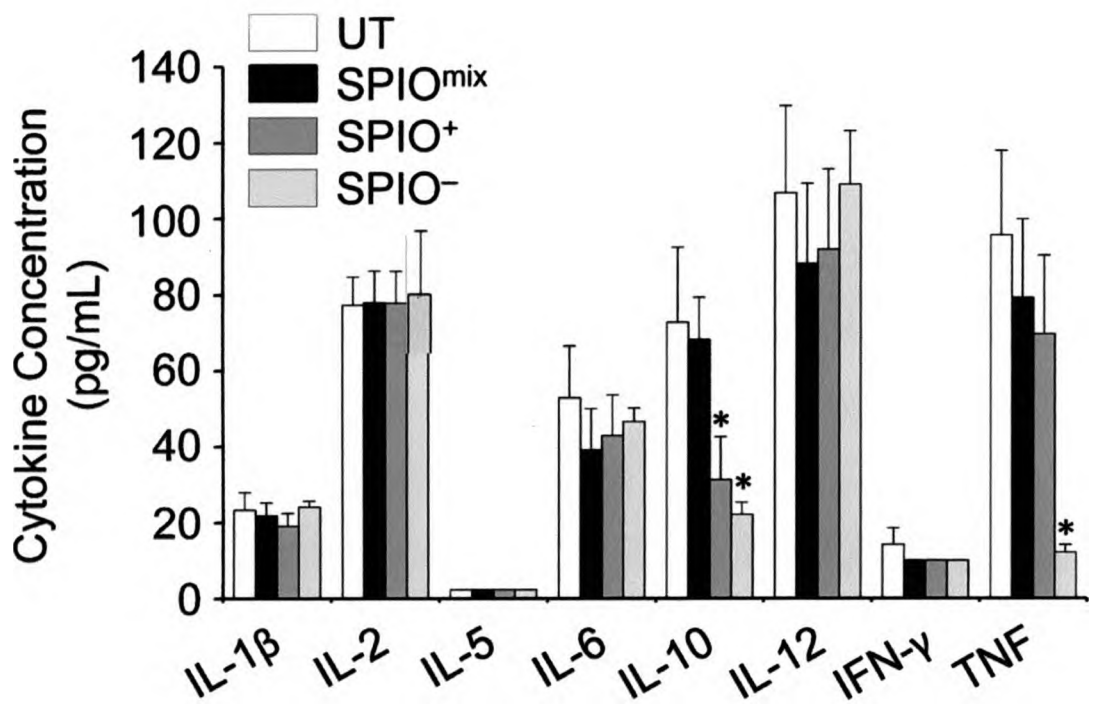
Furthermore, significantly less IL-10 was detected in the supernatants of SPIO<sup>+</sup> and SPIO<sup>-</sup> DCs. Still, amount of all cytokines released by all DC populations were below the biological levels required for normal function *in vivo*. Thus, at least with respect to cytokine expression, the SPIO<sup>+</sup> and SPIO<sup>-</sup> subpopulations were not substantially different from each other with the exception of TNF cytokine secretion, or from the UT and SPIO<sup>mix</sup> DCs, with the exception of and IL-10.

#### **2.3.4 UT DCs migrate preferentially to popliteal LNs compared to SPIO<sup>+</sup> DCs *in vivo***

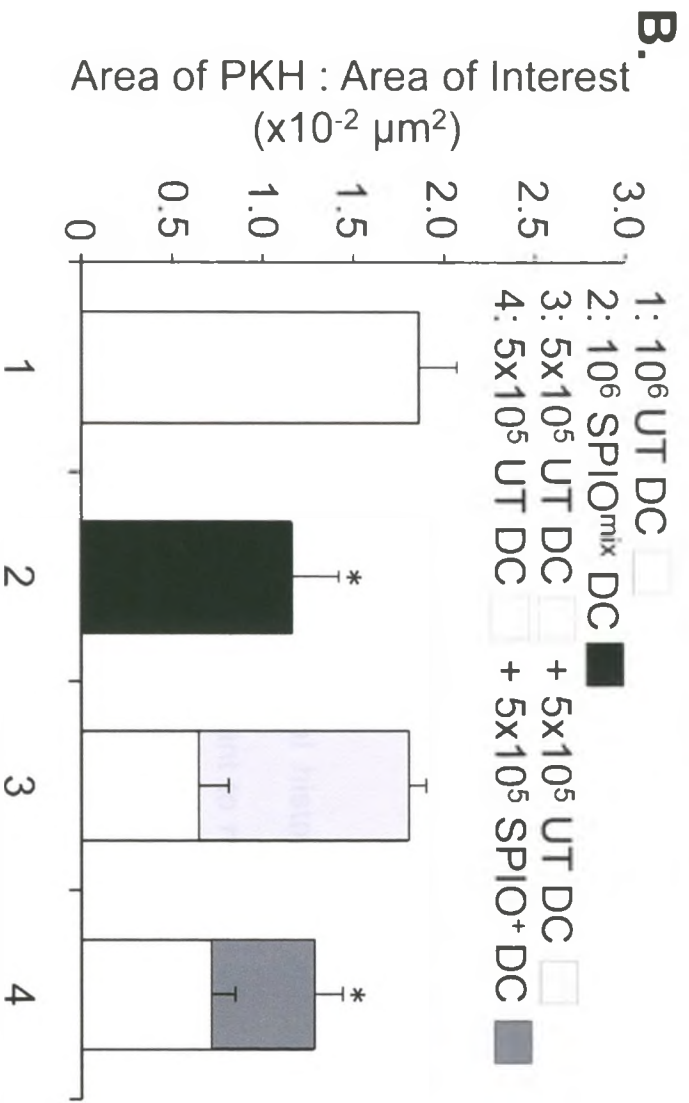
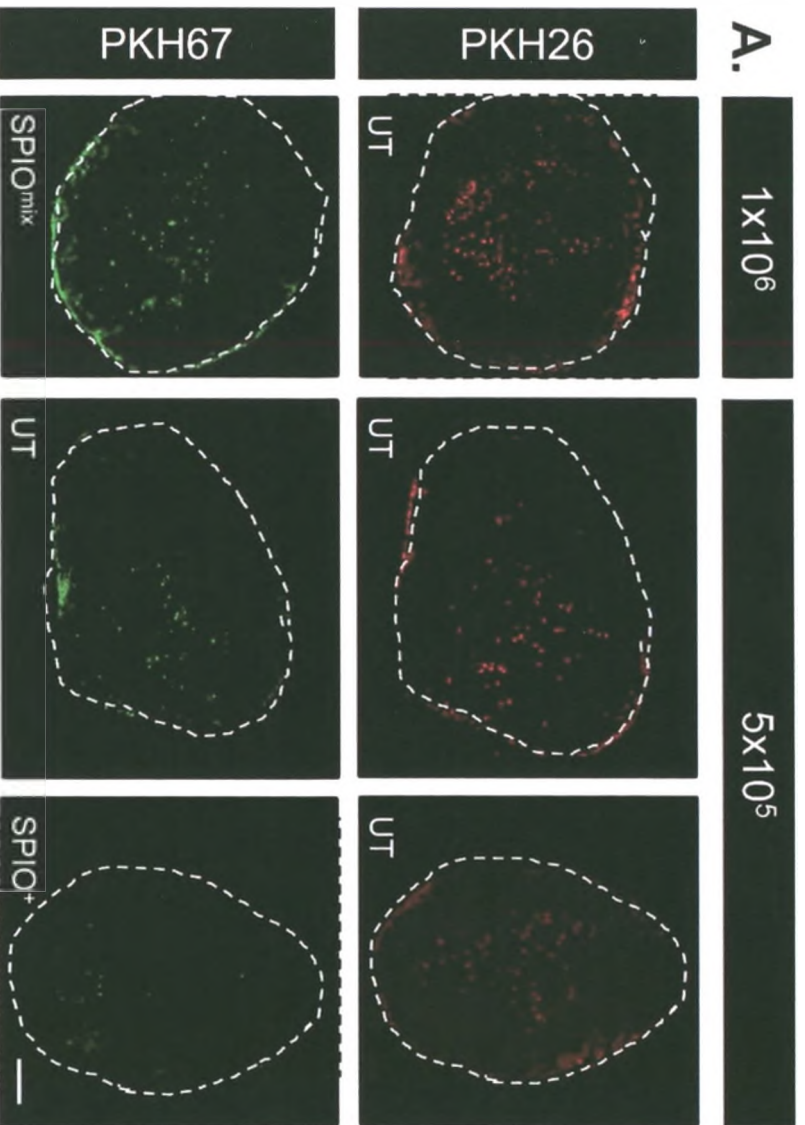
Due to the characterization of two phenotypically distinct sub-populations of DCs in our SPIO<sup>mix</sup> DC population, it was possible that this was affecting the overall migration of the SPIO<sup>mix</sup> DC population *in vivo*. Therefore we set out to investigate if there was competition between SPIO<sup>+</sup> and UT DCs to popliteal LNs. We investigated this by performing a mixing experiment, in which SPIO<sup>+</sup> DCs were magnetically separated from SPIO<sup>-</sup> DCs and injected in an equal 1:1 ratio with UT DCs (for a total of 10<sup>6</sup> cells) (Fig. 2.6). Results showed that the PKH26<sup>+</sup>UT DC: PKH67<sup>+</sup>UT DC (control mixture) had the same amount of migration as the UT control group ( $p > 0.50$ ). Furthermore, the PKH67<sup>+</sup>SPIO<sup>+</sup> DC: PKH26<sup>+</sup>UT DC mixture migrated to the same extent as the SPIO<sup>mix</sup> DC group. Results from this experiment indicated that from the injected mixture of the same amount of UT DCs migrated in both 1:1 mixtures of PKH67<sup>+</sup>UT DC: PKH26<sup>+</sup>UT DC and PKH67<sup>+</sup>SPIO<sup>+</sup> DC: PKH26<sup>+</sup>UT DC (while portion of columns 3 and 4). However, upon mixing SPIO<sup>+</sup> DCs with UT DCs, the amount of PKH67<sup>+</sup>DCs



**Figure 2.5. The cytokine profile of SPIO<sup>-</sup> DCs is different than that of UT, SPIO<sup>mix</sup>, and SPIO<sup>+</sup> DCs.** DCs were labelled with SPIO (FeREX) as per usual. On day 5, cells were collected, washed of free SPIO, magnetically separated, and equal numbers of each DC population were put back into overnight culture. On day 6, supernatants from UT, SPIO<sup>mix</sup>, SPIO<sup>+</sup>, and SPIO<sup>-</sup> DCs were collected and analyzed for cytokines using Luminex assays. IL-10 secretion by SPIO<sup>+</sup> and SPIO<sup>-</sup> DC populations is lower compared to UT and SPIO control groups. SPIO<sup>-</sup> DCs also secrete lower levels of TNF compared to UT, SPIO<sup>mix</sup>, and SPIO<sup>+</sup> DC populations. Data are means  $\pm$  SE and are representative of three independent experiments. Differences from controls are significant if  $p < 0.05$  (\*).



**Figure 2.6. *In vivo* migration suggests unlabelled DCs migrate to LNs preferentially compared to SPIO<sup>+</sup> DCs.** DCs were labelled with SPIO (Feridex) and stained with PKH67 (green) for *in vivo* detection. Untreated (UT) DCs were labelled with PKH26 (red) or PKH67 to serve as a control. Either 10<sup>6</sup> PKH67<sup>+</sup>SPIO<sup>mix</sup> DCs or 10<sup>5</sup> PKH26<sup>+</sup>UT + 10<sup>5</sup> PKH67<sup>+</sup>SPIO<sup>+</sup> DCs were injected subcutaneously into the right hind footpads of C57BL/6 mice. 10<sup>6</sup> PKH26<sup>+</sup>UT DCs or 10<sup>5</sup> PKH26<sup>+</sup>UT + 10<sup>5</sup> PKH67<sup>+</sup>UT DCs were injected as the respective controls into contralateral footpads. Two days post injection popliteal LNs were removed and analyzed using digital morphometry to determine the area of PKH<sup>+</sup> fluorescence. (A) Representative images of LNs for each group. Scale bar = 500  $\mu$ m. (B) SPIO<sup>+</sup> DC migration to popliteal LNs decreases when mixed with UT DCs. Data are means SE; n=4. Differences are significant from respective controls if p<0.05 (\*).



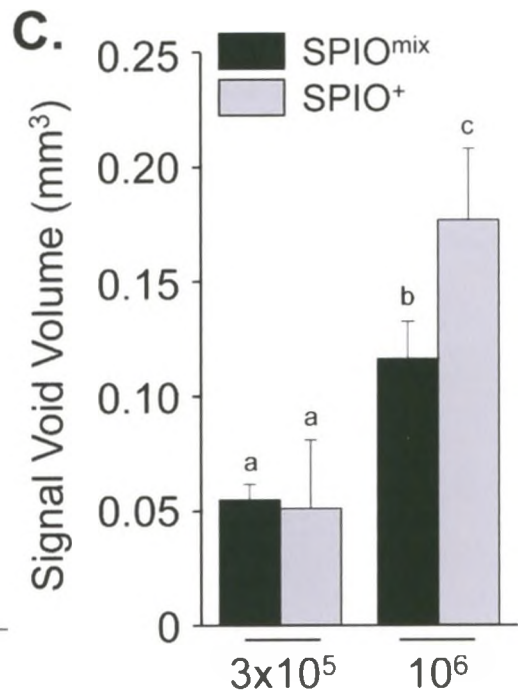
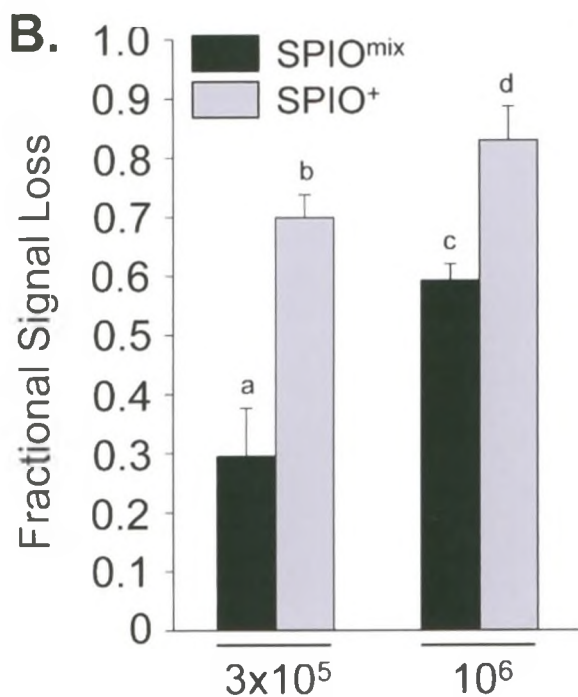
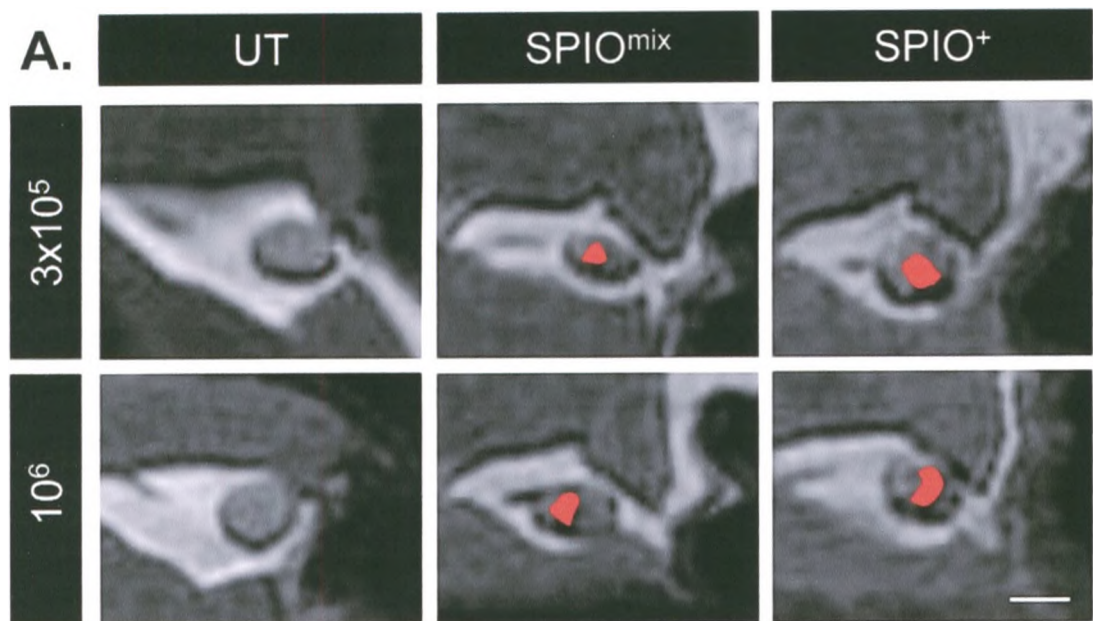
migrating to the LNs in the 1:1 DC mixtures was reduced by 50% (shaded portion of columns 3 and 4) (Fig. 2.6B). This suggests that SPIO<sup>+</sup> DCs do not migrate as well as UT DCs.

### **2.3.5 SPIO<sup>+</sup> DCs migrate more efficiently compared to SPIO<sup>mix</sup> DCs**

Based on the results following our *in vivo* competition experiment, we hypothesized that magnetically separating SPIO<sup>+</sup> DC from SPIO<sup>-</sup> DC before adoptive transfer would increase the number of SPIO<sup>+</sup> DCs that reach the LN. Adoptive transfer of either  $3 \times 10^5$  or  $10^6$  PKH<sup>+</sup>SPIO<sup>mix</sup> DCs or PKH<sup>+</sup>SPIO<sup>+</sup> DCs was performed and MRI and histological analysis was performed. Upon analysis of fractional signal loss (FSL) of the MR images obtained at two days post-injection, data revealed an increase in signal hypointensity for PKH<sup>+</sup>SPIO<sup>+</sup> DCs compared to PKH<sup>+</sup>SPIO<sup>mix</sup> DCs (Fig 2.7). Signal void volumes and LN volumes were also higher in mice given PKH<sup>+</sup>SPIO<sup>mix</sup> DCs (Fig 2.7C, D). Together, these data suggest that SPIO<sup>+</sup> DCs migrate more efficiently than SPIO<sup>mix</sup> DCs *in vivo*. Dose responsive increases in both FSL and signal void volume were also observed with increasing numbers of DC injected. This suggested that more cells migrated to the popliteal LNs.

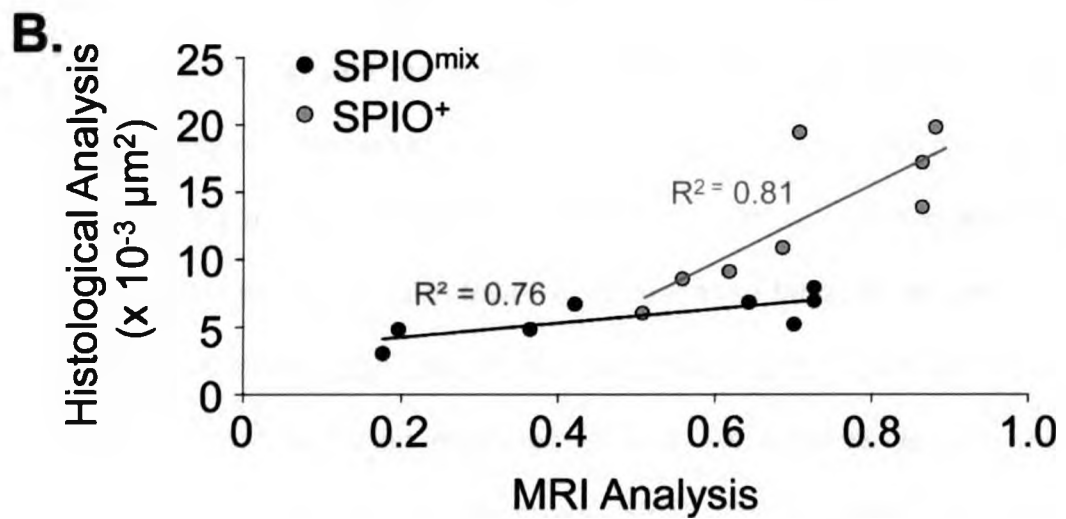
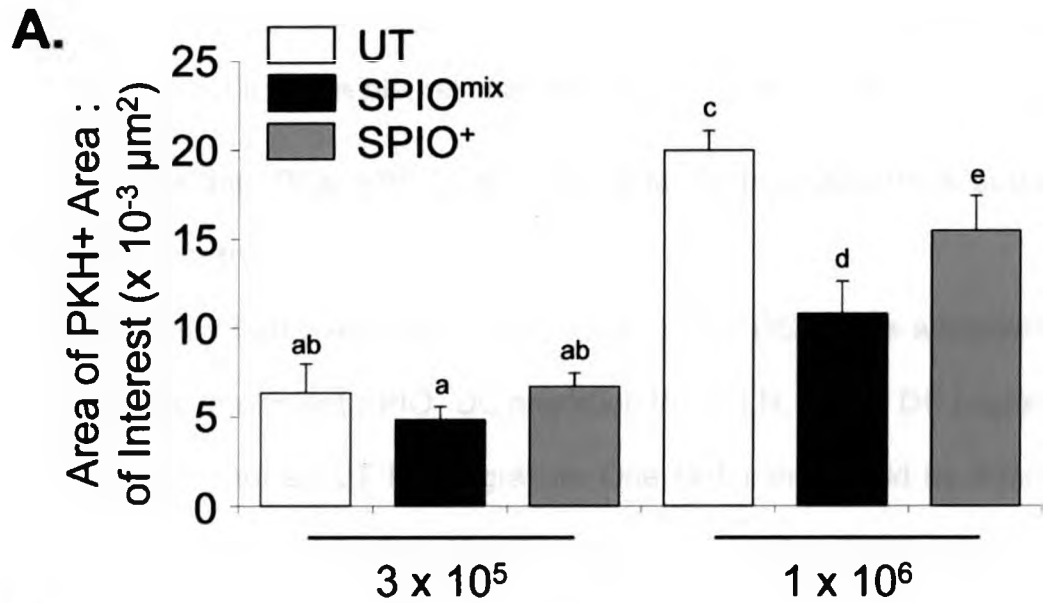
In order to verify MRI data, conventional histological analysis was performed on the popliteal LNs. First, it is important to note that DCs from all groups were located in the central, T cell-rich paracortical regions of the LNs. After calculating the ratio between the area of PKH<sup>+</sup> fluorescence: area of interest (popliteal LN), it was determined that SPIO<sup>+</sup> DCs migrated more efficiently compared to SPIO<sup>mix</sup> DCs, which supported our MR data (Fig. 2.8B).

**Figure 2.7. *In vivo* migration assays of DC migration demonstrate SPIO<sup>+</sup> DC migration is more efficient than SPIO<sup>mix</sup> DCs.** Either  $3 \times 10^5$  or  $1 \times 10^6$  PKH<sup>+</sup>SPIO<sup>+</sup> DCs or PKH<sup>+</sup>SPIO<sup>mix</sup> DCs were adoptively transferred via subcutaneous injection of the hind footpad of C57BL/6 mice. PKH<sup>+</sup> DCs were injected into the contralateral hind footpads to serve as a control. MRI scans were carried out 2 days post injection. (A) Representative MR images of popliteal LNs for each group. Scale bar = 2 mm. MR images were analyzed for (B) fractional signal loss (FSL) and (C) signal void volume. SPIO<sup>+</sup> DCs generate greater signal loss compared to SPIO<sup>mix</sup> DCs. Data are means  $\pm$  SE and n=4 for each group. If superscript letters are different, then means are significantly different ( $p < 0.05$ ).



**Figure 2.8. Histological analysis of *in vivo* DC migration correlates with MRI data.** Either  $3 \times 10^5$  or  $1 \times 10^6$  PKH<sup>+</sup>SPIO<sup>mix</sup> DCs or PKH<sup>+</sup>SPIO<sup>+</sup> DCs were adoptively transferred to C57BL/6 mice via subcutaneous hind footpad injections. PKH<sup>+</sup> DCs were injected into the contralateral hind footpads to serve as the control. Popliteal LNs were removed following MRI scans and were analyzed for the area of PKH<sup>+</sup> fluorescence. **(A)** SPIO<sup>+</sup> DC migration is less efficient than untreated (UT) DC migration but more efficient than SPIO<sup>mix</sup> DC migration *in vivo*. Data are means  $\pm$  SE and n=4 for each group. Differences are significant if superscript letters are different ( $p < 0.05$ ). **(B)** A positive, linear correlation between MRI analysis and histological analysis (correlation slope  $> 0$ ) is demonstrated for SPIO<sup>mix</sup> and SPIO<sup>+</sup> DC populations. The correlation between MR and histological data for SPIO<sup>+</sup> DC is stronger ( $R^2 > 0.81$ ) than that for the SPIO<sup>mix</sup> DC population ( $R^2 > 0.76$ ).





However, SPIO<sup>+</sup> DCs still migrated less efficiently to LNs compared to UT control DCs. Furthermore, it was determined that there was a positive linear correlation between FSL and histological data (Fig 2.8). Therefore, we concluded that MRI analysis of *in vivo* DC migration is correlative to conventional histological analysis, making it a feasible, reliable method for tracking *in vivo* cell migration.

### **2.3.6 Labelling DCs with SPIO mechanically impedes their subsequent migration *in vitro***




Although magnetically separating SPIO<sup>+</sup> from SPIO<sup>-</sup> DC before adoptive transfer resulted in more efficient SPIO<sup>+</sup> DC migration to the LN, SPIO<sup>+</sup> DC migration was still not as efficient as UT DC migration. One factor that could be affecting the migration of SPIO<sup>+</sup> DCs to LNs, however, is that the SPIO nanoparticle is impeding the DCs from migrating through the reticulo-endothelial cell junctions. We decided to investigate the effect of contrast agent nanoparticle size on DC migration using *in vitro* assays for two reasons. First, *in vitro* assays remove some of the biological complexities associated with *in vivo* migration studies. Second, *in vitro* assays require fewer cells. Because labelling efficiency of DCs with SPIO is relatively high, insufficient numbers of SPIO<sup>-</sup> DCs are obtained to allow us to investigate their migration *in vivo*. As a result, *in vitro* migration assays allowed us to directly compare SPIO<sup>+</sup> DC migration to SPIO<sup>-</sup> DC migration. Bangs Beads<sup>®</sup>, which are micron-sized iron oxide particles (MPIOs) averaging 0.9  $\mu\text{M}$  in diameter, were used as a larger nanoparticle comparison to SPIO (Fig. 2.9). First, results with the *in vitro* assays supported our *in vivo* migration assays (Fig. 2.8). Specifically, SPIO<sup>+</sup> DC migration efficiency was

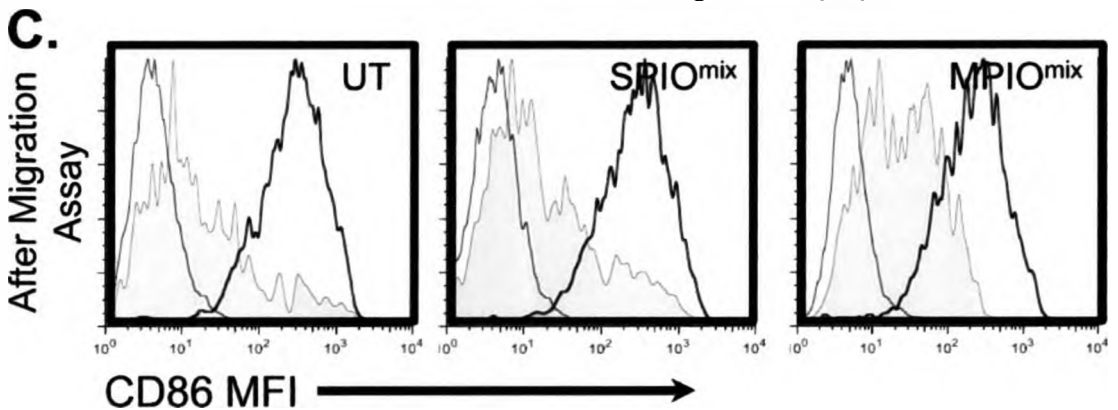
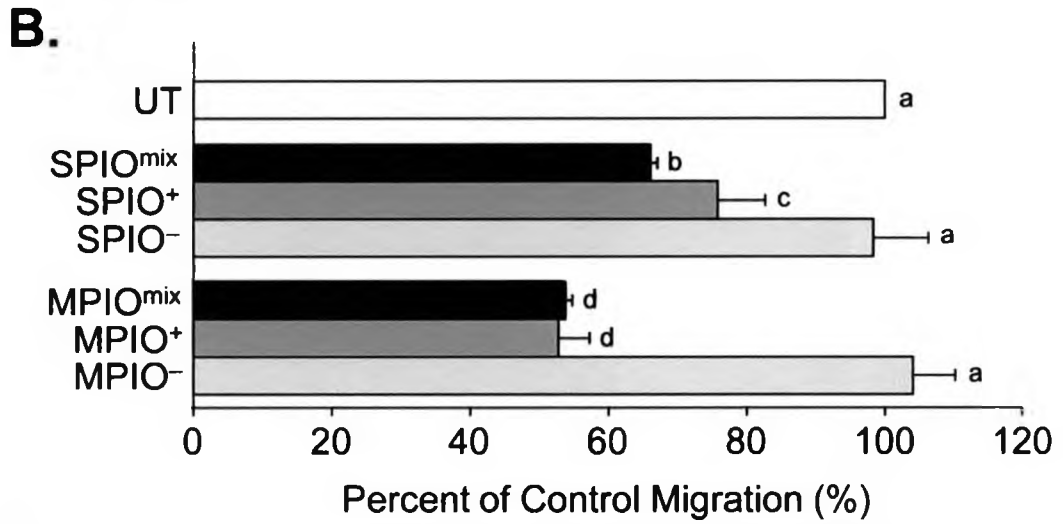
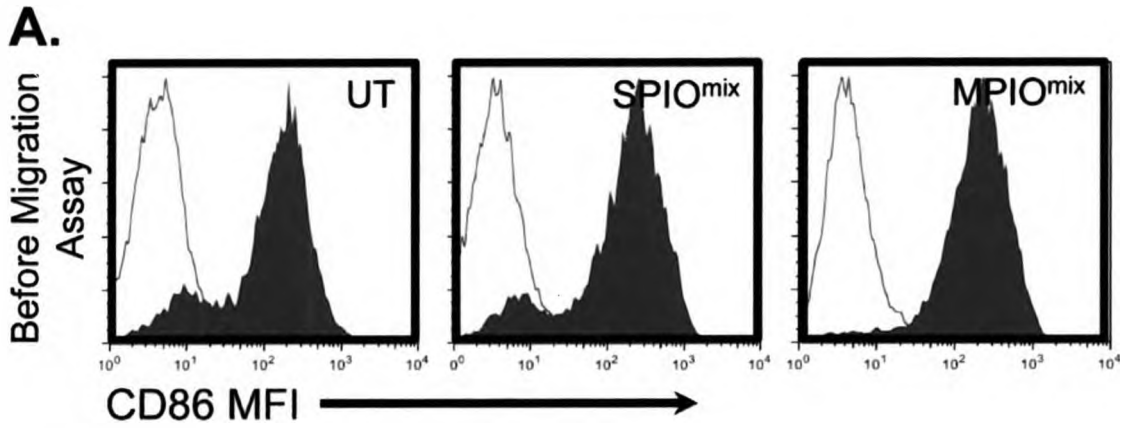
higher compared to that of SPIO<sup>mix</sup> DC migration ( $p < 0.05$ ). Furthermore, SPIO<sup>-</sup> DC migration was as efficient as UT DC migration (Figure 2.9A). Data also indicated that MPIO<sup>+</sup> DCs migrated 10% less efficiently than SPIO<sup>+</sup> DCs. This supports the theory that nanoparticle size inhibits DC migration in a size-related fashion. Furthermore, analysis of CD86 surface marker expression by cells that migrated through the membrane indicated that they were phenotypically more mature based on CD86 MFIs compared to those that did not (Fig. 2.9E, F, G).

### **2.3.7 SPIO labelling does not physically slow the kinetics of *in vivo* DC migration**

It is well established that *in vivo* migration of subcutaneously injected DCs to a target LN peaks two days post-injection. It is possible that the discrepancy between the *in vivo* migration of SPIO<sup>+</sup> and UT DCs is occurring because the presence of SPIO nanoparticles in DCs is actually delaying the peak migration by physically slowing their migration to LNs. The possibility that SPIO nanoparticles physically slow *in vivo* DC migration was investigated by performing a time-course experiment. The kinetic *in vivo* migration of SPIO<sup>+</sup> DCs was assessed using both MRI (Fig. 2.10) and histological analysis (Fig. 2.11). The amount of *in vivo* migration of UT DCs was used as the control. MRI analysis and histological analysis indicate that both SPIO<sup>+</sup> DC and UT DC migration to popliteal LN peaks at day two post injection. As a result, SPIO itself does not alter the kinetics of *in vivo* DC migration to target LNs. Although FSL decreases with time (Fig 2.10C), void volume increases with time for SPIO<sup>+</sup> DCs (Fig 2.10C). Consistent with our earlier results, throughout the time course UT DC were always present in greater



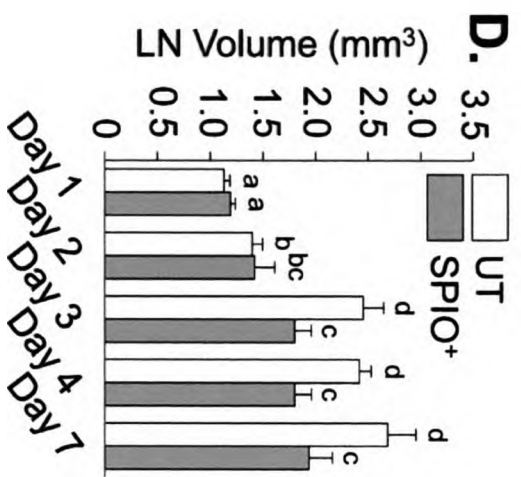
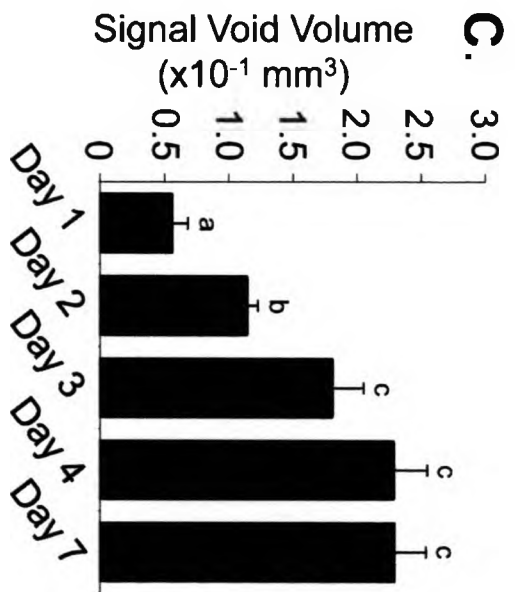
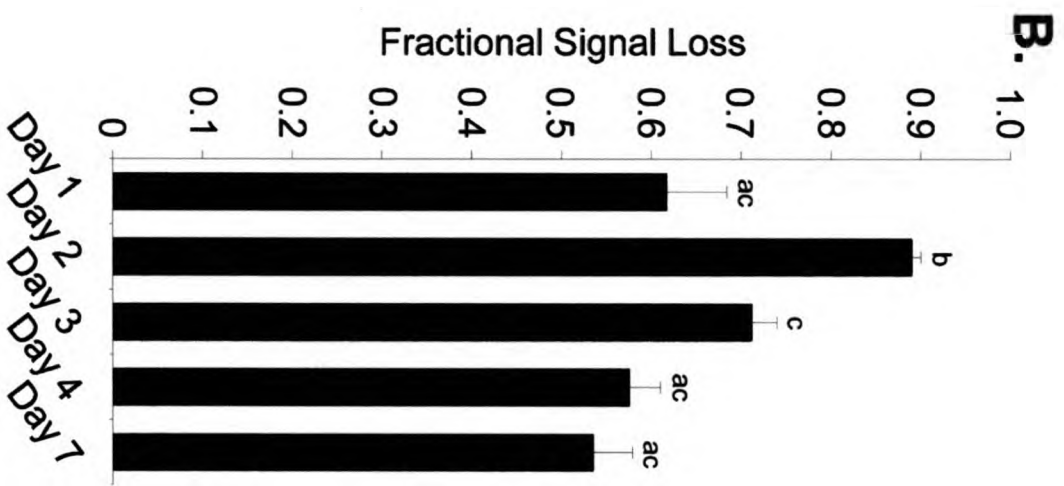
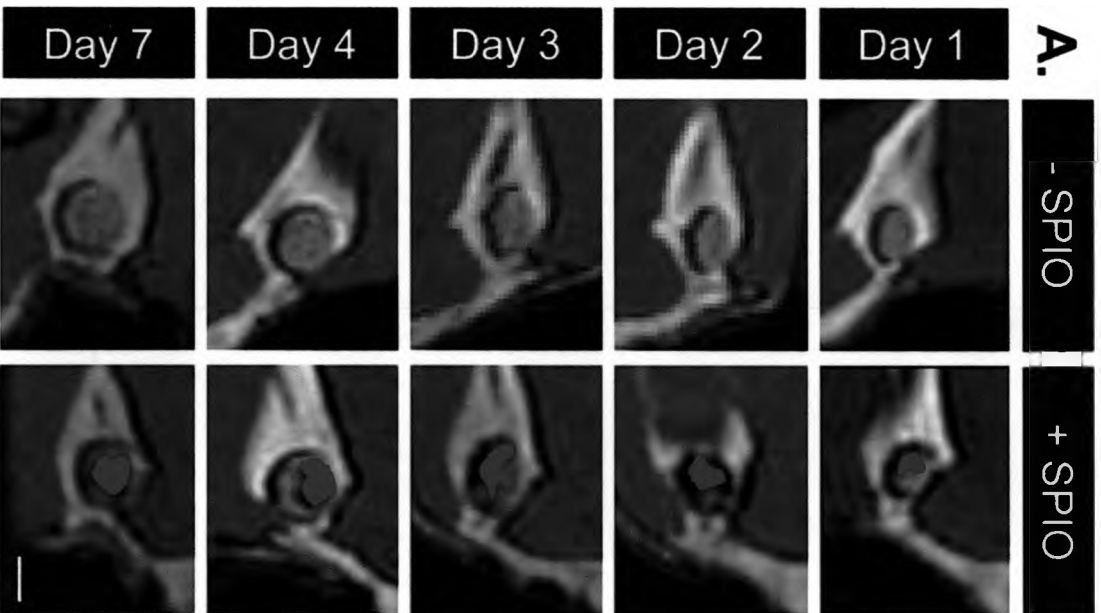
**Figure 2.9. *In vitro* migration assays show SPIO<sup>+</sup> DCs migrate more efficiently than MPIO<sup>+</sup> DCs.** DCs were labelled overnight with SPIO (FeREX), MPIO (Bangs Beads) or left untreated (UT). Cells were collected, some were magnetically separated, and *in vitro* migration assays were performed to determine *in vitro* migration efficiencies of each DC population to CCL19 and CCL21. (A) DCs were analyzed for CD86 surface expression using flow cytometry before migration assays were carried out. (B) After counting collected cells using flow cytometry, it was determined that MPIO<sup>+</sup> DCs migrated less efficiently than SPIO<sup>+</sup> DCs. Data are means of triplicate experiments  $\pm$  SE and are representative of 3 replicates. Means with different superscript letters indicate significant differences ( $p < 0.05$ ). (C) Analysis of surface CD86 expression using flow cytometry on cells collected following migration through transwell inserts (  ) and those that did not migrate through (  ) was carried out. DCs that were relatively more mature migrated through transwell inserts. Histograms are gated on viable CD11c<sup>+</sup> cells. Isotype control is demonstrated as  .



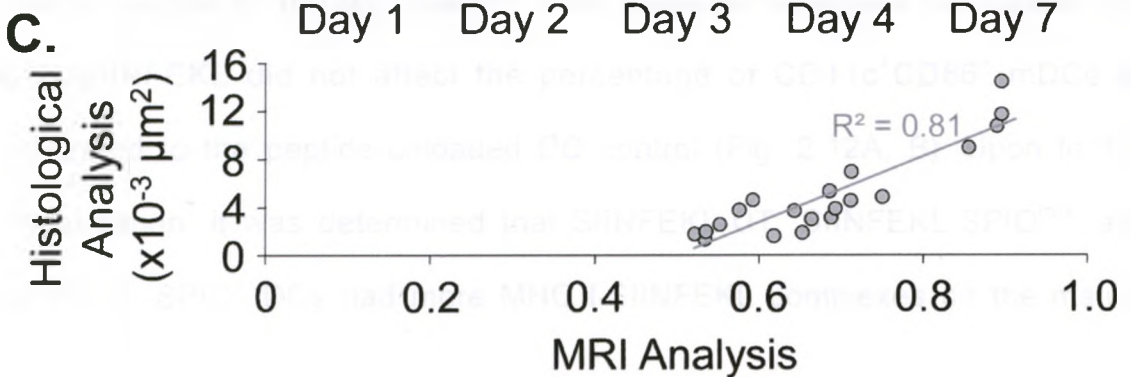
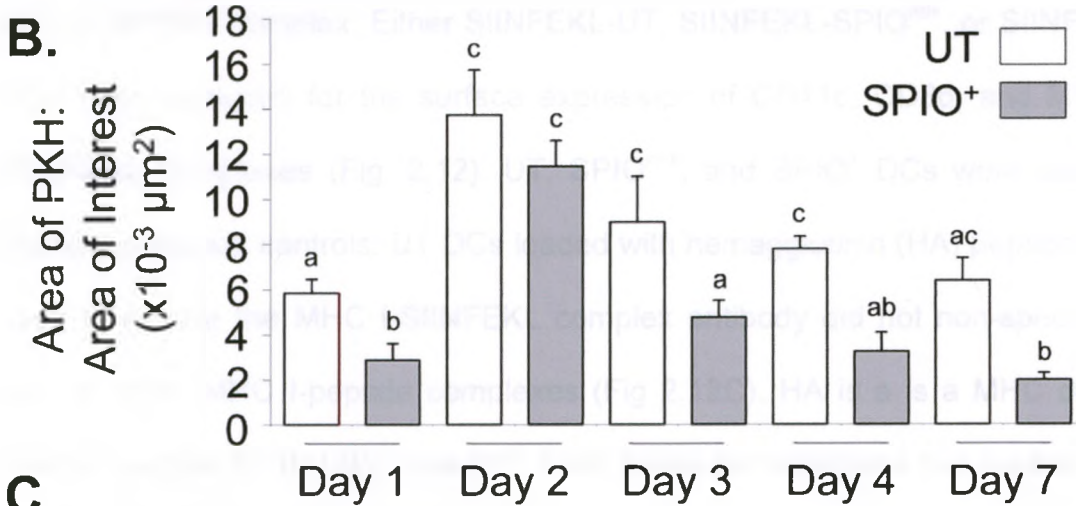
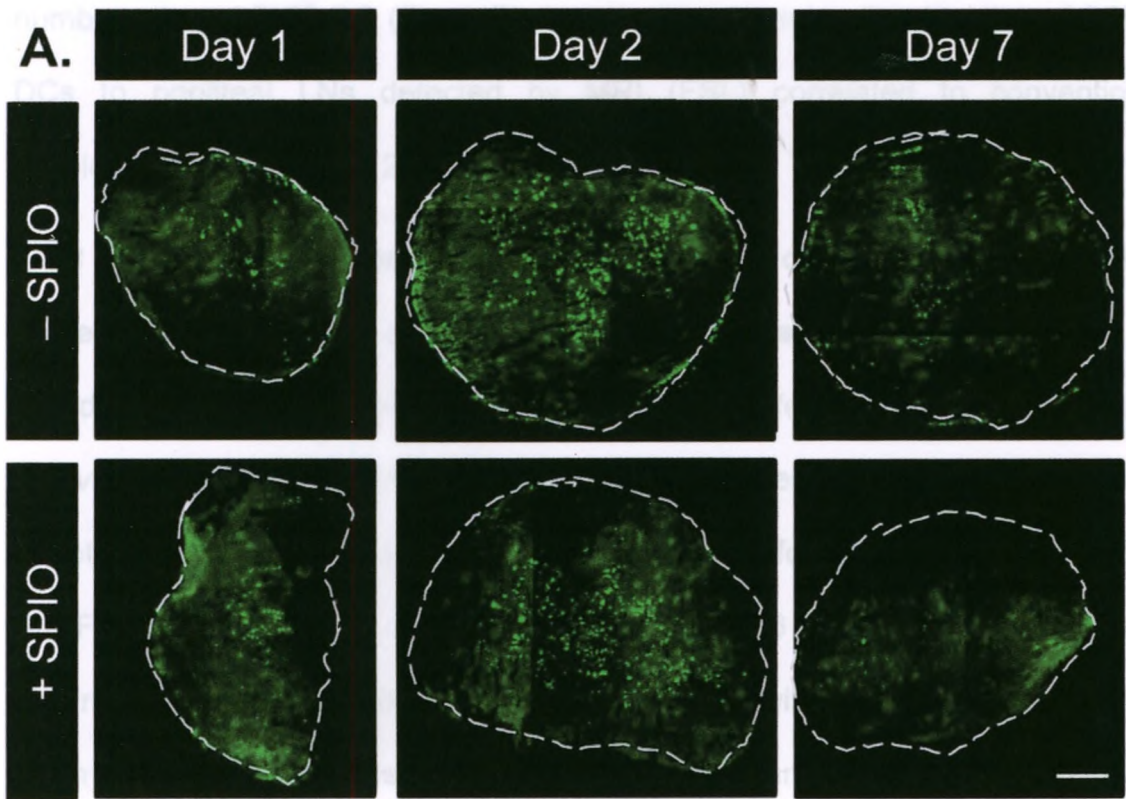


**Figure 2.10. *In vivo* migration of SPIO<sup>+</sup> DCs to popliteal LNs peaks at day 2.**  $1 \times 10^6$  PKH<sup>+</sup>SPIO<sup>+</sup> DCs were adoptively transferred via subcutaneous injection into the right hind footpads of C57BL/6 mice. PKH<sup>+</sup> DCs were injected into the contralateral hind footpads to serve as a control. MRI scans were carried out 1, 2, 3, 4, and 7 days post adoptive transfer. (A) Representative cropped MR images of popliteal LNs for each time point are shown. Areas of signal loss are pseudo-coloured in red. Scale bar = 2 mm. MR images were analyzed for (B) fractional signal loss (FSL), (C), signal void volume, and (D) LN volume. Signal loss is greatest at day 2 and recovers subsequently. Signal void volume increases and plateaus at day 3. Data are means  $\pm$  SE and  $n=4$  for each time point. Differences are significant if superscript letters are different ( $p < 0.05$ ).





**Figure 2.11. Histological analysis of DC migration kinetics to popliteal LNs correlates with MRI analysis.**  $1 \times 10^6$  PKH<sup>+</sup>SPIO<sup>+</sup>DCs were adoptively transferred to C57BL/6 mice via subcutaneous right hind footpad injections. PKH<sup>+</sup>DCs were injected into contralateral hind footpads to serve as a control. Following MRI scans 1, 2, 3, 4, and 7 days post injection, popliteal LNs were removed and analyzed using digital morphometry. (A) Representative images of popliteal LNs showing PKH<sup>+</sup> (green) DCs for Days 1, 2, and 7 are shown. Scale bar = 100  $\mu$ m. (B) Migration to LNs peaks at day 2 for SPIO<sup>+</sup> and UT DCs and declines subsequent to that. Data are means  $\pm$  SE; n=4 for each day. (C) Comparison of histological analysis with MRI analysis (FSL) indicates a positive linear correlation (correlation slope > 0).



numbers than SPIO<sup>+</sup> DC (Fig 11B). Importantly, the migration kinetics of SPIO<sup>+</sup> DCs to popliteal LNs detected by MRI (FSL) correlated to conventional histological analysis (Fig. 2.11C).

### **2.3.8 Differences between UT, SPIO<sup>mix</sup>, and SPIO<sup>+</sup> DCs migration correspond with *in vivo* antigen-specific T cells responses**

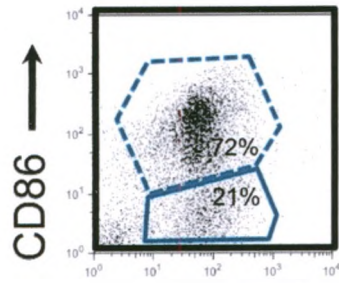
In order to demonstrate the biological relevance of effective DC migration to LNs *in vivo*, *ex vivo* antigen (Ag)-specific T cell responses were analyzed following adoptive transfer of Ag-loaded DCs. The Ag used for these experiments was SIINFEKL, a MHC class I specific peptide for C57BL/6 mice (K<sup>b</sup>). First, in order to confirm that DCs were being appropriately loaded with SIINFEKL peptide, flow cytometric analysis of DCs was performed using an antibody that recognizes the HC I-SIINFEKL complex. Either SIINFEKL-UT, SIINFEKL-SPIO<sup>mix</sup>, or SIINFEKL<sup>+</sup> DCs were analyzed for the surface expression of CD11c, CD86, and MHC I-SIINFEKL complexes (Fig. 2.12). UT, SPIO<sup>mix</sup>, and SPIO<sup>+</sup> DCs were used as peptide-unloaded controls. UT DCs loaded with hemagglutinin (HA) peptide were used to ensure the MHC I-SIINFEKL complex antibody did not non-specifically bind to other MHC I-peptide complexes (Fig 2.12C). HA is a is a MHC class I specific peptide for BALB/c mice (K<sup>d</sup>). First, it was demonstrated that loading DCs with SIINFEKL did not affect the percentage of CD11c<sup>+</sup>CD86<sup>+</sup> mDCs as compared to the peptide-unloaded DC control (Fig. 2.12A, B). Upon further investigation, it was determined that SIINFEKL-UT, SIINFEKL-SPIO<sup>mix</sup>, and SIINFEKL-SPIO<sup>+</sup> DCs had more MHC I-SIINFEKL complexes on the mature



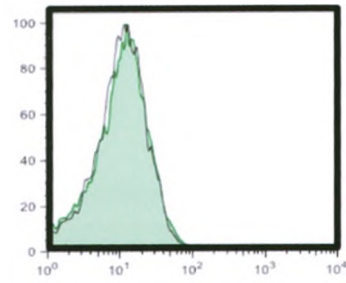
**Figure 2.12. MHC I-SIINFEKL peptide complexes are present on mature DCs.**

Following 2 hour incubation with SIINFEKL peptide, UT, SPIO<sup>mix</sup>, or SPIO<sup>+</sup> DCs were stained for surface MHC I-SIINFEKL peptide complexes and analyzed by flow cytometry. UT DCs not given SIINFEKL peptide or DCs given an irrelevant MHC I-specific hemagglutinin (HA) peptide served as controls. (A) Representative dot plot of UT DCs is shown. Mature CD11c<sup>+</sup>CD86<sup>+</sup> (□) and CD11c<sup>+</sup>CD86<sup>-</sup> (□) DC populations are gated on. (B) Representative dot plots for UT, SPIO<sup>mix</sup>, and SPIO<sup>+</sup> DCs loaded with SIINFEKL peptide are shown. Gates outline mature (□) and immature (□) DC populations. (C) UT DCs loaded with HA peptide (■) did not result in non-specific binding of MHC I-SIINFEKL antibody. (D) Histograms of UT, SPIO<sup>mix</sup>, or SPIO<sup>+</sup> SIINFEKL loaded DCs were analyzed for surface expression of MHC I-SIINFEKL peptide complexes. A comparison of CD11c<sup>+</sup>CD86<sup>+</sup> mature (■) and CD11c<sup>+</sup>CD86<sup>-</sup> immature (□) populations is shown for each DC population. MHC I-SIINFEKL complexes were found predominantly on CD11c<sup>+</sup>CD86<sup>+</sup> mature DC populations for all groups. Isotype controls are shown as □.

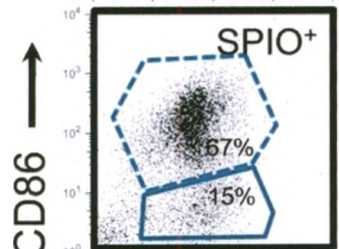
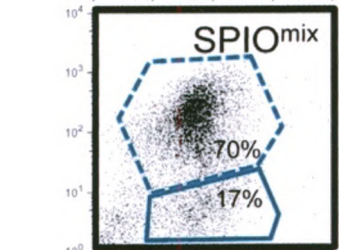
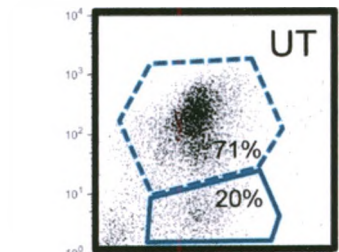
**A.** - SIINFEKL



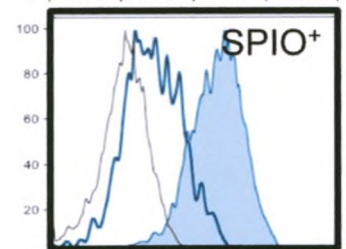
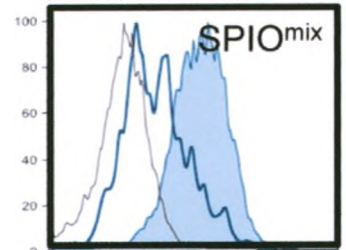
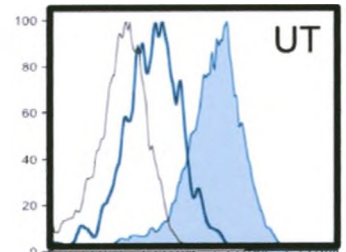
**C.** + Irrelevant



**B.** + SIINFEKL






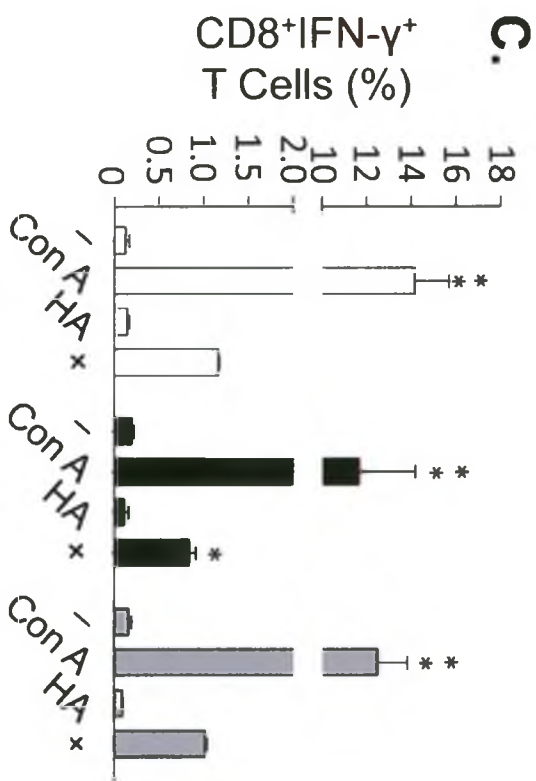
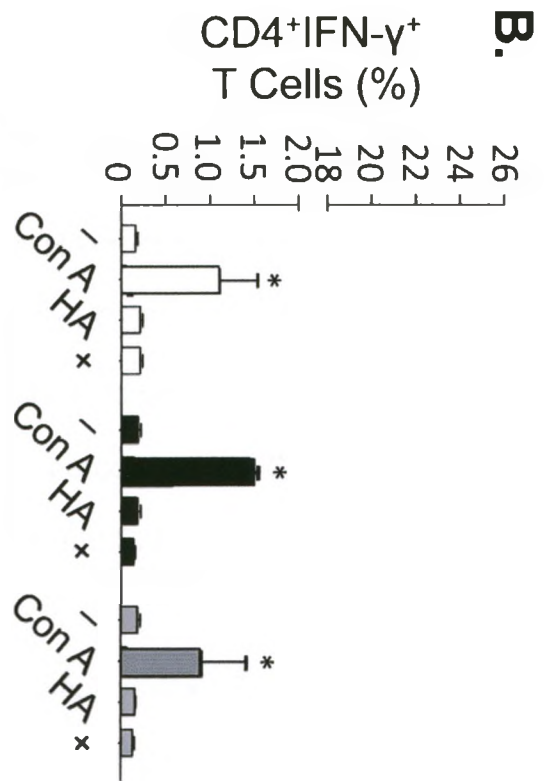
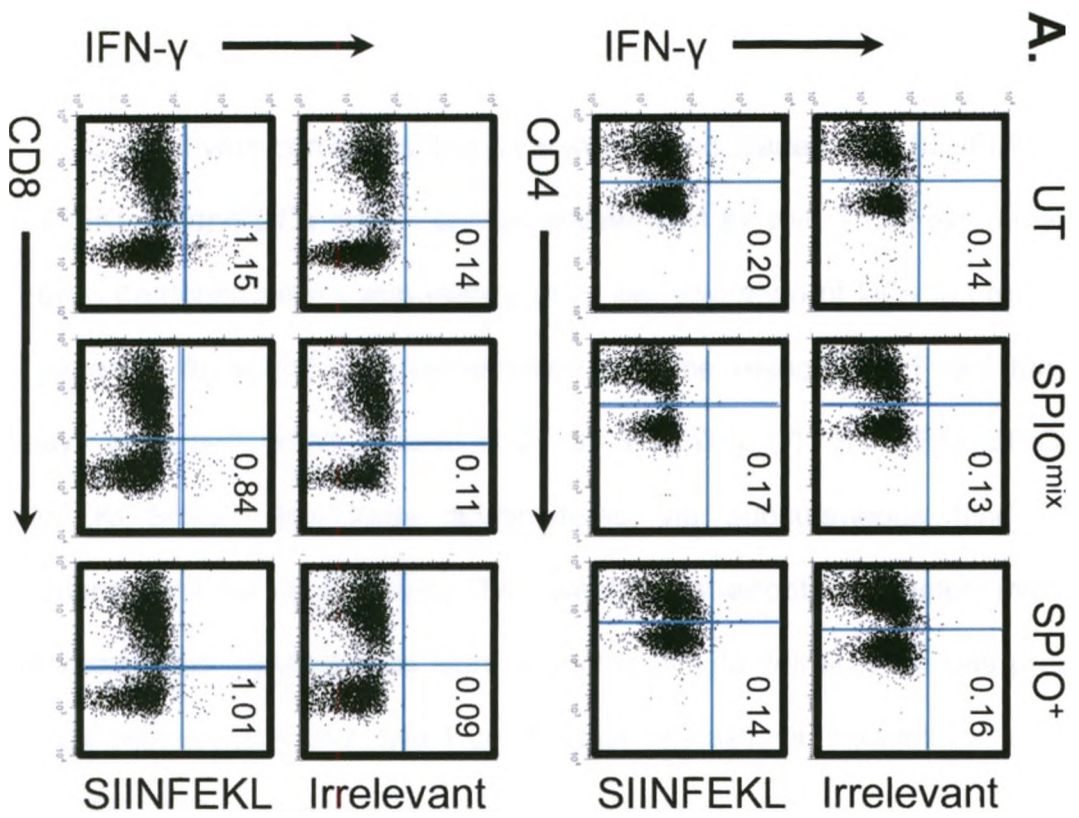
**D.** + SIINFEKL







**Figure 2.13. ICS for IFN- $\gamma$  indicates the presence of more CD8<sup>+</sup>IFN<sup>+</sup> T cells following adoptive transfer of either UT or SPIO<sup>+</sup> DCs.** Following adoptive transfer of either  $2 \times 10^6$  untreated (UT) (  ), SPIO<sup>mix</sup> (  ), or SPIO<sup>+</sup> (  ) DCs, popliteal LNs were removed, digested, and LN cells were incubated with either irrelevant peptide (hemagglutinin [HA]) or SIINFEKL for 2 hours and then an additional 3 hours in the presence of Brefeldin A. Concanavalin A (Con A) was used as an internal positive control and media was used as a negative control. All treatments were repeated in triplicate. **(A)** Representative dot plots for either CD4<sup>+</sup> or CD8<sup>+</sup> T cells are shown. Dot plots are gated on viable CD3<sup>+</sup> T cells. Analysis was carried out to determine the percentage of **(B)** CD3<sup>+</sup>CD4<sup>+</sup>IFN- $\gamma$ <sup>+</sup> or **(C)** CD3<sup>+</sup>CD8<sup>+</sup>IFN- $\gamma$ <sup>+</sup> T cells. Data are means  $\pm$  SE (n=4) and differences from the negative control are significant if  $p < 0.05$  (\*).



(CD11c<sup>+</sup>CD86<sup>+</sup>) subset as compared to the immature (CD11c<sup>+</sup>CD86<sup>-</sup>) subset (Fig. 2.12D).

Once it was confirmed that DCs were being loaded with SIINFEKL, these SIINFEKL-loaded DCs were used for subsequent *ex vivo* T cell experiments. In order to demonstrate the importance of *in vivo* migration of DCs to LNs in order to generate Ag-specific T cell-mediated immune responses, T cell functional assays were performed. A total of  $2 \times 10^6$  SIINFEKL-UT, SIINFEKL-SPIO<sup>mix</sup>, or SIINFEKL-SPIO<sup>+</sup> DCs were administered via subcutaneous hind footpad injections (n=4 for each group). Two weeks post-adoptive transfer, mice were euthanized and popliteal LNs were collected, single cell suspensions prepared, and LN cells were used in two T cell functionality assays: intracellular staining of IFN- $\gamma$  (Fig. 2.13) and tetramer staining (Fig 2.14).

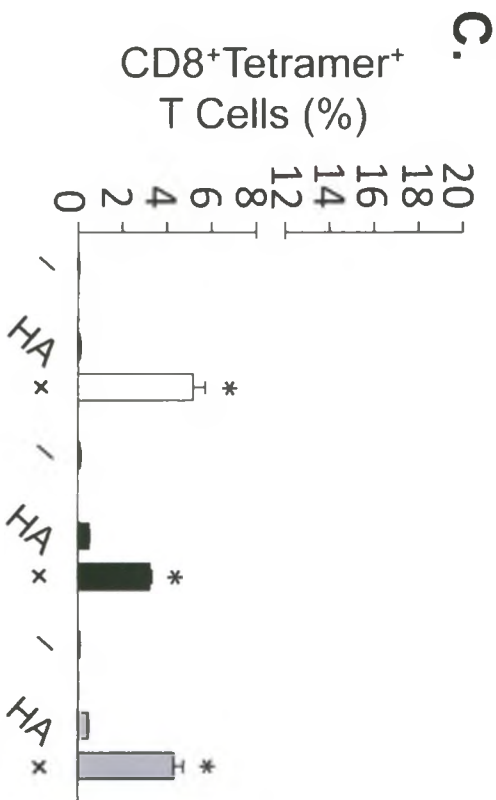
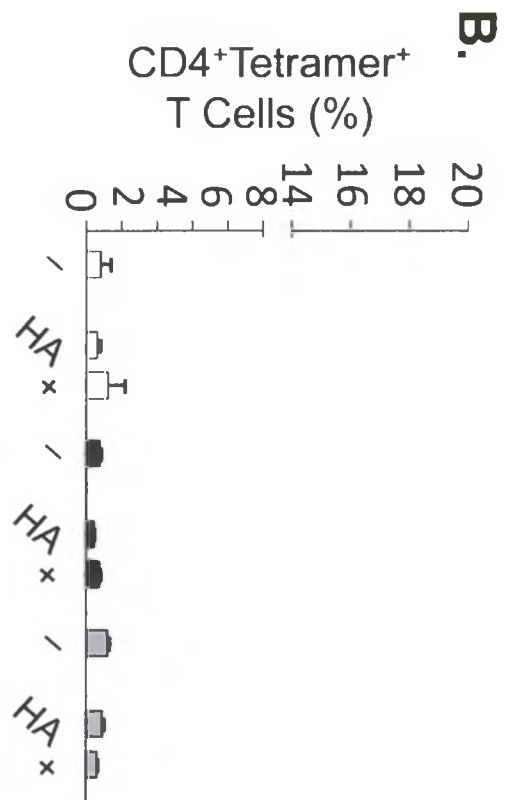
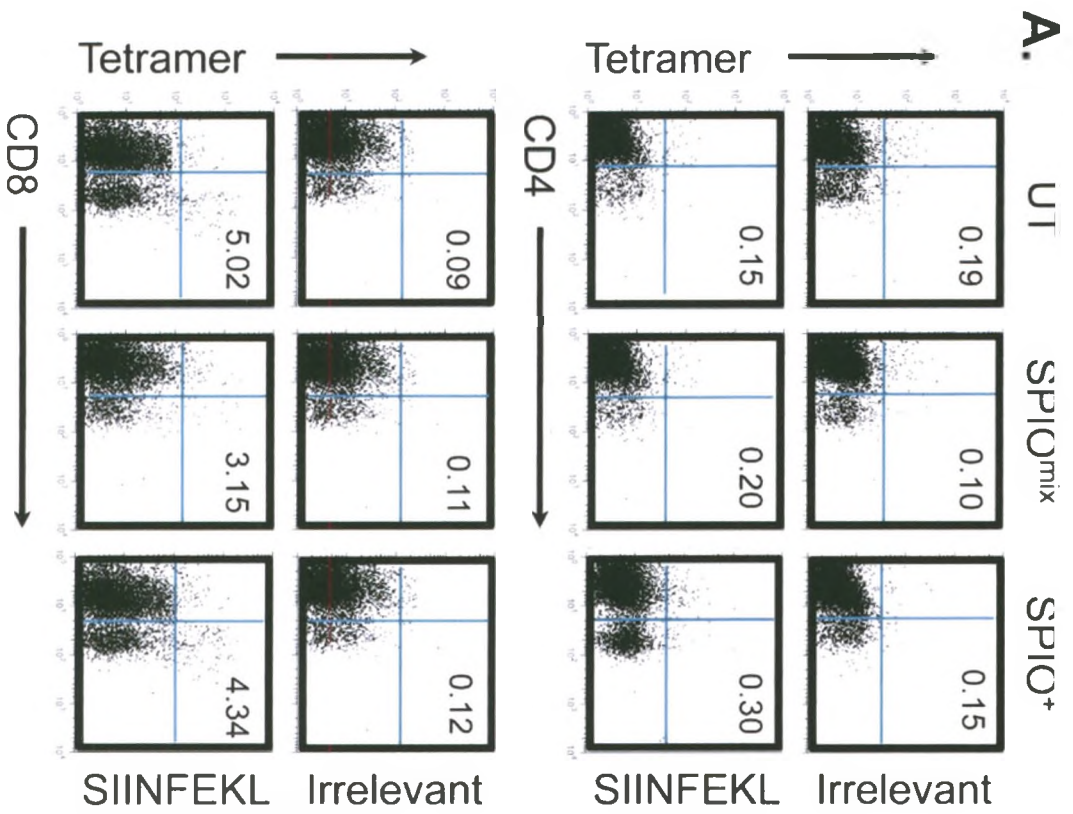
For ICS assays, either no peptide, non-specific HA peptide, or specific peptide (SIINFEKL) was used to re-stimulate T cell responses *in vitro*. It was determined that IFN- $\gamma$  production by CD8<sup>+</sup> T cells was SIINFEKL-specific as compared to the use of a non-specific HA control peptide for all three groups (Fig. 2.13). Furthermore, the percentage of CD8<sup>+</sup>IFN- $\gamma$ <sup>+</sup> T cells was significantly higher compared to CD4<sup>+</sup>IFN- $\gamma$ <sup>+</sup> T cells following peptide-specific (SIINFEKL) stimulation (Fig. 2.13B, C). Finally, the percentage of CD8<sup>+</sup>IFN- $\gamma$ <sup>+</sup> T cells was higher following transfer of SIINFEKL-UT and SIINFEKL-SPIO<sup>+</sup> DCs compared to SIINFEKL-SPIO<sup>mix</sup> DCs (Fig 2.13C).

The percentage of SIINFEKL-specific cytotoxic T lymphocytes (CTLs) was detected by re-stimulating LN cells with SIINFEKL and staining with a MHC-I-SIINFEKL-specific tetramer (H2K<sup>b</sup>-SIINFEKL). No peptide and non-specific HA

peptide controls were used to ensure T cell responses were SIINFEKL specific (Fig. 2.14). The percentage of SIINFEKL-specific CTLs generated following adoptive transfer of SPIO<sup>+</sup> DCs was not different from that of the UT DC control. However, 1.4% fewer SIINFEKL-specific CTLs were generated from mice that received SPIO<sup>mix</sup> DCs (Fig. 2.14C). This suggests that by magnetically separating SPIO<sup>+</sup> from SPIO<sup>-</sup> DCs in order to improve *in vivo* migration compared to SPIO<sup>mix</sup> DCs, as demonstrated in Figures 2.10 and 2.11, a corresponding increase in the Ag-specific T cell response was seen. As expected, no SIINFEKL-specific CD4<sup>+</sup> T cells were found (Fig. 2.14B).



**Figure 2.14. Tetramer staining indicates the presence of more CD8+ SIINFEKL-specific T cells following adoptive transfer of either UT or SPIO<sup>+</sup> DCs.** Following adoptive transfer of either  $2 \times 10^6$  untreated (UT) (□), SPIO<sup>mix</sup> (■), or SPIO<sup>+</sup> (▒) DCs, popliteal LNs were removed, digested, and LN cells were incubated with either irrelevant peptide (hemagglutinin [HA]) or SIINFEKL for two days. Media was used as a negative control. Treatments were repeated in triplicate. Following incubation, cells were collected and stained for MHC I-SIINFEKL specific tetramer. (A) Representative dot plots for either CD4<sup>+</sup> or CD8<sup>+</sup> T cells are shown. Dot plots are gated on viable CD3<sup>+</sup> T cells. Analysis was carried out to determine the percentage of (B) CD3<sup>+</sup>CD4<sup>+</sup> or (C) CD3<sup>+</sup>CD8<sup>+</sup> T cells specific for SIINFEKL peptide. Data are means  $\pm$  SE (n=4) and differences from negative control are significant if  $p < 0.05$  (\*).



## 2.4 Discussion

There is a need for a safe, non-invasive imaging modality to track the *in vivo* migration of clinical grade DCs in cancer patients in order to determine their location in the body following administration. To date, MRI appears to be feasible and applicable for human use [11, 12]. In order to distinguish cells of interest from surrounding tissues, cells must be labelled with a contrast agent. To date, negative contrast agents, particularly SPIO nanoparticles, are preferred because of the sensitivity of detection they provide. However, recent data from our laboratory [18] and one other laboratory demonstrated a discrepancy between the *in vivo* migration of SPIO<sup>mix</sup> DCs and UT DCs. The migration of DCs to LNs *in vivo* is crucial to generate appropriate T cell-mediated antigen-specific responses. In order for cellular MRI to be viable modality to track DC migration *in vivo*, the use of an MR contrast agent itself should not have any negative impact on DC biology and function *in vitro* or *in vivo*. As a result, this study set out to investigate the reason as to why SPIO-labelling is affecting the *in vivo* migration of DCs.

It is important to note that this study employs two brands of SPIO nanoparticles: Feridex and FeREX. Feridex was the SPIO we chose to use in many of our earlier experiments because of its prior availability for use in clinical trials. However, following the withdrawal of Feridex from the market, we began using FeREX, a SPIO of very similar composition (dextran-coated) and size (80-120 nm in diameter) to Feridex. Preliminary studies using FeREX were carried out to ensure there were no adverse effects of it on our DCs *in vitro*.



Furthermore, we determined that the trends in data obtained following the use of Feridex were not significantly different from those obtained using FeREX ( $p < 0.05$ , data not shown) with respect to DC phenotype, and cytokine profiles.

Although the effect of SPIO on DC viability has been previously tested [18, 20], we needed to specifically confirm if SPIO was pre-disposing cells to become apoptotic or necrotic before further assessing any other effect(s) FeREX<sup>®</sup> might have on DCs. Assessing DC viability with Trypan Blue and Annexin/7AAD staining indicated that SPIO labelling (Feridex or FeREX) has no significant effect on cell death. Therefore, it could be concluded that SPIO is not inducing early cell death *in vitro*, which could have explained the poor levels of DC migration *in vivo* compared to UT DCs. These results also correspond with other studies that have used SPIO to label DCs *in vitro*. Some have raised the question as to whether or not SPIO induces the production of reactive oxygen species (ROS) in cells following their uptake. It is known that generation of ROS by cells can result in disrupted mitochondrial membrane potential. A study by Frasa *et al.* [21] investigated the effect of mitochondrial membrane potential after blocking CD38. Data from this study demonstrated that CD38-blockade resulted in a reduction of mitochondrial membrane potential and decreasing the migratory capacity of their DCs *in vitro* and secretion of IL-12. As a result, the potential production of ROS following SPIO labelling would have negative implications. However, a study investigating the production of ROS in human macrophages following incubation with SPIO indicated no significant effects compared to control cells [22]. As such, the production of ROS following SPIO labelling by our DCs *in vitro* is an unlikely cause of the *in vivo* migration discrepancy compared to UT control DCs.

Our lab has previously investigated the effects of SPIO (Feridex) on DC phenotypic markers and cytokine secretion [18], but to our knowledge, there have been no extensive phenotypic and functional characterization of the effects of FeREX on DCs. We found no significant differences in terms of phenotype (surface marker expression) or function (cytokine profiling) between SPIO and UT DCs that could explain differences in migration abilities. Specifically, SPIO have no notable, significant effect on the expression of surface molecules relevant to DC migration (CCR7, CD38, CD11b).

The efficiency of labelling DCs with SPIO in our *in vitro* culture conditions is relatively high compared to other immune cells, such as lymphocytes, because of the inherent endocytic ability of DCs. However, 100% cell labelling was never achieved (Appendix 2). As a result, magnetic separation of SPIO<sup>mix</sup> DCs into two subpopulations (SPIO<sup>+</sup> DCs and SPIO<sup>-</sup> DCs) allowed us to further characterize them phenotypically and assess their cytokine secretion. It is known that DCs naturally down-regulate their endocytic abilities following sufficient maturation and activation [23]. Our data indicate SPIO<sup>-</sup> DCs were relatively more mature and active compared to SPIO<sup>+</sup> DCs. It follows, then, that SPIO<sup>-</sup> DCs were unable to take up SPIO nanoparticles in culture because they are phenotypically mature and active. We believe that it is likely that a subpopulation of CD11c<sup>+</sup>CD86<sup>Hi</sup>CD38<sup>Hi</sup>CD40<sup>Hi</sup>DCs can also be found in the UT DC population. However, our *in vitro* culture produces UT DCs which are highly heterogeneous in terms of surface marker expression, so it is likely that this small subpopulation's phenotype is being masked.

Upon examination of CD38 surface expression, we found that SPIO<sup>-</sup> DCs express higher levels of this ecto-enzyme on their mature (CD86<sup>+</sup>) populations compared to all other (UT, SPIO, SPIO<sup>+</sup>) DC populations. This suggests that SPIO<sup>-</sup> DCs migrate more efficiently compared to SPIO<sup>+</sup> DCs. The *in vitro* and *in vivo* migration studies which followed magnetic separation of SPIO<sup>mix</sup> DCs into the two subpopulations of SPIO<sup>+</sup> and SPIO<sup>-</sup> DCs provided support to this theory. These findings are supported by others, which have elucidated a role for CD38 in CCR7 receptor sensitization contributing to migrational competency [21, 24].

By examining the cytokine profiles of SPIO<sup>+</sup> and SPIO<sup>-</sup> DC populations with Luminex assays, we were able to detect some differences in the amount of TNF and IL-10 secretion. Specifically, SPIO<sup>-</sup> DCs secreted less TNF compared to all other DC populations. It has been found that APCs [25, 26], such as macrophages [27], express the insulin-like growth factor receptor II (IGFII)/mannose-6-phosphate (M6P) receptor complex. Dextran, which is used as a complex polymer of glucose, is used as the stabilizing coating to protect the iron nanoparticles from oxidizing and to improve biocompatibility of SPIO. However, it is possible that over time, this stable dextran coat spontaneously degrades to glucose, which is known to bind to the IGFII receptor. A study by Ikezu *et al.* [28] demonstrated that IGFII receptor signalling can be differentially coupled to various pathways under different conditions, one being the G protein-coupled receptor (GPCR) and cyclic adenosine monophosphate (cAMP) pathways. It has been shown that high levels of cAMP can lead to maturation and activation of DCs despite [29, 30] lowering the functional capabilities of these cells, specifically in terms of TNF- $\alpha$  [31, 32] production and secretion. This

phenomenon might provide an explanation as to why the SPIO<sup>-</sup> DC population is more mature and active, yet doesn't secrete expectedly higher levels of cytokines *in vitro*. However, more extensive studies will have to be carried out in order to properly confirm this theory. The amount of IL-10 for both SPIO<sup>+</sup> and SPIO<sup>-</sup> DC populations was lower compared to that found in the supernatants of SPIO<sup>mix</sup> and UT DC controls. As of yet, there is no known explanation for this phenomenon. Nevertheless, it is important to note that all cytokine levels detected were well below the biological levels believed to be required for *in vivo* function. Therefore, significance differences found *in vitro* might not directly correlate significantly to *in vivo* function.

Due to the presence of two phenotypically distinct sub-populations of DCs in our SPIO<sup>mix</sup> DC population, it was important to determine if there were differences in their *in vivo* migratory abilities. Our first investigation involved a competition experiment, which demonstrated that by mixing SPIO<sup>+</sup> DCs with UT DCs, it reduced the amount of SPIO<sup>+</sup> DC migration to LNs *in vivo*. This suggested that there was a preferential migration of UT DCs to LNs. As a result, we postulated that by magnetically separating SPIO<sup>+</sup> from SPIO<sup>-</sup> DCs before adoptive transfer could improve SPIO<sup>+</sup> migration to LNs *in vivo*. It was possible, however, that separating SPIO<sup>-</sup> DCs from SPIO<sup>+</sup> DCs could have resulted in less *in vivo* migration of SPIO<sup>+</sup> DCs to LNs compared to SPIO<sup>+</sup> DCs because we were removing the most migratory competent DCs. While our data support the idea generated from our competition experiment regarding an *in vivo* competition, we need to further investigate why removing SPIO<sup>-</sup> DCs from SPIO<sup>+</sup> actually

improves subsequent SPIO<sup>+</sup> migration *in vivo*. Further studies into this effect will need to be investigated.

We postulated that SPIO is physically impeding the migration of DCs through lymphatic cell junctions because these junctions average between 1-10 nm. In order to support this hypothesis, we used larger MPIO particles to compare the migratory abilities DCs *in vitro*. Our data indicate that labelling DCs with MPIO significantly reduces their migration *in vitro* compared to SPIO<sup>+</sup> and UT DC, thereby supporting our hypothesis.

Evaluation of the time course of DC migration using MRI and histology indicated that SPIO<sup>+</sup> DC migration peaks to popliteal LNs at 2 days following subcutaneous injection. This data are comparable to findings from a previous study [33]. Taken together, MRI and histological analysis of the kinetics of *in vivo* DC migration to LNs indicate SPIO uptake isn't physically slowing migration. Although SPIO appears to be physically impeding the *in vivo* migration of DCs to popliteal LNs, we do not believe these findings discount the use of SPIO as a viable contrast agent to track cells *in vivo* using MRI. Several other studies involved in tracking the *in vivo* migration of DCs using cellular MRI also use SPIO because it does not seem to have negative effects on cell viability [22]. Furthermore, because SPIO is coated in dextran, it is susceptible to degradation. Due to the dynamic nature of DC migration *in vivo*, as well as the short lifespan of migratory DCs, the fact that SPIO signal is transitory and reflects the presence of DCs *in vivo* makes it useful. This also provides the added advantage to clinicians of being able to administer and track the migration of multiple SPIO<sup>mix</sup> DC vaccinations to patients.

While non-invasively tracking *in vivo* migration of DCs is important, the ultimate goal remains to accurately quantify the amount of detected DC migration. This is because the amount of DC migration to LNs has been suggested to be related to the strength of the anti-tumour responses generated in patients [34]. This can be supported by our data that investigated T cell function *in vitro* following adoptive transfer of UT, SPIO<sup>mix</sup>, or SPIO<sup>+</sup> DCs. We demonstrated that following magnetic separation of SPIO<sup>+</sup> from SPIO<sup>-</sup> we detected a greater percentage of CD8<sup>+</sup> CTLs following *in vitro* re-stimulation compared to adoptive transfer of SPIO<sup>mix</sup> DCs. This data supports the idea that more DC migration generates a greater T cell functional response *in vivo* [35]. Ultimately, methods to enhance *in vivo* migration of DCs to target LNs can be assessed effectively in patients if a non-invasive imaging modality is capable of accurately quantifying DC migration. By magnetically separating SPIO<sup>+</sup> from SPIO<sup>-</sup> DCs prior to adoptive transfer, we also improved the correlation between histological and MRI data. This means that by purifying SPIO<sup>+</sup> DCs before adoptive transfer via magnetic separation, we can be confident that signal generated from *in vivo* MR images is truly reflective of cell numbers present in LNs. Taken together, results from this study have led us to routinely magnetically separate our SPIO<sup>+</sup> from SPIO<sup>-</sup> DCs in preparation for adoptive transfer. This strengthens our assumption that the negative signal generated in the LNs of MR images is due to the presence of SPIO<sup>+</sup> DCs.

There is a need by clinicians to be able to track the *in vivo* migration of clinical grade DCs in cancer patients. This data will provide relevant information to help improve the overall efficacy of cell-based vaccination strategies. MRI is

one of the preferred methods to track cells *in vivo* because of its safety, lack of ionizing radiation, and non-toxic contrast agents. Although SPIO appears to be physically impeding *in vivo* migration of DCs, the use of a MRI contrast agent which provides the ability to generate a dynamic signal in MR images truly reflective of the biological function of DCs *in vivo* in addition to sensitive spatial localization is important. Our laboratory will continue to work towards methods to develop and refine reliable strategies to help make cellular MRI a useful cell tracking modality in clinical settings.

## 2.5 References

1. Banchereau, J., et al., *Immunobiology of dendritic cells*. Annu Rev Immunol, 2000. **18**: p. 767-811.
2. Miyake, T., et al., *Poly I:C-induced activation of NK cells by CD8 alpha+ dendritic cells via the IPS-1 and TRIF-dependent pathways*. J Immunol, 2009. **183**(4): p. 2522-8.
3. Zaini, J., et al., *OX40 ligand expressed by mouse DCs stimulates NKT and CD4+ Th antitumor immunity*. J Clin Invest, 2007. **117**(11): p. 3330-8.
4. Ardavin, C., S. Amigorena, C. Reis Sousa, *Dendritic cells: immunobiology and cancer immunotherapy*. Immunity, 2004. **20**(1): p. 17-23.
5. Levine, B.L., et al., *CD28 ligands CD80 (B7-1) and CD86 (B7-2) induce long-term autocrine growth of CD4+ T cells and induce similar patterns of cytokine secretion in vitro*. Int Immunol, 1995. **7**(6): p. 891-904.
6. Santana, M.A., F. EsquivelGuadarrama, and W.J. Kwang, *Cell Biology of T Cell Activation and Differentiation*, in *International Review of Cytology*. 2006, Academic Press. p. 217-274.
7. Adema, G.J., et al., *Migration of dendritic cell based cancer vaccines: in vivo veritas?* Curr Opin Immunol, 2005. **17**(2): p. 170-4.
8. Chaudhuri, D., et al., *Targeting the immune system in cancer*. Curr Pharm Biotechnol, 2009. **10**(2): p. 166-84.
9. Curigliano, G., M. Rescigno, and A. Goldhirsch, *Immunology and breast cancer: Therapeutic cancer vaccines*. The Breast, 2007. **16**(2): p. 20-26.
10. Baumjohann, D. and M.B. Lutz, *Non-invasive imaging of dendritic cell migration in vivo*. Immunobiology, 2006. **211**(6-8): p. 587-597.
11. de Vries, I.J., et al., *Magnetic resonance tracking of dendritic cells in melanoma patients for monitoring of cellular therapy*. Nat Biotechnol, 2005. **23**(11): p. 1407-13.
12. Kiessling, F., *Noninvasive cell tracking*. Handb Exp Pharmacol, 2008(185 Pt 2): p. 305-21.
13. Halwani, R., et al., *Generation and maintenance of human memory cells during viral infection*. Semin Immunopathol, 2006. **28**(3): p. 197-208.
14. Martin-Fontecha, A., et al., *Regulation of dendritic cell migration to the draining lymph node: impact on T lymphocyte traffic and priming*. J Exp Med, 2003. **198**(4): p. 615-21.
15. Nguyen, C.L., et al., *Mechanisms of enhanced antigen-specific T cell response following vaccination with a novel peptide-based cancer vaccine and systemic interleukin-2 (IL-2)*. Vaccine, 2003. **21**(19-20): p. 2318-28.
16. Liu, W. and J.A. Frank, *Detection and quantification of magnetically labeled cells by cellular MRI*. European Journal of Radiology, 2009. **70**(2): p. 258-264.
17. Heyn, C., et al., *Detection threshold of single SPIO-labeled cells with FIESTA*. Magn Reson Med, 2005. **53**(2): p. 312-20.
18. Dekaban, G.A., et al., *Semiquantitation of mouse dendritic cell migration in vivo using cellular MRI*. J Immunother, 2009. **32**(3): p. 240-51.
19. Caux, C., et al., *Activation of human dendritic cells through CD40 cross-linking*. J Exp Med, 1994. **180**(4): p. 1263-72.
20. De Vries, I.J., et al., *Effective migration of antigen-pulsed dendritic cells to lymph nodes in melanoma patients is determined by their maturation state*. Cancer Res, 2003. **63**(1): p. 12-7.
21. Frasca, L., et al., *CD38 orchestrates migration, survival, and Th1 immune response of human mature dendritic cells*. Blood, 2006. **107**(6): p. 2392-9.



22. Oude Engberink, R.D., et al., *Comparison of SPIO and USPIO for in vitro labeling of human monocytes: MR detection and cell function*. *Radiology*, 2007. **243**(2): p. 467-74.
23. Ardavin, C., et al., *Origin and differentiation of dendritic cells*. *Trends in Immunology*, 2001. **22**(12): p. 691-700.
24. Sanchez-Sanchez, N., L. Riol-Blanco, and J.L. Rodriguez-Fernandez, *The multiple personalities of the chemokine receptor CCR7 in dendritic cells*. *J Immunol*, 2006. **176**(9): p. 5153-9.
25. Kleijmeer, M.J., et al., *MHC class II compartments and the kinetics of antigen presentation in activated mouse spleen dendritic cells*. *J Immunol*, 1995. **154**(11): p. 5715-24.
26. Waguri, S., et al., *Different distribution patterns of the two M-6-phosphate receptors in rat liver*. *J Histochem Cytochem*, 2001. **49**(11): p. 1397-405.
27. Rabinowitz, S., et al., *Immunocytochemical characterization of the endocytic and phagolysosomal compartments in peritoneal macrophages*. *J Cell Biol*, 1992. **116**(1): p. 95-112.
28. Ikezu, T., et al., *In vivo coupling of insulin-like growth factor II/mannose 6-phosphate receptor to heteromeric G proteins. Distinct roles of cytoplasmic domains and signal sequestration by the receptor*. *J Biol Chem*, 1995. **270**(49): p. 29224-8.
29. Kambayashi, T., R.P. Wallin, and H.G. Ljunggren, *cAMP-elevating agents suppress dendritic cell function*. *J Leukoc Biol*, 2001. **70**(6): p. 903-10.
30. Rieser, C., et al., *Prostaglandin E2 and tumor necrosis factor alpha cooperate to activate human dendritic cells: synergistic activation of interleukin 12 production*. *J Exp Med*, 1997. **186**(9): p. 1603-8.
31. Altmayr, F., G. Jusek, and B. Holzmann, *Neuropeptide CGRP causes repression of TNF transcription and suppression of ATF-2 promoter recruitment in Toll-like receptor-stimulated DCs*. *J Biol Chem*, 2009.
32. Zhou, W., et al., *Prostaglandin I2 analogs inhibit proinflammatory cytokine production and T cell stimulatory function of dendritic cells*. *J Immunol*, 2007. **178**(2): p. 702-10.
33. Lappin, M.B., et al., *Analysis of mouse dendritic cell migration in vivo upon subcutaneous and intravenous injection*. *Immunol* 1999. **98**(2): p. 181-8.
34. Kimber, I., et al., *Correlation between Lymphocyte Proliferative Responses and Dendritic Cell Migration in Regional Lymph Nodes following Skin Painting with Contact-Sensitizing Agents*. *International Archives of Allergy and Immunology*, 1990. **93**(1): p. 47-53.
35. Fong, L., et al., *Altered peptide ligand vaccination with Flt3 ligand expanded dendritic cells for tumor immunotherapy*. *Proc Natl Acad Sci U S A*, 2001. **98**(15): p. 8809-14.

## **CHAPTER 3      CELLULAR MRI AS A SENSITIVE, NON-INVASIVE MODALITY SUITABLE FOR DETECTING DIFFERENCES BETWEEN THE MIGRATORY EFFICIENCIES OF DIFFERENT DENDRITIC CELL POPULATIONS *IN VIVO***

### **3.1 Introduction**

Dendritic cells (DCs) are the most potent antigen-presenting cells (APCs) of the immune system [1], particularly because of their ability to directly prime naïve T cells in lymph nodes (LNs) [2]. As a result, the use of DCs as adjuvants in immunotherapies such as cell-based cancer vaccines has become an expanding field of research [3-5]. Pre-clinical studies in animal models [6-8] as well as early-phase clinical trials [9-11] have provided promising results in regards to the feasibility and safety of the DC-based cancer vaccine. However, the overall efficacy of this emerging immunotherapy, while superior to alternative cancer vaccine strategies [3, 12], remains low and has yet to reach its full therapeutic potential [13, 14].

Several studies have stressed the importance of the stage of maturation and activation of *ex vivo*-prepared DCs prior to their administration to a patient [15-19]. Mature and active DCs are characterized by a functional shift from antigen up-take to antigen presentation, requiring an increase in surface expression of antigen presentation molecules (MHC class I and II) in conjunction with co-stimulatory molecules (CD80 and CD86) to ensure a non-tolerogenic T cell response. CD40 surface up-regulation is also required for activation of T cells via CD40L ligation [20-26]. DCs remaining in an immature or semi-mature state can induce tolerance against the presented antigen [1, 23, 27-31]. As a result,

investigations into reagents able to mature and activate DCs *in vitro* effectively without resulting in cell exhaustion have been undertaken. DC exhaustion results when these cells are over-activated before reaching the LNs [32], oftentimes resulting in DCs incapable of T cell activation and premature DC death [2]. Recently, a maturation cocktail has been introduced by Jonuleit *et al.*, which consists of TNF- $\alpha$ , IL-1 $\beta$ , IL-6, and PGE<sub>2</sub> [33]. This cytokine cocktail (CC) is considered to be a 'gold standard' that has been used in several DC vaccine clinical studies [34-36]. While this protocol has proven effective at maturing and initiating DC activation, the addition of toll-like receptor (TLR) ligands to cytokine cocktails has been shown to enhance the level of DC maturation and activation [37]. As a result, this study employs a cocktail consisting of TNF- $\alpha$ , IL-1 $\beta$ , IL-6, and PGE<sub>2</sub> and includes the TLR9 ligand CpG on *ex vivo*-generated DCs.

DC maturation also induces a shift in chemokine receptor (CCR) expression, resulting in the down-regulation of CCRs important for tissue confinement (CCR1, CCR5) and the concurrent up-regulation of surface proteins important for migration towards LNs (CCR7, CD38) [38-42]. Increased surface expression of CD38 by mature DCs (mDCs) is important to trigger Ca<sup>2+</sup>-mediated intracellular signalling cascades required to sensitize surface CCR7 responsive to its chemokine ligands (CCLs) 19 and 21 [39, 43]. Therefore, CD38<sup>+</sup>CCR7<sup>+</sup> mDCs migrate efficiently to LNs. It follows, then, that by improving the level of maturation and activation of DCs, there will be a corresponding increase the efficiency with which these mDCs migrate to LNs [16, 17, 44] *in vivo*. As a result, the use of the TLR9 ligand CpG combined with the standard cytokine cocktail

(CpG-CC) was used to mature *ex vivo*-prepared DCs. This CpG-CC stimulated DC population should be more efficient at migration towards target LNs *in vivo*.

It is important to achieve appropriate levels of maturation and activation of *ex vivo*-generated DCs. Nevertheless, in the case of cancer patients, qualitatively and quantitatively assessing which stimulatory cocktail works most effectively at enhancing subsequent *in vivo* DC migration is difficult and conventionally invasive. Thus, a non-invasive imaging modality capable of monitoring the *in vivo* migration of DCs is required. We address this issue in a mouse model and determine if cellular MRI is sufficiently sensitive to quantify differences in the migratory abilities of two different DC populations: untreated vs. *ex vivo*-matured. In order to distinguish our *ex vivo*-generated DCs of interest from surrounding tissues in MR images, DCs must be labelled with an MR contrast agent. For this study, DCs were labelled *in vitro* with the superparamagnetic iron oxide (SPIO) nanoparticle FeREX<sup>®</sup>. First, it was confirmed that the presence of SPIO itself has no effect on DC maturation and activation induced by CpG-CC. Thus, characterization of DC phenotype and function following addition of CpG-CC in the presence and absence of SPIO was carried out. Conventional histological techniques were used to verify the quantitative data obtained from MR images. This study provides important information relevant to tracking the *in vivo* migration of *ex vivo*-prepared and stimulated DCs. Furthermore, it demonstrates that cellular MRI is capable of detecting differences in the migratory efficiencies of different DC populations. Ultimately, results of this study can be applied towards addressing important questions regarding DC-based cancer vaccine optimization for use in human clinical trials.

## **3.2 Methods**

### **3.2.1 Animal Care**

C57BL/6 male mice (6 – 12 weeks) were obtained from Charles River Laboratories Inc. (Kingston, NY) and housed in pathogen-free conditions in the Robarts Barrier Facility at the Robarts Research Institute (London, Ontario) until use. All experiments were undertaken in accordance with Animal Care guidelines with the approval from the Animal Use Subcommittee at the University of Western Ontario, London, Ontario (Appendix 1).

### **3.2.2 Reagents**

RPMI 1640 culture medium (Gibco, Burlington, ON) was supplemented with 10% FBS (Hyclone, Logan, USA), 5 mL penicillin-streptomycin, 5 mL L-glutamine, 5 mL MEM non-essential amino acids, 5 mL sodium pyruvate, 5 mL HEPES buffer solution, and 500 µL 2-mercaptoethanol (Invitrogen, Burlington, ON). Hanks buffered salt solution (HBSS) was from Invitrogen and bovine serum albumin (BSA) was purchased from Sigma-Aldrich (Oakville, ON). Mouse GM-CSF and IL-4 were gifts from Dr. Peta O'Connell (Robarts Research Institute, London, ON) originally provided by Schering-Plough (Kenilworth, NJ). FeREX<sup>®</sup> was obtained from BioPAL (Worcester, MA). Anti-mouse CD11c, CD86, CD80, CD40, and I-A<sup>B</sup> (MHC II) fluorescence conjugated antibodies were purchased from Becton, Dickinson and Co. (BD, Mississauga, ON). Anti-CD8 $\alpha$ , CD11b, CD54, CCR7, and biotinylated CD36, and CD38 antibodies and secondary antibodies (streptavidin-phycoerythrin [SA-PE]) were purchased from eBioscience (San Diego, CA). Respective isotype controls were purchased from the same

companies. Normal goat serum (NGS) was purchased from Sigma-Aldrich (Oakville, ON). Recombinant mouse TNF- $\alpha$  was purchased from R&D systems (Burlington, ON), PGE<sub>2</sub> was obtained from Sigma-Aldrich, recombinant mouse IL-1 $\beta$  and IL-6 were from PeproTech (Rocky Hill, NJ), and un-methylated CpG (ODN1826) was from InvivoGen (San Diego, CA).

### **3.2.3 Generation of murine bone marrow-derived DCs**

DCs used for these experiments were mouse bone marrow-derived DCs (BMDCs). DCs were prepared and enriched as previously described [45]. Briefly, bone marrow cells were collected from the femurs and tibias of C57BL/6 mice and red blood cells (RBCs) were lysed using ACK lysis buffer. B220 and MHC II positive cells were depleted using antibody-specific complement-mediated lysis (Cedarlane Laboratories, Burlington, ON). Cells were re-suspended at a concentration of  $3 \times 10^5$  cells/mL in complete RPMI 1640 medium and cultured for 4 days at 37°C in the presence of GM-CSF (4 ng/mL media) and IL-4 (1000 U/mL media). Enrichment of DCs was performed on day 4 using HistoDenz (13.5% w/v, Sigma-Aldrich) gradient centrifugation.

### **3.2.4 DC Maturation Cocktail**

Following enrichment on day 4, DCs were treated overnight with the maturation cocktail (CpG-CC) in order to mature and activate them. TNF- $\alpha$  (25 nM), IL-1 $\beta$  (10 nM), IL-6 (25 nM), PGE<sub>2</sub> ( $10^{-6}$  M), and CpG (0.2  $\mu$ M) were added and cells were left to incubate overnight for 20 hours at 37°C. DCs were left untreated to serve as a control.

### **3.2.5 SPIO Labelling**

SPIO labelling (FeREX, 200 µg Fe/mL) was carried out after enrichment during overnight incubation for 20 hours at 37°C in the presence of CpG-CC stimulation. Cells stimulated with CpG-CC but not given SPIO served as the appropriate control.

### **3.2.6 Magnetic separation of SPIO<sup>+</sup> DCs from SPIO<sup>-</sup> DCs**

SPIO DCs were collected on day 5 and washed 3 times with cold HBSS + 0.1% bovine serum albumin (BSA) to remove any free iron nanoparticles. Cells were transferred to a 12x75 mm tube and re-suspended in 2.5 mLs of cold HBSS + 0.1% BSA. The tube was put in an EasySep magnet (StemCell Technologies, Vancouver, BC) for 5 minutes. The supernatant was poured off into a second 12x75 mm tube, which was subsequently put into the EasySep magnet to collect any remaining SPIO-labelled DCs. The supernatant containing unlabelled (SPIO<sup>-</sup>) cells was poured off into another 12x75 mm tube. SPIO-labelled (SPIO<sup>+</sup>) cells were pooled together. Both cell populations were counted to determine the efficiency of SPIO labelling.

### **3.2.7 Detection of surface antigens**

Cells were collected from overnight cultures on day 5 and washed 3X with HBSS + 0.1% BSA. Cells were blocked in 5% v/v normal goat serum (NGS) and washed 1X following a 20-minute incubation at 4°C (on ice). CCR7 staining was carried out first at 20°C (room temperature) for 20 minutes in the dark. Cells were washed 1X and stained with all other required antibodies at 4°C (on ice) in the

dark. Flow cytometry was performed using a FACSCalibur (BD) and analyzed with CellQuest Pro (BD) and FlowJo software (Tree Star Inc., Ashland, OR).

### **3.2.8 Luminex<sup>®</sup> cytokine assays**

The Luminex<sup>®</sup> Cytokine Mouse 10-plex Panel antibody detection kit, reagents, and buffers were obtained from Invitrogen. The Luminex<sup>®</sup> assay was used according to the manufacturer's protocol to analyze the cytokine profiles of supernatants collected from overnight cultures of DCs that received CpG-CC and/or SPIO. Supernatants collected from UT DCs or CpG-CC DCs served as controls. All incubations were carried out at room temperature in the dark. Briefly, test samples or serial dilutions of kit standards were incubated for 2 hours with the Luminex detection beads provided. After washing with assay wash buffer, biotinylated primary antibody was added and incubated for 1 hour. Following another wash step, SA-PE was added to wells and plates were incubated for an additional 30 minutes. After a final three washes, plates were analyzed using the Luminex 100 plate reader and IS 2.3 Software (both from Luminex Corporation, Austin, TX). A minimum of 400 events (beads) was collected for each cytokine per sample, and mean fluorescence intensities were obtained.

### **3.2.9 Labelling DCs with PKH**

DCs were collected from day 5 cultures and washed 1X in cold PBS. The membrane intercalating dye, PKH26 (red), was used to label DCs for histological detection as per manufacturer's instructions (Sigma-Aldrich). Briefly, DCs were re-suspended in Diluent C (Sigma Aldrich) and incubated with  $2 \times 10^{-6}$  M of PKH dye for no longer than 3 minutes. Excess dye was removed by incubating cells



with 2 mLs of FBS for 1 minute. Cells were washed, first in complete RPMI 1640 media, then in HBSS + 0.1% BSA, and finally in PBS. Following the final wash, cells were re-counted and re-suspended accordingly in PBS for adoptive transfer.

### **3.2.10 Adoptive transfer of DCs**

PKH-labelled DCs were adoptively transferred via subcutaneous injection into the hind footpads of C57BL/6 mice. Briefly, either  $3 \times 10^5$  or  $1 \times 10^6$  PKH-labelled SPIO<sup>+</sup> or CpG-CC-SPIO<sup>+</sup> DCs were administered into the right hind footpads (n=4). Untreated or CpG-CC DCs were used as the respective controls and were administered to the contralateral footpads at the appropriate dose.

### **3.2.11 Magnetic resonance imaging of DC migration**

Mice were imaged 2 days post-adoptive transfer. MRI was performed using a 1.5T clinical scanner (GE Medical Systems, Milwaukee, WI) with a custom gradient-coil insert as previously described [45]. Briefly, a 3-D FIESTA (GE Medical Systems) imaging pulse sequence was used, and scan times averaged 23 minutes. Spatial resolution was  $200 \mu\text{m}^3$  and slice thickness was 200  $\mu\text{m}$ . MR images were analyzed for signal void volume, and fractional signal loss (FSL) as previously described (Chapter 2.2).

### **3.2.12 LN removal and cryostat sectioning**

Following MR scans, mice were euthanized by CO<sub>2</sub> inhalation and popliteal LNs (behind the knee) were removed. LNs were fixed overnight in 4% v/v paraformaldehyde (PFA) at 4°C, LNs were cryo-protected by overnight incubations in increasing concentrations of sucrose (10%, 20%, 30%) to prepare

them for cryostat sectioning. For sectioning, LNs were embedded in optimal cutting temperature (OCT) compound (Sakura Finetek U.S.A. Inc., Torrance, CA) and serial sections were cut using a Leica CM3050S cryostat (Leica Microsystems, Wetzlar, Germany). Serial sections were cut and mounted onto sets of four alternating Plus Slides (VWR International, Westchester, PA). Slides were cover-slipped with PBS for histological analysis.

### **3.2.13 Histological analysis and quantification**

To verify MR results of *in vivo* DC migration, conventional histological analysis of DC migration was performed. To determine the area of PKH26 (red) fluorescence, digital images (10X) were collected using an Olympus BX50 microscope (Olympus America Inc. Centre Valley, PA) equipped with an Olympus IX50 digital camera (Olympus America Inc.) and digital morphometry (Image Pro v4.0) was used to determine the area of fluorescence (DCs): area of interest (popliteal LN) [45]. Briefly, the area of interest was selected manually and a threshold for fluorescence intensity was set such that any PKH<sup>+</sup> fluorescence above this threshold was included in the area of fluorescence.

### **3.2.14 Statistical analysis**

All data were expressed as means and standard error means. Statistical significance was determined using a repeated measures ANOVA followed by a post-hoc Tukey's Test. Differences were considered significant if  $p < 0.05$ . Correlation between MRI and histological data was determined using a linear rank correlation.

### 3.3 Results

#### 3.3.1 CpG and cytokine cocktail (CpG-CC) stimulation leads to a DC population with a mature and migratory competent phenotype

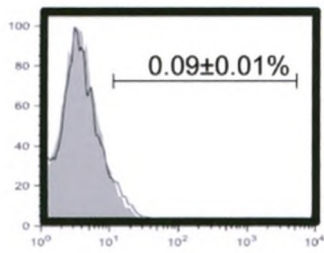
In order to determine if cellular MRI is capable of detecting differences in migration to popliteal LNs between control and matured and activated DCs, a mature, active, and therefore migratory competent DC population was required. Various stimulatory reagents in different combinations were used to determine which were the most effective at maturing and activating our DCs *in vitro*. The TLR 9 ligand CpG was used in these studies because it is known to trigger potent Th 1 type maturation/activation of DCs [46, 47]. It is important to note that while TLR 9 is known to be expressed by human myeloid DCs [48], there is debate as to whether mouse monocyte-derived DCs express TLR 9. However, intracellular staining for TLR 9 demonstrated that our mouse bone marrow-derived DCs used in these experiments express TLR 9 (Fig. 3.1). These findings confirm the results of other studies investigating the expression of TLR 9 by mouse DCs [49, 50]. Importantly, SPIO has no effect on TLR 9 expression.

The standard CC (IL-1 $\beta$ , IL-6, TNF- $\alpha$ , and PGE<sub>2</sub>) with the addition of CpG (CpG-CC) was used to mature and activate enriched DCs overnight. UT cells were used as controls. Flow cytometric analysis was used to determine the effect of each of these treatments on DC maturation (CD86), migration (CCR7, CD38), and activation (CD40) (Fig. 3.2). It was determined that overnight stimulation of DCs with CC stimulation only enhanced the maturation of the DC population based on the percentage of CD86+ cells, PGE<sub>2</sub> had no significant effect on



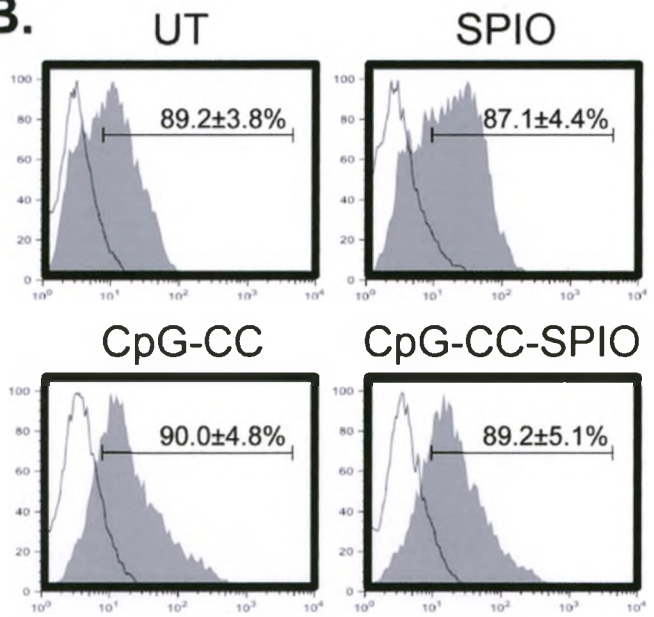
**Figure 3.1. Mouse BMDCs express intracellular TLR9.** DCs were stimulated with CpG-CC overnight in the presence or absence of SPIO. Cells were left untreated to serve as a control. Intracellular staining for TLR9 and flow cytometric analysis were used in order to confirm expression of TLR9 by mouse DCs. **(A)** Cells not permeabilized prior to TLR9 antibody staining served as a negative control. **(B)** Both CpG-CC and UT DCs express TLR9. SPIO has no significant effect on its expression. Histograms are gated on viable CD11c<sup>+</sup> cells and are representative of 3 independent experiments. Numbers above the bars are mean positive cells (%)  $\pm$  SE from three independent experiments; differences are not significant ( $p > 0.05$ ).

**A.**



MFI  $\longrightarrow$

**B.**

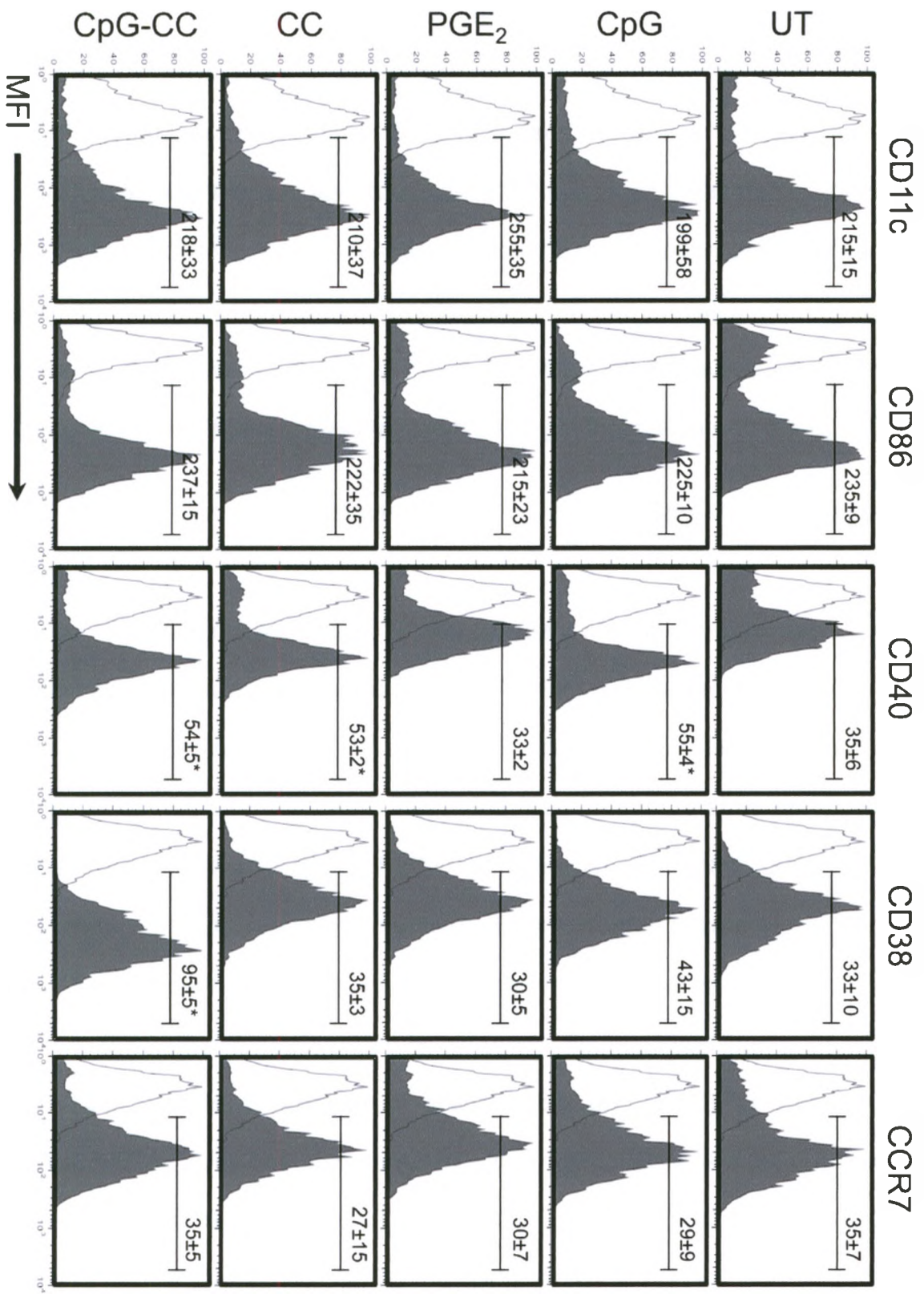


MFI  $\longrightarrow$



**Figure 3.2. *In vitro* CpG-CC stimulation produces a mature and active population of DCs.** DCs were treated with the TLR 9 ligand CpG, PGE<sub>2</sub>, CC, or CpG-CC. Following overnight incubation for 20 hours, cells were phenotypically characterized by staining for several DC surface markers and analyzed using flow cytometry. Untreated (UT) DCs served as a control. CpG-CC stimulation significantly increased surface expression (MFI) of DC migration (CD38) and activation (CD40) markers. CD11c histograms are gated on viable cells, while all other histograms are also gated on CD11c<sup>+</sup> cells. Histograms are representative of 3 independent experiments. Numbers in top right corners indicate the mean MFI ± SE for all three experiments combined. Differences for each marker are significantly different from control (UT) if p<0.05 (\*).





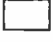


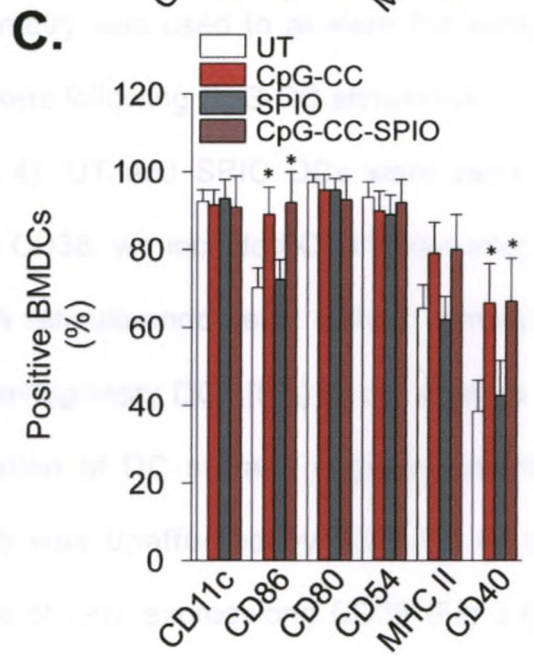
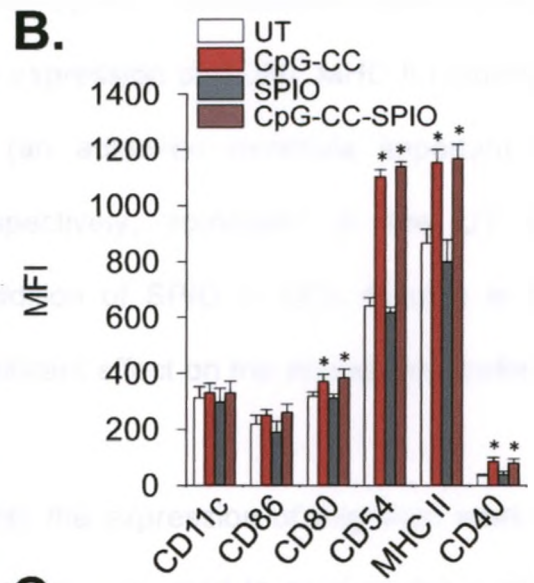
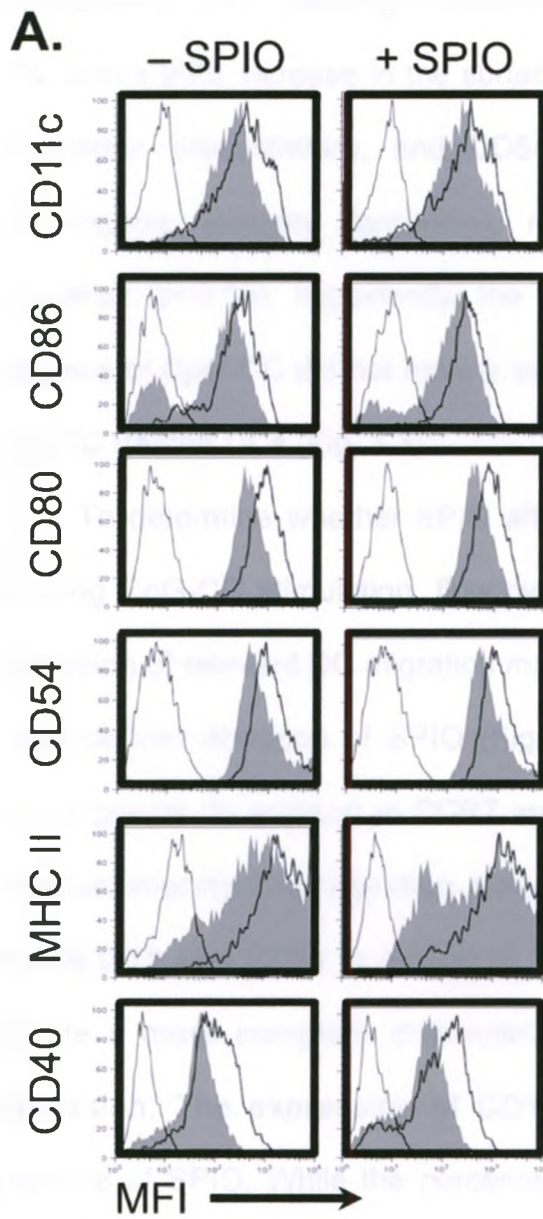
surface expression of any of the maturation or activation markers. TLR (CpG) and CpG-CC stimulation enhanced both the number of cells by how much and the MFI by how much of CD86 and CD40 surface expression. However, only the CpG-CC combination was able to enhance by how much the surface expression of proteins important for DC migration. Since the combination of both the TLR9 ligand CpG and the CC resulted in both maturation and activation plus induced a migration competent phenotype in the day 5 DC, in all subsequent experiments DC were matured and activated using an overnight incubation with the CpG-CC .

### **3.3.2 SPIO has no significant effects on *in vitro* CpG-CC stimulation of DCs**

Cellular MRI requires the use of a contrast agent in order to distinguish cells of interest from the surrounding tissues in MR images. As a result, we needed to verify that SPIO labelling did not significantly affect CpG-CC-induced maturation and activation of DCs. DCs were stimulated overnight in the absence (CpG-CC) and presence (CpG-CC-SPIO) of SPIO nanoparticles. Untreated (UT) and SPIO DCs were used as respective controls. Flow cytometric analysis of several important DC maturation and activation markers was carried out (Fig. 3.3). In order to determine the expression levels (mean fluorescence intensities [MFIs]) (Fig. 3.3B) and the percentage of positive cells (Fig. 3.3C) for each surface marker, CD11c<sup>+</sup> histograms were gated with a 5% confidence interval based on the appropriate isotype controls. CpG-CC DCs show, on average, a 20% increase in the percentage of CD11c<sup>+</sup> cells which express CD86 (Fig. 3.3C) compared to UT DCs. The level of CD40 surface expression increased by 2.4X





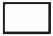
**Figure 3.3. SPIO labelling does not affect CpG-CC-induced phenotypic maturation and activation of DCs.** DCs were stimulated overnight with TLR-CC in the absence or presence of SPIO. Untreated cells (UT) or cells labelled with SPIO served as controls. **(A)** Representative histograms for each DC marker from 3 independent experiments are shown. Cells stimulated with CpG-CC are shown as  while cells left unstimulated are depicted as . Isotypes are depicted as . CD11c histograms are gated on viable cells, while all other histograms are also gated on CD11c<sup>+</sup> cells. Quantification of flow cytometry results was carried out to determine the **(B)** mean fluorescence intensities (MFI) and **(C)** percentage of cells positive for each DC marker analyzed. SPIO has no effect on either the MFI or the percentage of positive cells following CpG-CC stimulation. Data are means  $\pm$  SE (n=3). Differences are significant from control cells if  $p < 0.05$  (\*).



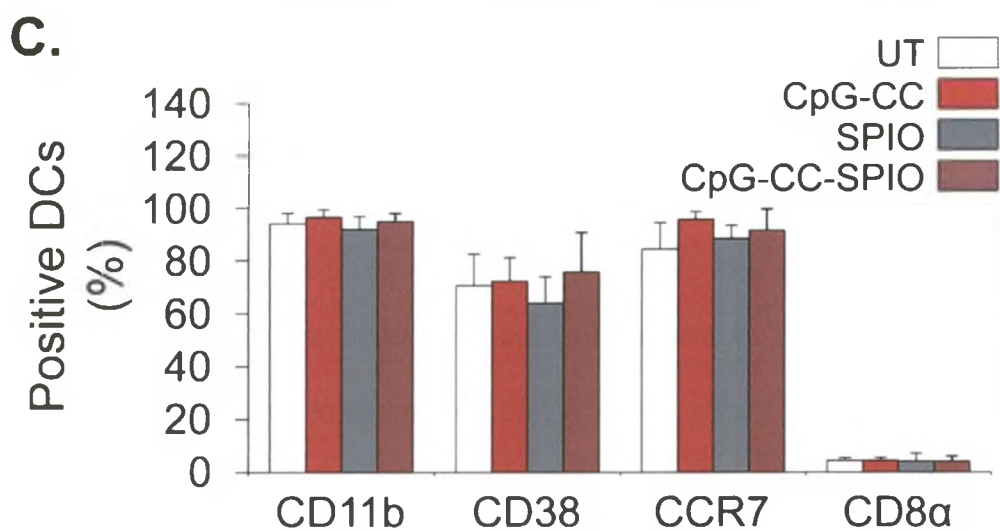
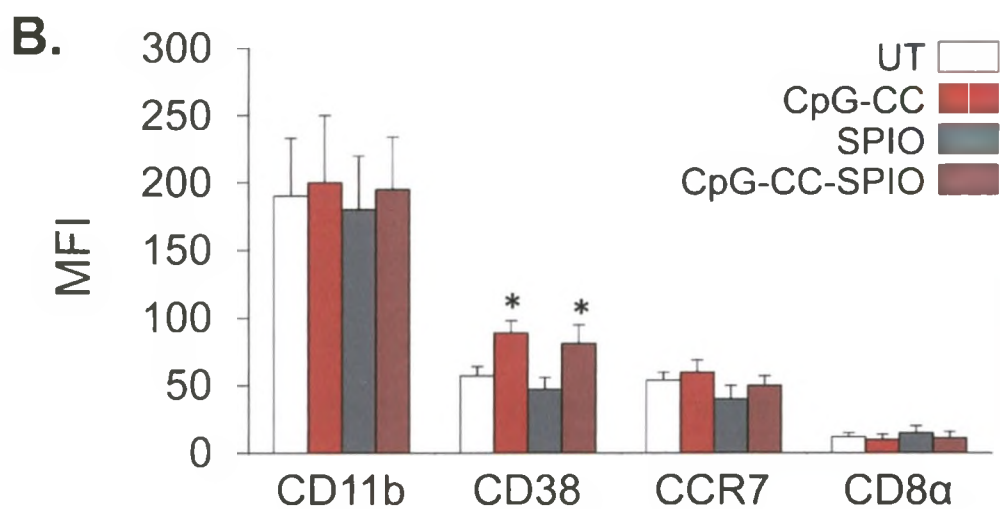
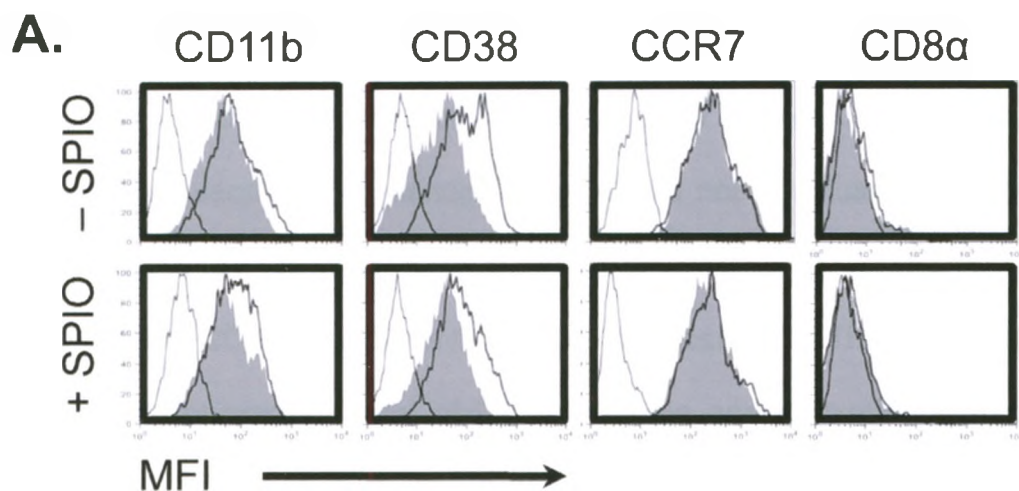
following CpG-CC stimulation (Fig. 3.3B) and the percentage of CD40<sup>+</sup> DCs roughly doubled by 50% (Fig. 3.3C). This trend was significant ( $p < 0.05$ ) and was unaffected by SPIO labelling. Furthermore, CpG-CC stimulation induced a 10%, 30%, and a 90% increase in the surface expression of CD80, MHC II (important for antigen presentation), and CD54 (an adhesion molecule important for immunogenic synapse formation), respectively, compared to the UT DC population ( $p < 0.05$ ). Importantly, the addition of SPIO to DCs cultures in the presence of CpG-CC did not have a significant effect on the phenotypic profile of CpG-CC treated DCs (Fig. 3.3).

To determine whether SPIO affects the expression of migration markers following CpG-CC stimulation, flow cytometry was used to analyze the surface expression of relevant DC migration markers following CpG-CC stimulation in the presence and absence of SPIO (Fig 3.4). UT and SPIO DCs were used as control groups. In addition to CCR7 and CD38, we included CD11b (an integrin molecule important to migration through reticulo-endothelial cells of lymphatic vessels [51]) and CD8 $\alpha$  (a marker of non-migratory DCs [52]) in our analysis to provide a more complete characterization of DC surface migration marker expression. The expression of CD11b was unaffected by CpG-CC or the presence of SPIO. While the percentage of cells expressing CD38 (Fig 3.4C) remained unaltered by either the CpG-CC and SPIO, culturing with CpG-CC significantly enhanced the level of surface expressed CD38 by XX% (Fig. 3.4B). Neither the percentage of CCR7<sup>+</sup> DC nor the level of CCR7<sup>+</sup> surface expression was affected by the CpG-CC and SPIO (Fig. 3.4C) following stimulation of DCs (Fig. 3.4B). Also, both level and percentage expression of CD8 $\alpha$  was not



**Figure 3.4. SPIO labelling does not affect CpG-CC-induced surface expression of DC migration markers.** Flow cytometry was used to characterize DCs for several surface markers relevant to migration following overnight incubation with CpG-CC in the absence or presence of SPIO. Untreated (UT) and SPIO DCs served as respective controls. **(A)** Representative histograms for each DC migration marker from 3 independent experiments. Cells stimulated with CpG-CC are shown as  while cells left unstimulated are depicted as . Isotypes are depicted as . CD11c histograms are gated on viable cells, while all other histograms are also gated on CD11c<sup>+</sup> cells. Quantification of flow cytometry results was carried out to determine the **(B)** mean fluorescence intensities (MFI) and **(C)** percentage of cells positive for each DC migration marker analyzed. SPIO has no effect on the percentage of positive cells following CpG-CC stimulation. Data are means  $\pm$  SE (n=3). Differences are significant from control cells if  $p < 0.05$  (\*).





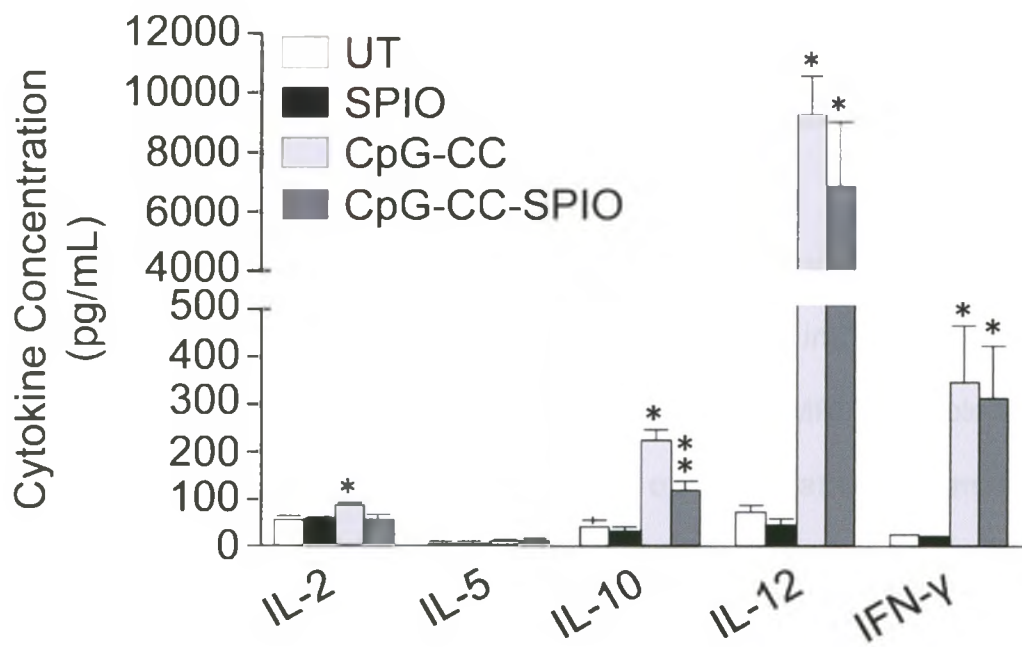
significantly different than that of the isotype control as one would expect for a migratory competent population of DC. Overall, the addition of SPIO had no significant effects on the expression of migratory markers of CpG-CC-DCs (Fig. 3.4). Consequently, SPIO nanoparticles should not significantly affect the ability of these cells to migrate *in vivo*.

### **3.3.3 CpG-CC-DCs secrete cytokines necessary for Th1 type responses**

While the appropriate level of DC maturation and activation surface marker expression is important in mediating T cell-mediated anti-tumour responses *in vivo*, the secretion of cytokines which favour immunogenic (IL-2, IL-12, IFN- $\gamma$ ) rather than tolerogenic (IL-10) is of equal importance. To confirm that CpG-CC stimulation produces DCs capable of stimulating T cell-mediated immunogenic responses *in vivo*, we analyzed the cytokine profiles of our DCs, important for future studies in our laboratory. Furthermore, it was important to determine if SPIO labelling was affecting the secreted cytokine profiles of CpG-CC-DCs. Supernatants from CpG-CC-DCs cultured in the presence or absence of SPIO nanoparticles were analyzed using the Luminex cytokine mouse 10-plex (IL-1  $\beta$ , IL-2, IL-4, IL-5, IL-6, IL-10, IL-12, GM-CSF, TNF- $\alpha$ , IFN- $\gamma$ ). Supernatants from UT and SPIO DCs were used as appropriate controls. It is important to note that our DC *in vitro* culture protocol requires the addition of mouse IL-4 and GM-CSF. In addition, CpG-CC contains the mouse cytokines IL-1 $\beta$ , IL-6, and TNF- $\alpha$ . As a result, no conclusive statements can be made about these cytokines in regards to CpG-CC stimulation and they were accordingly excluded from our analysis. Significant increases in secretion of IL-12 and IFN- $\gamma$  were observed following cocktail stimulation ( $p < 0.05$ ), important mediators of Th1 type



**Figure 3.5. CpG-CC stimulation induces BMDCs to secrete Th 1 type cytokines *in vitro*.** Supernatants were collected from overnight cultures of DCs stimulated with CpG-CC in the absence and presence of SPIO. Supernatants from untreated (UT) and SPIO DCs were used as respective controls. Luminex assays were used to analyze the cytokines secreted by each DC population. A significant increase in IL-12 secretion was induced following CpG-CC stimulation. Significant increases in IFN- $\gamma$  and IL-10 were also seen compared to UT control cells. While SPIO labelling has no effect on Th 1 type cytokine release (IL-12, IFN- $\gamma$ ), it does significantly decrease the CpG-CC-induced increase in IL-10 secretion by DCs *in vitro*. Data are means  $\pm$  SE from 3 independent experiments. Differences are significant from UT or SPIO controls (\*) and CpG-CC and CpG-CC SPIO are significantly different from each other (\*\*) if  $p < 0.05$ .



responses (Fig. 3.5). While there was a significant increase in IL-10 secretion for CpG-CC and CpG-CC-SPIO DCs compared to the UT and SPIO DC controls. However, the levels of IL-10 secretion was significantly lower than that of IL-12 levels ( $P>0.05$ ) in the presence and absence of SPIO following CpG-CC stimulation. The secretion levels of the other cytokines analyzed (IL-2 and IL-5) were not significantly altered following cocktail stimulation ( $p>0.05$ ). Importantly, there were no significant effects of SPIO on CpG-CC-induced cytokine secretion ( $p>0.05$ ).

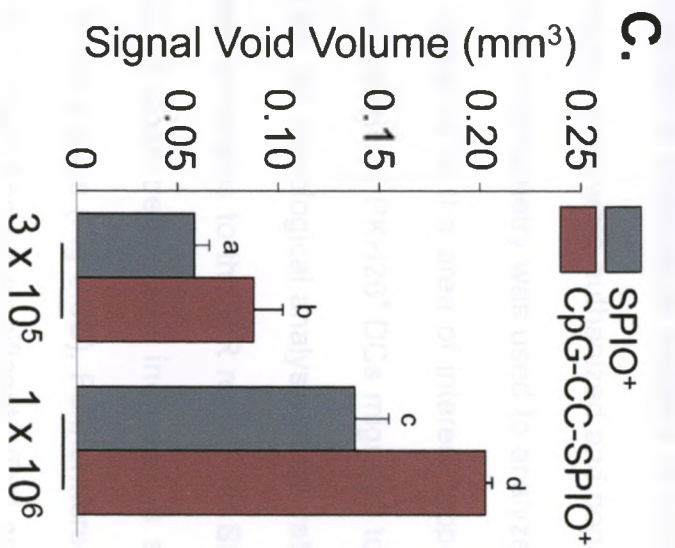
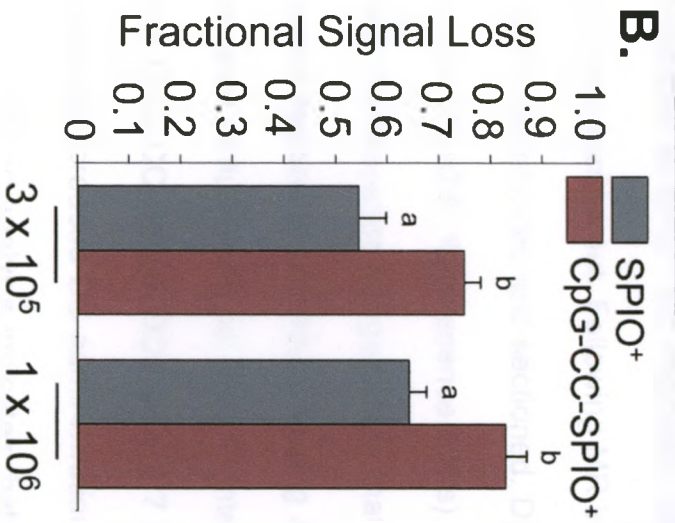
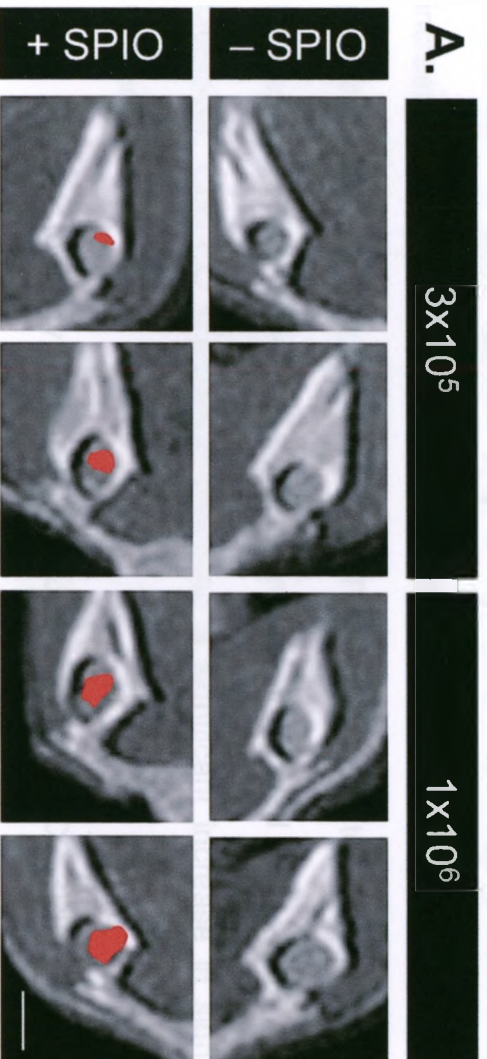
#### **3.3.4 CpG-CC stimulation enhances DC migration to target LNs *in vivo*, as assessed with cellular MRI**

It was confirmed that labelling our DCs with the MR contrast agent SPIO was not significantly affecting the maturation and activation induced by CpG-CC stimulation. As a result, I wanted to determine if cellular MRI was able to detect differences between the *in vivo* migration of the relatively immature DC population (SPIO<sup>+</sup>) and the mature and active DC population (CpG-CC-SPIO<sup>+</sup>) to popliteal LNs. Adoptive transfer of either  $3 \times 10^5$  or  $10^6$  SPIO<sup>+</sup> and CpG-CC-SPIO<sup>+</sup> DCs was performed via subcutaneous injection into right hind footpads of C57BL/6 mice ( $n=4$  for each treatment). UT (no CpG-CC treatment) and CpG-CC DCs served as the respective controls and were injected into the left hind footpads. Two days post injection, cellular MRI was used to assess the *in vivo* migration of our two DC populations (Fig. 3.6). Fractional signal loss (FSL) and the signal void volume can be used to determine the amount of signal lost due to the presence of the SPIO negative contrast agent. Therefore, FSL was



**Figure 3.6. MRI can detect differences between migration of SPIO<sup>+</sup> and CpG-CC-SPIO<sup>+</sup> DCs *in vivo*.** Either  $3 \times 10^5$  or  $1 \times 10^6$  PKH<sup>+</sup>SPIO<sup>+</sup> or PKH<sup>+</sup>CpG-CC-SPIO<sup>+</sup> DCs were adoptively transferred into C57BL/6 mice (n=4) via subcutaneous hind footpad injections. Control cells (PKH<sup>+</sup>DCs or PKH<sup>+</sup>CpG-CC DCs) were injected into contralateral hind footpads. Mice were imaged with MRI 2 days post adoptive transfer. (A) Representative cropped images of popliteal LNs from each group are shown and are representative of 2 independent experiments. Areas of signal void are pseudocoloured in red. Scale bar = 2 mm. MR images were analyzed for (B) fractional signal loss (FSL) and (C) signal void volumes. CpG-CC-SPIO<sup>+</sup> DCs migrated more efficiently than SPIO<sup>+</sup> DCs, resulting in greater FSLs and larger signal void volumes at both doses. Furthermore, a dose-responsive increase in signal void volume was observed when more DCs were administered. Data are means  $\pm$  SE and are significantly different if superscript letters are different (p<0.05).



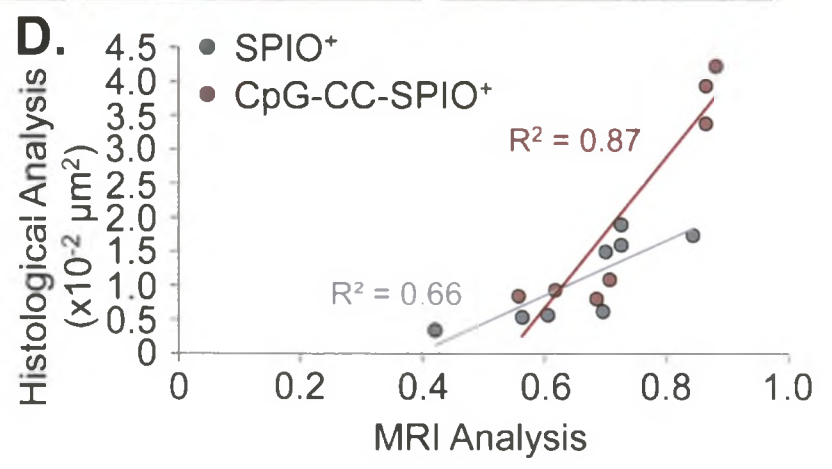
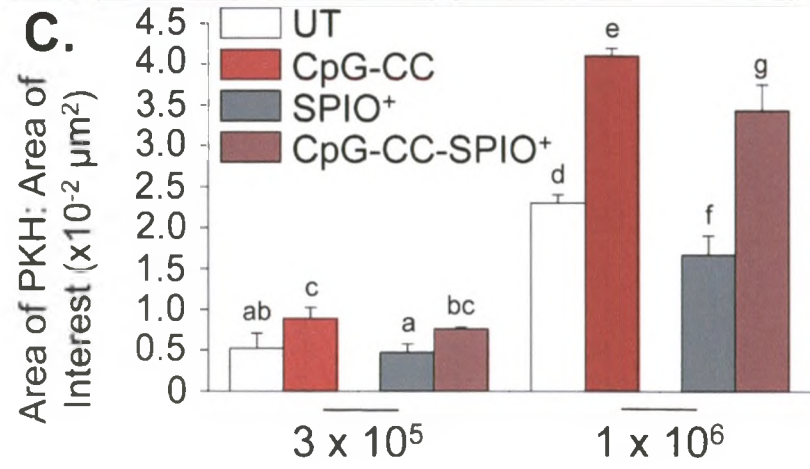
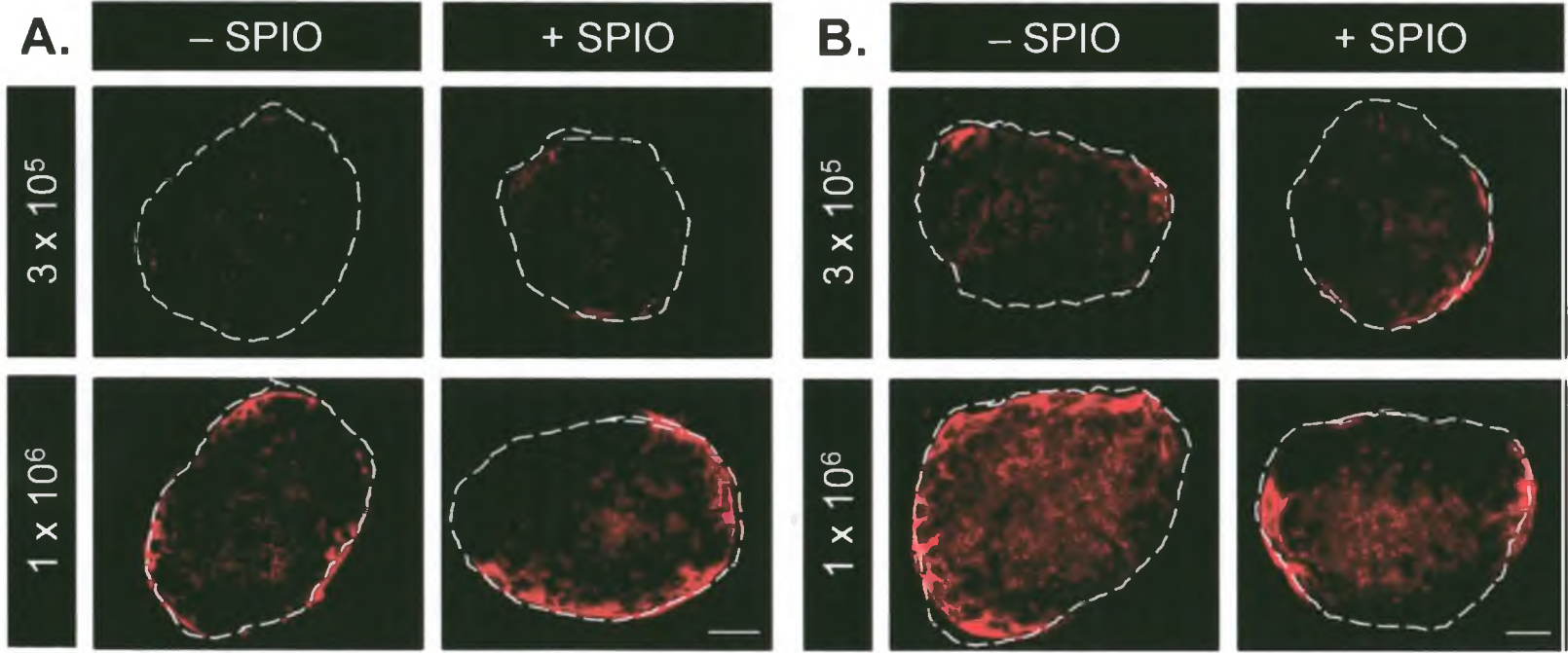


calculated based on the signal intensity measured in the LNs which received DCs labelled with SPIO (SPIO<sup>+</sup> or CpG-CC-SPIO<sup>+</sup>) from MR images. According to the FSL, DC prepared in the presence of the CpG-CC exhibited significantly enhanced *in vivo* migration (Fig. 3.6B). Also, there was a dose-dependent increase in FSL with increasing DC number. Measuring the signal void volume in popliteal LNs that received CpG-CC-SPIO<sup>+</sup> DCs indicated a dose responsive increase in void volume as cell numbers increased (Fig. 3.6C,  $p < 0.05$ ). Moreover, CpG-CC stimulation produced a significant increase in signal void volume.

In order to verify MRI-detected increases in CpG-CC-SPIO<sup>+</sup> DC migration compared to SPIO<sup>+</sup> DC migration, conventional histological analysis of popliteal LNs was carried out. Following MR imaging, mice were euthanized and popliteal LNs were removed and sectioned. Digital morphometry was used to analyze the area of PKH26<sup>+</sup> fluorescence (DCs) compared to the area of interest (popliteal LN). Fluorescence images show that all groups of PKH26<sup>+</sup> DCs migrated to the central regions of popliteal LNs (Fig 3.6A, B). Histological analysis of the ratio of the area of fluorescence: area of interest correlates to the MR results for SPIO<sup>+</sup> and CpG-CC-SPIO<sup>+</sup> DCs (Fig 3.7 C). A dose-dependent increase is seen following increased DC administration for all groups (Fig 3.6C). Furthermore, the morphometric analysis indicates that SPIO itself has no significant effect on the enhancement of migration following CpG-CC stimulation. Importantly, histological data shows a correlation with MRI analysis of void volume (Fig. 3.7D).



**Figure 3.7. Histological analysis of *in vivo* migration correlates with MRI data and indicates SPIO has no effect on CpG-CC-enhanced *in vivo* migration.** Either  $3 \times 10^5$  or  $1 \times 10^6$  PKH<sup>+</sup>SPIO<sup>+</sup> or PKH<sup>+</sup>CpG-CC-SPIO<sup>+</sup> DCs were adoptively transferred into C57BL/6 mice (n=4) via subcutaneous hind footpad injections. Control cells (PKH<sup>+</sup>DCs or PKH<sup>+</sup>CpG-CC DCs) were injected into contralateral hind footpads. Following MRI scans 2 days post adoptive transfer, popliteal LNs were removed and analyzed for the area of PKH<sup>+</sup> fluorescence using digital morphometry. Representative images of LNs from mice administered either (A) UT DCs or (B) CpG-CC DCs are shown. Data are representative of 2 independent experiments. Scale bar = 500  $\mu$ m. (C) CpG-CC stimulation is able to significantly enhance *in vivo* migration of DCs. Importantly, SPIO does not interfere with the enhancement of *in vivo* migration by CpG-CC stimulation. Data are means  $\pm$  SE and are different if superscript letters are different ( $p < 0.05$ ). (D) Linear correlation of histological analysis with MRI analysis (FSL) indicates a positive correlation (slope  $> 0$ ) between between the two data sets.



### 3.4 Discussion

The targeted migration of clinical-grade DCs to LNs in cancer patients *in vivo* is critical for generating effective T cell-mediated anti-tumour responses. Based on data compiled from recent DC-based cancer vaccine clinical trials, the efficacy of this emerging immunotherapy has not yet reached its full potential. In part, this is due to the fact that fewer than 5% of *ex vivo*-generated DCs are actually reaching target LNs [44]. It has been determined that efficient migration to LNs is a hallmark of mature and appropriately activated DCs [16, 17, 53]. Therefore, the ability to generate a mature and an appropriately activated population of DCs *in vitro* is of significant importance when it comes to improving DC-based cancer vaccines. While a number of studies have investigated various pro-inflammatory agents and developed a number of cocktails capable of achieving DC maturation *in vitro* [33, 44, 54-57], their relative abilities to actually improve *in vivo* migration to LNs in clinical patients is largely unknown. Specifically, a non-invasive imaging modality sensitive enough to track and quantify the amount of *in vivo* migration of clinical-grade DCs in patients would be useful in determining which maturation agents are most beneficial. This, in turn, can be related qualitatively and quantitatively to the tumour antigen-specific immune responses being elicited by the DC-based cancer vaccine. Therefore, this study set out to determine if cellular MRI is capable of detecting differences between the *in vivo* migration efficiencies of a mature DC population compared to a control, resting (unstimulated) DC population in a mouse model.

Immature mouse DCs generated from bone marrow monocyte precursors *in vitro* exhibit higher expression levels of MHC and co-stimulatory molecules on their surface compared to immature DCs *in vivo* due to the presence of GM-CSF and IL-4 in the culture medium [58]. Regardless, these DCs are neither sufficiently phenotypically nor functionally mature. In order to generate an *ex vivo* population of DCs that are properly mature and activated, incubation with a cytokine cocktail (CC) of pro-inflammatory cytokines (IL-1 $\beta$ , IL-6, TNF- $\alpha$ , and PGE $_2$ ) has been used [33]. However, these CC-treated DCs do not produce significant levels of IL-12-p70, the active form of IL-12 [57], which is important for polarizing Th cells towards the Th 1 phenotype. Similarly, DCs matured with only TNF- $\alpha$  acted to tolerize CD4 $^+$  T cells *in vivo* [59]. Thus, insufficient or inappropriate maturation can produce DCs that are still not optimal for use in cell-based vaccines [16, 29, 60, 61]. DCs recognize evolutionarily conserved pathogen-associated molecular patterns (PAMPs). PAMPs are recognized by DCs by pattern recognition receptors (PRRs), or Toll-like receptors (TLRs), which are transmembrane receptors. Stimulation of DCs using PAMPs induces DC maturation along with appropriate Th 1 type cytokine production. For instance, DCs matured with lipopolysaccharide (LPS) plus anti-CD40 induced a Th 1 phenotype and did not mediate tolerance [62-65]. Recently, Napolitani *et al* [62] demonstrated that TLR ligation leads to the induction of high amounts of IL-12, leading to a Th 1 polarized helper T cell response. Furthermore, it has also been demonstrated that the use of TLR ligands in combination with pro-inflammatory cytokines is able to produce a DC population with a more mature and active phenotype [37]. Taken together, these data suggest that the use of the gold

standard CC in conjunction with TLR ligation might be optimal in inducing DC maturation that supports efficient migration to a lymph node and Th 1-type response required for a cancer vaccine to be effective.

Based on this rationale, the TLR 9 ligand CpG and pro-inflammatory cytokines were used in various combinations to determine which would result in a phenotypically mature, active, and therefore migratory competent DC population. Overnight culture of DCs with CpG, PGE<sub>2</sub>, or the CC alone produced mixed results. CpG was able to enhance the level of DC maturation and activation, as determined by an increase in surface expression of CD86 and CD40, respectively, while stimulation with PGE<sub>2</sub> or the CC alone only produced modest increases in these two surface markers. These results are consistent with findings from another study [50], which determined that CpG is capable of inducing immature mouse DCs to mature and activate into competent, APCs. While CpG appeared effective in terms of CD86 and CD40 expression, the surface expression of CCR7 and CD38, both important for the migration of DCs to LNs, remained unaffected. Likewise, neither CC nor PGE<sub>2</sub> stimulation was able to enhance the surface expression of these migration markers. Interestingly, PGE<sub>2</sub> was unable to improve CD38 expression, although it is known to be linked to its surface expression. Related studies investigating the effects of PGE<sub>2</sub> on CD38 expression involved longer PGE<sub>2</sub>-mediated stimulation (48-72 hours) of DCs *in vitro*. This could provide an explanation as to why no change in surface CD38 expression was seen following overnight PGE<sub>2</sub> stimulation (20 hours) used by these experiments [33, 40, 42, 66, 67]. The combination of CpG with CC (CpG-CC) stimulation resulted in the up-regulation of CD86 and CD40, as well as



key mediators of *in vivo* DC migration (CCR7 and CD38). Recently, it has been determined that although the surface expression of CCR7 is required for the migration of DCs to chemokine ligands 19 and 21 (CCL19, CCL21), it is not sufficient [66, 68]. A study investigating the role of PGE<sub>2</sub> suggested that CCR7 pathways must be activated by activating Ca<sup>2+</sup> channels, which is mediated by the ecto-enzyme CD38 [66].

My ultimate goal was to investigate the ability of cellular MRI to detect differences of *in vivo* migration between UT DCs and DCs matured and activated with the CpG-CC. In order to do this, I labelled DCs with SPIO (FeREX) to detect them in MR images. Therefore, I needed to confirm that SPIO was not affecting the TLR-CC-mediated stimulation of the DCs cultured *in vitro*. I performed a more complete analysis of DC surface marker expression using flow cytometry. Following CpG-CC stimulation, an enhanced expression level and rate of the important co-stimulatory molecules (CD80, CD86) and antigen presentation molecules (MHC) was observed. The co-expression of co-stimulatory molecules and antigen presentation molecules is important for DCs to have an immunostimulatory rather than a tolerogenic phenotype [29].

It was also important to ensure that the effect of the CpG-CC in the presence of SPIO did not alter the expression of surface molecules important to DC migration. In the context of DC migration, I assessed whether SPIO induced the expression of CD8 $\alpha$ , believed to be expressed by non-migratory DCs [69]. Specifically, CD11c<sup>+</sup>CD8 $\alpha$ <sup>+</sup> DCs migrate less efficiently compared to CD11c<sup>+</sup>CD8 $\alpha$ <sup>-</sup> DCs. However, it is important to note that for mouse DC this finding is controversial, as other studies have claimed that CD11c<sup>+</sup>CD8 $\alpha$ <sup>+</sup> define

cells with high migratory capacity *in vivo* [70, 71]. Nevertheless, my data supports the theory that CD8 $\alpha$  is not expressed by mouse BMDCs matured and activated by CpG-CC, as suggested by the insignificant surface expression of CD8 $\alpha$ . Furthermore, DC stimulated with the CpG-CC underwent migration following injection. Importantly, the surface expression of the integrin CD11b, which has been shown to play an important role in DC adhesion and migration into the lymphatics remained unaffected following CpG-CC stimulation. Combined these experiments determined that SPIO had no effect on CpG-CC stimulation of our DCs *in vitro*.

Next, it was important to determine if the CpG-CC DC cytokine secretion was affected by SPIO. It is now accepted that Th 1 type responses play important roles in the generation of cellular immunity and are most useful in terms of cancer immunotherapeutics [1, 17, 44]. The key cytokine mediators which have been shown to play an important role in the control of Th 1/Th 2 balance are IL-2, IL-12, IFN- $\gamma$ , IL-4 and IL-10. To determine if CpG-CC cultured DC could potentially generate a Th 1-type response *in vivo*, we investigated the cytokines secreted by these cells. The production of IL-12 and IL-10, which play an important role in the shift of Th cells into Th 1 or Th 2 cells [27, 72], respectively, were noted. Importantly, CpG-CC stimulation increased the production of IL-12 while having no biologically significant effect on IL-10 secretion by DCs *in vitro*. SPIO did not alter this response. This suggests CpG-CC SPIO<sup>+</sup> DCs are capable of eliciting a Th 1-type response *in vivo*. While appropriate secretion of IL-12 is important to generating a Th 1-type response *in vivo*, it is also important to ensure *ex vivo* DC stimulation is not leading to

premature DC exhaustion. This exhaustion would result in DCs no longer capable of secreting cytokines at biologically relevant levels once in the LN. Exhausted DC migration to LNs *in vivo* would lead to stimulation of T cells in the absence of appropriate levels of pro-inflammatory cytokines and result in T cell anergy [25]. In a study investigating the kinetics of IL-12 secretion [73], it was suggested that DCs secrete IL-12 in two stages: the first is in response to initial exposure to a TLR agonist (10-15 ng/mL) and the second, delayed burst of IL-12 is significantly higher (20-25 ng/mL), in response to CD40 ligation (by CD4+ helper T cells), which occurs in the LN. It has been suggested that this staged IL-12 secretion by DCs *in vivo* could be a physiologic response to postpone DC exhaustion prior to their arrival in the lymph node. Based on the level of IL-12 secreted by our DCs *in vitro* following CpG-CC stimulation (, the levels are below those of the second stage of IL-12 secretion. Ultimately, our data suggest that our DCs are not exhausted following *in vitro* CpG-CC stimulation. Long-term cytokine secretion profiles in response to CD40 ligation following *in vitro* CpG-CC stimulation of our DCs would be interesting to carry out in order to confirm this.

Another related study investigated the secretion of cytokines by terminally-matured DCs in response to lipopolysaccharide (LPS; a TLR 4 ligand) stimulation [61]. Data from this study demonstrated that terminally-matured DCs produce significantly higher IFN- $\gamma$  and IL -10, while IL-12 production was suppressed in response to further *in vitro* stimulation. These data suggest that terminally-matured DCs are not exhausted, but reprogrammed with a distinct cytokine-secreting profile. Under the conditions used in the present experiments and independent of the presence of SPIO, the DC secreted low to modest levels of

IFN- $\gamma$  and IL-10 without dampening IL-12 production following *in vitro* CpG-CC stimulation. Taken together, our data suggest that we are not terminally-maturing our DCs *in vitro* following CpG-CC stimulation, still capable of secreting IL-12.

In order to confirm that CpG-CC DCs migrate more efficiently compared to UT DCs, *in vivo* migration experiments were carried out and assessed using MRI and conventional histology. In order to safely and non-invasively track our cells of interest *in vivo* using MRI, the negative contrast agent SPIO (FeREX<sup>®</sup>) was used. As a result, we first confirmed in this and previous investigations that SPIO has no significant negative effects on DC maturation, activation, or functionality. Directly related to this study in particular, SPIO had no significant effects on DC phenotype, CpG-CC stimulation, or functionality (cytokine secretion).

Previous studies have indicated that MRI is sensitive enough to detect low numbers of cells *in vivo* [45, 74], which was confirmed again in this study. In order to confirm that the differences detected in the migratory capacity between SPIO<sup>+</sup> and CpG-CC-SPIO<sup>+</sup> DCs by cellular MRI, conventional histological techniques were used. Importantly, the enhanced migratory capacity of CpG-CC-SPIO<sup>+</sup> DCs was detected following the analysis of the MR images and confirmed using digital morphometry. Furthermore, there was a strong correlation between quantitative MRI analysis and the digital morphometric analysis. Notably, the morphometric data indicated that SPIO labelling had no impact on the enhancement of migration resulting from CpG-CC stimulation. Also of importance is that histological results indicated that DCs migrated to the central areas of the LNs, regardless of SPIO labelling. This is important, because naïve T cells reside in the central areas of the LNs, and because when DCs migrate to these areas,

they are more likely to come into contact and potentially activate naïve T cells, which will then go on to produce antigen-specific immune responses. However, in order to appropriately determine if *in vivo* responses are generated, *in vivo* proliferation assays and *ex vivo* functional T cell assays (tetramer and IFN- $\gamma$  staining) will need to be performed. These results only confirm that our DCs are migrating to target LNs and entering the T cell rich areas of the nodes.

In summary, it was observed that CpG-CC stimulation up-regulates key co-stimulatory, migratory, and activation molecules on mouse DCs with no negative impact of SPIO on this stimulation. CpG-CC stimulation produces a correlating increase in DC function (cytokine secretion and migratory capacity), suggesting overall that CpG-CC DCs are able to stimulate Th 1 type responses *in vivo*. The use of SPIO labelling also allows for the tracking of DC migration *in vivo* safely and non-invasively using MRI, something which is especially useful when it comes to a clinical application. An important goal of DC immunotherapy is to target DCs to LNs, but as of yet, there is no reliable and non-invasive available for routine use in clinics. Because cellular MRI is non-toxic to cells and doesn't rely on ionizing radiation, unlike other non-invasive imaging modalities (PET, CT), it is also useful for long-term imaging studies. Furthermore, PET is also unlikely to be able to detect small numbers of cells with the same range of sensitivity as seen from our experiments. Ultimately, results from this investigation provide the evidence that cellular MRI is a non-invasive imaging modality with the sensitivity to track and quantify differences in migration between different DC populations *in vivo*. Furthermore, data from this investigation can be applied to the use of MRI for tracking clinical-grade DCs in

patients. Importantly, by providing clinicians with a sensitive and non-invasive imaging modality such as cellular MRI, useful information regarding the most effective DC population for use in patients can be obtained. Taken together, this investigation provides the proof-of-principle experiments that demonstrate MRI is a viable tool for use in patients, capable of tracking and quantifying *in vivo* DC migration.

### 3.5 References

1. Banchereau, J., et al., *Immunobiology of dendritic cells*. Annu Rev Immunol, 2000. **18**: p. 767-811.
2. Langenkamp, A., et al., *Kinetics of DC activation: impact on priming of TH1, TH2 and nonpolarized T cells*. Nat Immunol, 2000. **1**(4): p. 311-6.
3. Chan, T., et al., *HER-2/neu-gene engineered dendritic cell vaccine stimulates stronger HER-2/neu-specific immune responses compared to DNA vaccination*. Gene Ther, 2006. **13**(19): p. 1391-402.
4. Berntsen, A., et al., *Therapeutic dendritic cell vaccination of patients with metastatic renal cell carcinoma: a clinical phase 1/2 trial*. J Immunother, 2008. **31**(8): p. 771-80.
5. Hersey, P., et al., *Phase I/II study of treatment with matured dendritic cells with or without low dose IL-2 in patients with disseminated melanoma*. Cancer Immunol Immunother, 2008. **57**(7): p. 1039-51.
6. Gauvrit, A., et al., *Measles virus induces oncolysis of mesothelioma cells and allows dendritic cells to cross-prime tumor-specific CD8 response*. Cancer Res, 2008. **68**(12): p. 4882-92.
7. Pellegatta, S., et al., *Dendritic cells pulsed with glioma lysates induce immunity against syngeneic intracranial gliomas and increase survival of tumor-bearing mice*. Neurol Res, 2006. **28**(5): p. 527-31.
8. Iankov, I.D., et al., *Demonstration of anti-tumor activity of oncolytic measles virus strains in a malignant pleural effusion breast cancer model*. Breast Cancer Res Treat, 2009.
9. Ovali, E., et al., *Active immunotherapy for cancer patients using tumor lysate pulsed dendritic cell vaccine: a safety study*. J Exp Clin Cancer Res, 2007. **26**(2): p. 209-14.
10. Gregoire, M., et al., *Anti-cancer therapy using dendritic cells and apoptotic tumour cells: pre-clinical data in human mesothelioma and acute myeloid leukaemia*. Vaccine, 2003. **21**(7-8): p. 791-4.
11. Meidenbauer, N., R. Andreesen, and A. Mackensen, *Dendritic cells for specific cancer immunotherapy*. Biol Chem, 2001. **382**(4): p. 507-20.
12. Lotze, M.T., et al., *The role of interleukin-2, interleukin-12, and dendritic cells in cancer therapy*. Cancer J Sci Am, 1997. **3 Suppl 1**: p. S109-14.
13. Wierdecky, J., et al., *Immunologic and clinical responses after vaccinations with peptide-pulsed dendritic cells in metastatic renal cancer patients*. Cancer Res, 2006. **66**(11): p. 5910-8.
14. Fricke, I., et al., *Vascular endothelial growth factor-trap overcomes defects in dendritic cell differentiation but does not improve antigen-specific immune responses*. Clin Cancer Res, 2007. **13**(16): p. 4840-8.
15. Colic, M., et al., *Differentiation of human dendritic cells from monocytes in vitro using granulocyte-macrophage colony stimulating factor and low concentration of interleukin-4*. Vojnosanit Pregl, 2003. **60**(5): p. 531-8.
16. De Vries, I.J., et al., *Effective migration of antigen-pulsed dendritic cells to lymph nodes in melanoma patients is determined by their maturation state*. Cancer Res, 2003. **63**(1): p. 12-7.
17. de Vries, I.J., et al., *Maturation of dendritic cells is a prerequisite for inducing immune responses in advanced melanoma patients*. Clin Cancer Res, 2003. **9**(14): p. 5091-100.

18. Haining, W.N., et al., *CpG oligodeoxynucleotides alter lymphocyte and dendritic cell trafficking in humans*. Clin Cancer Res, 2008. **14**(17): p. 5626-34.
19. Wurzenberger, C., et al., *Short-term activation induces multifunctional dendritic cells that generate potent antitumor T-cell responses in vivo*. Cancer Immunol Immunother, 2009. **58**(6): p. 901-13.
20. Dai, Z., B.T. Konieczny, and F.G. Lakkis, *The dual role of IL-2 in the generation and maintenance of CD8+ memory T cells*. J Immunol, 2000. **165**(6): p. 3031-6.
21. Levine, B.L., et al., *CD28 ligands CD80 (B7-1) and CD86 (B7-2) induce long-term autocrine growth of CD4+ T cells and induce similar patterns of cytokine secretion in vitro*. Int Immunol, 1995. **7**(6): p. 891-904.
22. Santana, M.A., F. EsquivelGuadarrama, and W.J. Kwang, *Cell Biology of T Cell Activation and Differentiation*, in *International Review of Cytology*. 2006, Academic Press. p. 217-274.
23. Ragazzo, J.L., et al., *Costimulation via lymphocyte function-associated antigen 1 in the absence of CD28 ligation promotes anergy of naive CD4+ T cells*. Proc Natl Acad Sci U S A, 2001. **98**(1): p. 241-6.
24. Thebeau, L.G., et al., *B7 costimulation molecules expressed from the herpes simplex virus 2 genome rescue immune induction in B7-deficient mice*. J Virol, 2007. **81**(22): p. 12200-9.
25. Tuettenberg, A., et al., *The role of ICOS in directing T cell responses: ICOS-dependent induction of T cell anergy by tolerogenic dendritic cells*. J Immunol, 2009. **182**(6): p. 3349-56.
26. Bedoui, S., et al., *Characterization of an immediate splenic precursor of CD8+ dendritic cells capable of inducing antiviral T cell responses*. J Immunol, 2009. **182**(7): p. 4200-7.
27. Kubach, J., et al., *Dendritic cells: sentinels of immunity and tolerance*. Int J Hematol, 2005. **81**(3): p. 197-203.
28. Kubach, J., et al., *Human CD4+CD25+ regulatory T cells: proteome analysis identifies galectin-10 as a novel marker essential for their anergy and suppressive function*. Blood, 2007. **110**(5): p. 1550-8.
29. Lutz, M.B. and G. Schuler, *Immature, semi-mature and fully mature dendritic cells: which signals induce tolerance or immunity?* Trends in Immunology, 2002. **23**(9): p. 445-449.
30. Ardavin, C., S. Amigorena, C. Reis Sousa, *Dendritic cells: immunobiology and cancer immunotherapy*. Immunity, 2004. **20**(1): p. 17-23.
31. Ahangarani, R.R., et al., *In vivo induction of type 1-like regulatory T cells using genetically modified B cells confers long-term IL-10-dependent antigen-specific unresponsiveness*. J Immunol, 2009. **183**(12): p. 8232-43.
32. Kajino, K., et al., *Involvement of IL-10 in exhaustion of myeloid dendritic cells and rescue by CD40 stimulation*. Immunology, 2007. **120**(1): p. 28-37.
33. Jonuleit, H., et al., *Pro-inflammatory cytokines and prostaglandins induce maturation of potent immunostimulatory dendritic cells under fetal calf serum-free conditions*. Eur J Immunol, 1997. **27**(12): p. 3135-42.
34. Banerjee, D.K., et al., *Expansion of FOXP3high regulatory T cells by human dendritic cells (DCs) in vitro and after injection of cytokine-matured DCs in myeloma patients*. Blood, 2006. **108**(8): p. 2655-61.
35. Ridolfi, R., et al., *Evaluation of in vivo labelled dendritic cell migration in cancer patients*. J Transl Med, 2004. **2**(1): p. 27.
36. Thurner, B., et al., *Vaccination with mage-3A1 peptide-pulsed mature, monocyte-derived dendritic cells expands specific cytotoxic T cells and induces regression of some metastases in advanced stage IV melanoma*. J Exp Med, 1999. **190**(11): p. 1669-78.



37. Boullart, A.C., et al., *Maturation of monocyte-derived dendritic cells with Toll-like receptor 3 and 7/8 ligands combined with prostaglandin E2 results in high interleukin-12 production and cell migration*. *Cancer Immunol Immunother*, 2008. **57**(11): p. 1589-97.
38. Allavena, P., et al., *Chemokine receptor switch paradigm and DC migration: significance in tumor tissues*. *Immunol Rev*, 2000. **177**: p. 141-9.
39. Partida-Sanchez, S., et al., *Chemotaxis of mouse bone marrow neutrophils and dendritic cells is controlled by adp-ribose, the major product generated by the CD38 enzyme reaction*. *J Immunol*, 2007. **179**(11): p. 7827-39.
40. Scandella, E., et al., *CCL19/CCL21-triggered signal transduction and migration of dendritic cells requires prostaglandin E2*. *Blood*, 2004. **103**(5): p. 1595-601.
41. Vecchi, A., et al., *Differential responsiveness to constitutive vs. inducible chemokines of immature and mature mouse dendritic cells*. *J Leukoc Biol*, 1999. **66**(3): p. 489-94.
42. Scandella, E., et al., *Prostaglandin E2 is a key factor for CCR7 surface expression and migration of monocyte-derived dendritic cells*. *Blood*, 2002. **100**(4): p. 1354-61.
43. Brueggemeier, R.W. and E.S. Diaz-Cruz, *Relationship between aromatase and cyclooxygenases in breast cancer: potential for new therapeutic approaches*. *Minerva Endocrinol*, 2006. **31**(1): p. 13-26.
44. Adema, G.J., et al., *Migration of dendritic cell based cancer vaccines: in vivo veritas? Curr Opin Immunol*, 2005. **17**(2): p. 170-4.
45. Dekaban, G.A., et al., *Semiquantitation of mouse dendritic cell migration in vivo using cellular MRI*. *J Immunother*, 2009. **32**(3): p. 240-51.
46. Weeratna, R.D., et al., *CpG ODN can re-direct the Th bias of established Th2 immune responses in adult and young mice*. *FEMS Immunol Med Microbiol*, 2001. **32**(1): p. 65-71.
47. Davis, H.L., et al., *CpG DNA is a potent enhancer of specific immunity in mice immunized with recombinant hepatitis B surface antigen*. *J Immunol*, 1998. **160**(2): p. 870-6.
48. Masten, B.J., et al., *Characterization of myeloid and plasmacytoid dendritic cells in human lung*. *J Immunol*, 2006. **177**(11): p. 7784-93.
49. Uchijima, M., et al., *IFN-gamma overcomes low responsiveness of myeloid dendritic cells to CpG DNA*. *Immun Cell Biol*, 2005. **83**(1): p. 92-5.
50. Theiner, G., et al., *TLR9 cooperates with TLR4 to increase IL-12 release by murine dendritic cells*. *Mol Immunol*, 2008. **45**(1): p. 244-52.
51. D'Amico, G., et al., *Adhesion, transendothelial migration, and reverse transmigration of in vitro cultured DCs*. *Blood*, 1998. **92**(1): p. 207-14.
52. Kronin, V., et al., *Differential effect of CD8+ and CD8- dendritic cells in the stimulation of secondary CD4 T cells*. *Int Immunol*, 2001. **13**(4): p. 465-73.
53. de Vries, I.J., et al., *Magnetic resonance tracking of dendritic cells in melanoma patients for monitoring of cellular therapy*. *Nat Biotechnol*, 2005. **23**(11): p. 1407-13.
54. Nestle, F.O., et al., *Vaccination of melanoma patients with peptide- or tumor lysate-pulsed dendritic cells*. *Nat Med*, 1998. **4**(3): p. 328-32.
55. Knippertz, I., et al., *Generation of human dendritic cells that simultaneously secrete IL-12 and have migratory capacity by adenoviral gene transfer of hCD40L in combination with IFN-gamma*. *J Immunother*, 2009. **32**(5): p. 524-38.
56. Trapp, S., et al., *Double-stranded RNA analog poly(I:C) inhibits human immunodeficiency virus amplification in dendritic cells via type I interferon-mediated activation of APOBEC3G*. *J Virol*, 2009. **83**(2): p. 884-95.
57. Trepiakas, R., et al., *Addition of interferon-alpha to a standard maturation cocktail induces CD38 up-regulation and increases dendritic cell function*. *Vaccine*, 2009. **27**(16): p. 2213-9.

58. Otten, M.A., et al., *Inefficient antigen presentation via the IgA Fc receptor (Fc[alpha]RI) on DCs*. Immunobiology, 2006. **211**(6-8): p. 503-510.
59. Decker, W.K., et al., *Deficient T(H)-1 responses from TNF-alpha-matured and alpha-CD40-matured DCs*. J Immunother, 2008. **31**(2): p. 157-65.
60. Schuler, G. and N. Romani, *Generation of mature dendritic cells from human blood. An improved method with special regard to clinical applicability*. Adv Exp Med Biol, 1997. **417**: p. 7-13.
61. Kalinski, P., et al., *Final maturation of dendritic cells is associated with impaired responsiveness to IFN-gamma and to bacterial IL-12 inducers: decreased ability of mature dendritic cells to produce IL-12 during the interaction with Th cells*. J Immunol, 1999. **162**(6): p. 3231-6.
62. Napolitani, G., et al., *Selected Toll-like receptor agonist combinations synergistically trigger a T helper type 1-polarizing program in dendritic cells*. Nat Immunol, 2005. **6**(8): p. 769-76.
63. Caux, C., et al., *Activation of human dendritic cells through CD40 cross-linking*. J Exp Med, 1994. **180**(4): p. 1263-72.
64. Loskog, A. and T.H. Totterman, *CD40L - a multipotent molecule for tumor therapy*. Endocr Metab Immune Disord Drug Targets, 2007. **7**(1): p. 23-8.
65. Clarke, S.R., *The critical role of CD40/CD40L in the CD4-dependent generation of CD8+ T cell immunity*. J Leukoc Biol, 2000. **67**(5): p. 607-14.
66. Frasca, L., et al., *CD38 orchestrates migration, survival, and Th1 immune response of human mature dendritic cells*. Blood, 2006. **107**(6): p. 2392-9.
67. Rieser, C., et al., *Prostaglandin E2 and tumor necrosis factor alpha cooperate to activate human dendritic cells: synergistic activation of interleukin 12 production*. J Exp Med, 1997. **186**(9): p. 1603-8.
68. Kabashima, K., et al., *CXCL12-CXCR4 engagement required for migration of cutaneous dendritic cells*. Am J Pathol, 2007. **171**(4): p. 1249-57.
69. Jakubzick, C., et al., *Optimization of methods to study pulmonary dendritic cell migration reveals distinct capacities of DC subsets to acquire soluble versus particulate antigen*. J Immunol Methods, 2008. **337**(2): p. 121-31.
70. Liu, K., et al., *In vivo analysis of dendritic cell development and homeostasis*. Science, 2009. **324**(5925): p. 392-7.
71. Jakubzick, C., et al., *Lymph-migrating, tissue-derived dendritic cells are minor constituents within steady-state lymph nodes*. J Exp Med, 2008. **205**(12): p. 2839-50.
72. Enk, A.H., *DCs and cytokines cooperate for the induction of tregs*. Ernst Schering Res Found Workshop, 2006(56): p. 97-106.
73. Czerniecki, B.J., et al., *Targeting HER-2/neu in early breast cancer development using dendritic cells with staged interleukin-12 burst secretion*. Cancer Res, 2007. **67**(4): p. 1842-52.
74. Heyn, C., et al., *Detection threshold of single SPIO-labeled cells with FIESTA*. Magn Reson Med, 2005. **53**(2): p. 312-20.

## CHAPTER 4            SUMMARY

### 4.1 Discussion

The DC-based cancer vaccine, an active form of immunotherapy, is a promising emerging cancer therapy. This immunotherapy, if successful, is capable of providing high specificity for tumour cells with low toxicity to patients [1-5]. Importantly, it provides the advantage of long-lasting immunological memory against tumour antigens [6], protecting against tumour recurrence and metastasis [7-9]. To date, the safety and feasibility of this immunotherapy has been demonstrated [10, 11], but the DC-based cancer vaccine has yet to reach its full potential in regards to efficacy [4, 12-14]. Pre-clinical studies involving small animal models [15, 16] as well as early-phase clinical trials [9, 17-20] have elucidated many important aspects of DC biology pertinent to vaccine immunotherapy. However, several aspects of the overall vaccination strategy remain to be fully elucidated before experimental results can be translated to the clinic. To date, *ex vivo* generation of autologous patient DCs is commonly used. This method not only ensures adequate numbers of DCs are generated [21], but also that these cells are of the correct phenotype [19, 22] and are administered to patients at sites preferentially away from the immunosuppressive tumour environment [23, 24]. As a result, clinicians require a non-invasive imaging modality in order to determine the fate of injected DCs once they are administered to patients. The use of an accurate, reliable non-invasive imaging modality would provide a means to ensure DCs are reaching target LNs. Furthermore, tracking labelled DCs can be used to determine the optimal route of

administration, provide feedback as to the optimal *ex vivo* maturation protocol, and help in determining the appropriate dosing schedule and DC numbers required in order to achieve the desired therapeutic outcome.

MRI is one of the most commonly used imaging modalities to track labelled cells *in vivo* [25-29] because it is non-invasive, generates high-resolution images, and does not rely on radioactive isotopes. Due to the lack of ionizing energy, this provides MRI an important advantage for repeated use in patients, as well as for longitudinal studies [29-33]. Cellular MRI combines the ability of MRI with contrast agents for labelling cells providing dynamic assessment of cell migration into target tissues. Labelling cells with superparamagnetic iron oxide (SPIO) nanoparticles allows for the possibility of detecting single or clusters of labelled cells within tissues.

#### **4.1.1 Labelling DCs with SPIO**

Gadopentetate dimeglumine was the first MRI contrast agent approved for use in patients by the American Food and Drug Administration (FDA) [34]. Marketed as Magnevist<sup>®</sup> by Bayer Schering Pharma, it was first introduced in 1988 and it is used to assist in imagining blood vessels of inflamed or diseased tissues [35]. Magnevist<sup>®</sup> acts to reduce the T1 relaxation time, thereby acting as a positive contrast agent [34]. Despite Magnevist<sup>®</sup> being available on the market first, by far the preferred MR contrast agent to label DCs for *in vivo* migration studies is SPIO.

SPIO nanoparticles are approved for use in patients by the FDA in the form of ferumoxides (Feridex, Bayer HealthCare), ferucarbotran, and ferumoxtran 10. Feridex was originally developed as a liver contrast agent and

FDA approved in 1996, but was recently taken off the market with claims of poor sales [30]. As a result, these studies used FeREX, a SPIO nanoparticle which has little to no effects on DC phenotype and *in vitro* function according to the results presented in this thesis. While there are currently no published studies tracking FeREX-labelled cells, this MRI contrast agent was chosen by our laboratory because it is a very similar to Feridex in its size, magnetic properties, and chemical nature [36]. Whether the company manufacturing FeREX will seek FDA approval is currently unknown. Thus, it is possible that alternative contrast agents, such as ferucarbotran, may need to be employed in the future.

SPIO nanoparticles perturb the static magnetic field out to a distance many times that of its diameter due to the inherent magnetic properties of its structure [27, 37, 38]. This results in a dramatic reduction in T2, which produces negative contrast. Because the contrast effect of SPIO is stronger than that of positive contrast agents, they potentially provide clinicians with the ability to detect single cells *in vivo* [27, 33]. Another important aspect of the SPIO nanoparticle is its biodegradable coating, which acts to stabilize the magnetic core *in vivo*. Specifically, FeREX is coated with a dextran polymer. This dextran coating allows DCs, which are naturally endocytic, to be labelled *in vitro* passively before administration to patients. Furthermore, SPIO nanoparticles coated with dextran show improved biocompatibility and biodegradability [27].

#### **4.1.2 Detection Threshold Using MRI**

The detection threshold for SPIO labelled cells is affected by a number of factors, including field strength, signal-to-noise ratio, pulse sequence, and acquisition

parameters [39, 40]. Heyn *et al.* concluded that under certain conditions, MRI cell tracking with iron oxide particles could actually be more sensitive than nuclear techniques, which have a sensitivity of a few hundred cells [37]. There are a number of different studies which have detected as few as 500 cells *in vivo* using scanners of at least 3 Tesla (T) in strength [41-43]. Kircher *et al.* reported the detection of 3 labelled T cells migrating *in vivo* using a 3 T scanner [44]. However, clinical scanners range in field strength from 0.5 – 2 T. As a result, the ability to detect low numbers of cells using field strengths of 2 T or lower is of more routine clinical relevance. Recently, Foster-Gareau *et al.* showed that single cells labelled with SPIO nanoparticles could be imaged with a 1.5 T clinical scanner [45].

The differences in the limit of detection between studies is probably attributable to variances in hardware, image resolution, magnetic field strength of the MRI scanner (i.e. number of T), and the efficiency of SPIO uptake by cells. Although DCs are capable of passively taking up nanoparticles in culture via endocytosis, various alternate approaches have been developed to improve the amount of contrast agent uptake. For instance, our laboratory has developed a technique to improve labelling efficiency of DCs *in vitro* using magnetic plates, a process known as magnetofection (Appendix Fig. 3). Other groups have used magnetofection, a mechanical approach, which essentially uses an externally-applied magnetic field to draw DNA-SPIO complexes into close proximity of the cell, thereby enhancing SPIO-uptake. Finally, the use of cationic lipid-based transfection agents, such as protamine sulphate, in conjunction with SPIO has

also been used. However, the possibility of these transfection agents affecting DC function is unknown and might prove detrimental.

#### **4.1.3 Quantification of SPIO-labelled DCs**

Overall, there is a great emphasis placed on tracking DC migration *in vivo*, which can be achieved using MRI. However, equal consideration must also be given to the fact that DC-induced T and B cell specific immunity is also based on the actual number of DCs that successfully migrate to target LNs. Therefore, the clinical relevance of being able to track the migration of DCs *in vivo* becomes that much more clinically relevant if the degree of *in vivo* DC migration can be successfully quantified.

Bulte *et al.* [46] and Bos *et al.* [47] have demonstrated a linear relationship between the signal generated in T2 and T2\* relaxation rates, respectively, and iron concentration within a voxel. However, currently, quantification of the number of labelled cells in tissues using MRI remains inexact and therefore at best semi-quantitative for several reasons [48]. First, quantification of SPIO nanoparticles is hindered and influenced by surrounding tissue associated inhomogeneities. These inhomogeneities can lead to an overestimation of the concentration of labelled DCs within a tissue [49]. However, the use of a steady state acquisition sequence, such as FIESTA (fast imaging employing steady state acquisition), can remove or minimize these artifacts [37], which can be caused by air/tissue interfaces or hemorrhage. Another type of artifact, known as a chemical shift artifact, occurs at the interface between two tissues due to differences between their inherent chemical properties (i.e. between surrounding

fat and LN tissue). Secondly, quantification of SPIO-labelled DCs *in vivo* can be complicated by the existence of non-compartmentalized iron oxide (free iron). However, free iron produces a larger signal in MR images, and measuring both the T2 and T2\* relaxation rates could reduce the interference from this iron pool and lead to a more accurate quantification of DCs [50]. Importantly, it should be noted that quantification of SPIO-labelled cells is technically an indirect technique [33]. The signal can change due to the local concentration of SPIO nanoparticles and not necessarily due to the total number of SPIO containing cells. Furthermore, SPIO-labelled DCs which die and undergo apoptosis *in vivo* could be internalized by macrophages and these newly SPIO-labelled macrophages could migrate to the LNs in lieu of the DCs. However, Pawelczyk *et al.* have recently shown that the amount of iron transferred from a labelled stem cell to activated macrophages is less than 10% of the total iron load injected into the tissue [51]. As a result, this iron transfer is most likely insufficient to contribute to the total signal detected in MR images.

In order to perfect quantification techniques, we must be able to properly correlate the signal generated with the number of cells migrating *in vivo*. In order to effectively do this, the labelling efficiency of DCs must also be considered. In chapter two, the issue concerning the observation that labelling DCs *in vitro* with SPIO does not achieve 100% efficiency was investigated to see if improvements could be achieved. I was able to effectively separate two cell populations from the SPIO<sup>mix</sup> DC population: those that were labelled with SPIO (SPIO<sup>+</sup>) and those which remained unlabelled (SPIO<sup>-</sup>). Therefore, subsequent experiments were



carried out with SPIO<sup>+</sup> DCs. This added confidence to MR analysis as it was demonstrated that by using a uniformly SPIO labelled population of DCs there was an improved correlation between the semi-quantitative MR data and the histological quantitative data which represented the amount of DC migration to target LNs (Chapter 2).

#### **4.1.4. Limitations of Cellular MRI**

Based on initial studies from our lab and supported by experiments conducted for this thesis, it is clear that nanoparticles can affect the *in vivo* migration of DCs, at least in a mouse model. However, it has yet to be determined if this issue is pertinent to the migration of SPIO-labelled DCs in human clinical patients, as both DCs and reticulo-endothelial cell junctions are larger in humans compared to mice. Perhaps, however, the use of a SPIO with a relatively smaller diameter, such as Molday nanoparticles (~50 nm), would provide a useful alternative to FeREX if, in fact, nanoparticle size does play a factor in the migration of human DCs in patients.

Furthermore, in the context of MR contrast agents, it is important to note that although several MR contrast agents available on the market are FDA approved, using them to label cells is an off-label application not approved for routine clinical application. Therefore, contrast agents developed for use in pre-clinical studies must undergo further clinical trials and approval processes in order to be used readily in the clinics for tracking cell migration.

The current conventional method of *in vivo* cell tracking remains to be histological analysis, which includes partial or full tissue biopsy and quantitative

morphometric analysis [52]. Due to the nature of SPIO-based MRI and the issues discussed above, the sensitivity and quantitative nature of this imaging modality (although correlative to histological analysis, as found by my studies) is not as accurate as conventional histology. However, further refinement of MR imaging techniques, MRI signal acquisition protocols, and MRI hardware technology (scanners and radiofrequency insert coils) will improve the overall sensitivity and therefore accuracy of the quantitative aspects of this imaging modality [53-55]. Another alternative to improving the accuracy of MR results is to use a multimodal imaging technique, such as through the combination of MRI and PET/SPECT. The latter techniques provide direct positive quantitative data although with less sensitivity and depend on the MR image to provide the 3D anatomical placement of the signal.

The detection of labelled DCs *in vivo* in patients is limited by partial volume effects, in which signal void detection is dependent on the resolution of the image [39]. To improve the sensitivity of MR detection, increasing field strength to reduce voxel size can overcome partial volume effects. [56]. However, increasing field strength is probably not feasible in a clinical setting, as higher T MR scanners are generally more expensive to run and maintain and the long term consequences on human health are unknown. As a result, improvements in hardware, cell labelling, and image acquisition techniques are more feasible with respect to improving image resolution. Another point to consider, however, is the scan times required to be able to accurately detect DCs in patients. While longer scan times improve the signal to noise ratio, these longer scan times also mean

increased costs. However, it is unclear if shortening scan times is reliable enough to produce accurate, reproducible quantitative MRI data.

## **4.2 Conclusion**

In order for the DC-based cancer vaccine to become an integral part of routine and personalized cancer therapy, the development of non-invasive imaging techniques is vital in order to provide clinicians with qualitative and quantitative feedback as to their *in vivo* migration. Currently, imaging techniques and MR hardware are being optimized in order to provide accurate and reproducible quantification of MR signals generated by DCs *in vivo*. In the future, cellular MRI may be used routinely in the clinics to track the migration of DC-based cancer vaccines, as well as to quantify and correlate migration to *in vivo* anti-tumour responses. Ultimately, tracking DCs *in vivo* with MRI will provide insight into this cell-based cancer vaccine, with the aim of accurately depicting DC migration, allowing for the optimization of vaccination strategies and correlation to patient responses.

### 4.3 References

1. Ardavin, C., S. Amigorena, and C. Reis e Sousa, *Dendritic cells: immunobiology and cancer immunotherapy*. *Immunity*, 2004. **20**(1): p. 17-23.
2. Banchereau, J., et al., *Immunobiology of dendritic cells*. *Annu Rev Immunol*, 2000. **18**: p. 767-811.
3. Basak, S.K., et al., *Increased dendritic cell number and function following continuous in vivo infusion of granulocyte macrophage-colony-stimulating factor and interleukin-4*. *Blood*, 2002. **99**(8): p. 2869-79.
4. Baxevasis, C.N., S.A. Perez, and M. Papamichail, *Cancer immunotherapy*. *Crit Rev Clin Lab Sci*, 2009. **46**(4): p. 167-89.
5. Berntsen, A., et al., *Therapeutic dendritic cell vaccination of patients with metastatic renal cell carcinoma: a clinical phase 1/2 trial*. *J Immunother*, 2008. **31**(8): p. 771-80.
6. Liu, Q., et al., *Abrogation of local cancer recurrence after radiofrequency ablation by dendritic cell-based hyperthermic tumor vaccine*. *Mol Ther*, 2009. **17**(12): p. 2049-57.
7. Kouivavskaia, D.V., et al., *Vaccination with agonist peptide PSA: 154-163 (155L) derived from prostate specific antigen induced CD8 T-cell response to the native peptide PSA: 154-163 but failed to induce the reactivity against tumor targets expressing PSA: a phase 2 study in patients with recurrent prostate cancer*. *J Immunother*, 2009. **32**(6): p. 655-66.
8. Di Nicola, M., et al., *Vaccination with autologous tumor-loaded dendritic cells induces clinical and immunologic responses in indolent B-cell lymphoma patients with relapsed and measurable disease: a pilot study*. *Blood*, 2009. **113**(1): p. 18-27.
9. Carrasco, J., et al., *Vaccination of a melanoma patient with mature dendritic cells pulsed with MAGE-3 peptides triggers the activity of nonvaccine anti-tumor cells*. *J Immunol*, 2008. **180**(5): p. 3585-93.
10. Sampson, J.H., et al., *An epidermal growth factor receptor variant III-targeted vaccine is safe and immunogenic in patients with glioblastoma multiforme*. *Mol Cancer Ther*, 2009. **8**(10): p. 2773-9.
11. Beran, J., et al., *Intradermal influenza vaccination of healthy adults using a new microinjection system: a 3-year randomised controlled safety and immunogenicity trial*. *BMC Med*, 2009. **7**: p. 13.
12. Ferguson, A.R., et al., *Strategies and challenges in eliciting immunity to melanoma*. *Immunol Rev*, 2008. **222**: p. 28-42.
13. Awasthi, S., et al., *Efficacy of antigen 2/proline-rich antigen cDNA-transfected dendritic cells in immunization of mice against *C. posadasii**. *J Immunol*, 2005. **175**(6): p. 3900-6.
14. Farkas, A., et al., *Current state and perspectives of dendritic cell vaccination in cancer immunotherapy*. *Skin Pharmacol Physiol*, 2006. **19**(3): p. 124-31.
15. Francia, G., et al., *Long-term progression and therapeutic response of visceral metastatic disease non-invasively monitored in mouse urine using beta-human choriogonadotropin secreting tumor cell lines*. *Mol Cancer Ther*, 2008. **7**(10): p. 3452-9.
16. Haenssle, H.A., et al., *Intracellular delivery of major histocompatibility complex class I-binding epitopes: dendritic cells loaded and matured with cationic peptide/poly(I:C) complexes efficiently activate T cells*. *Exp Dermatol*, 2009.
17. Chan, T., et al., *HER-2/neu-gene engineered dendritic cell vaccine stimulates stronger HER-2/neu-specific immune responses compared to DNA vaccination*. *Gene Ther*, 2006. **13**(19): p. 1391-402.

18. Toh, H.C., et al., *Clinical Benefit of Allogeneic Melanoma Cell Lysate-Pulsed Autologous Dendritic Cell Vaccine in MAGE-Positive Colorectal Cancer Patients*. Clin Cancer Res, 2009. **15**(24): p. 7726-7736.
19. De Vries, I.J., et al., *Effective migration of antigen-pulsed dendritic cells to lymph nodes in melanoma patients is determined by their maturation state*. Cancer Res, 2003. **63**(1): p. 12-7.
20. de Vries, I.J., et al., *Maturation of dendritic cells is a prerequisite for inducing immune responses in advanced melanoma patients*. Clin Cancer Res, 2003. **9**(14): p. 5091-100.
21. Colic, M., et al., *Differentiation of human dendritic cells from monocytes in vitro using granulocyte-macrophage colony stimulating factor and low concentration of interleukin-4*. Vojnosanit Pregl, 2003. **60**(5): p. 531-8.
22. Gieseler, R., et al., *In-vitro differentiation of mature dendritic cells from human blood monocytes*. Dev Immunol, 1998. **6**(1-2): p. 25-39.
23. Williams, C.A., R.A. Harry, and J.D. McLeod, *Apoptotic cells induce dendritic cell-mediated suppression via interferon-gamma-induced IDO*. Immunology, 2008. **124**(1): p. 89-101.
24. Jurgens, B., et al., *Interferon-gamma-triggered indoleamine 2,3-dioxygenase competence in human monocyte-derived dendritic cells induces regulatory activity in allogeneic T cells*. Blood, 2009. **114**(15): p. 3235-43.
25. Helfer, B.M., et al., *Functional assessment of human dendritic cells labeled for in vivo (19)F magnetic resonance imaging cell tracking*. Cytotherapy.
26. Loebinger, M.R., et al., *Magnetic resonance imaging of mesenchymal stem cells homing to pulmonary metastases using biocompatible magnetic nanoparticles*. Cancer Res, 2009. **69**(23): p. 8862-7.
27. Zhang, Z., et al., *Comparison of superparamagnetic and ultrasmall superparamagnetic iron oxide cell labeling for tracking green fluorescent protein gene marker with negative and positive contrast magnetic resonance imaging*. Mol Imaging, 2009. **8**(3): p. 148-55.
28. Kim, Y.J., et al., *In vivo magnetic resonance imaging of injected mesenchymal stem cells in rat myocardial infarction; simultaneous cell tracking and left ventricular function measurement*. Int J Cardiovasc Imaging, 2009. **25 Suppl 1**: p. 99-109.
29. Ye, Q., et al., *Longitudinal tracking of recipient macrophages in a rat chronic cardiac allograft rejection model with noninvasive magnetic resonance imaging using micrometer-sized paramagnetic iron oxide particles*. Circulation, 2008. **118**(2): p. 149-56.
30. Bulte, J.W., *In vivo MRI cell tracking: clinical studies*. AJR Am J Roentgenol, 2009. **193**(2): p. 314-25.
31. de Vries, I.J., et al., *Magnetic resonance tracking of dendritic cells in melanoma patients for monitoring of cellular therapy*. Nat Biotechnol, 2005. **23**(11): p. 1407-13.
32. Kiessling, F., *Noninvasive cell tracking*. Handb Exp Pharmacol, 2008(185 Pt 2): p. 305-21.
33. Liu, W. and J.A. Frank, *Detection and quantification of magnetically labeled cells by cellular MRI*. European Journal of Radiology, 2009. **70**(2): p. 258-264.
34. Schmiedl, U., et al., *Contrast-enhancing properties of Gd-DTPA at 2.0 Tesla*. Radiat Med, 1987. **5**(1): p. 1-5.
35. DeLeo, M.J., 3rd, et al., *Carotid artery brain aneurysm model: in vivo molecular enzyme-specific MR imaging of active inflammation in a pilot study*. Radiology, 2009. **252**(3): p. 696-703.
36. Molday, R.S. and D. MacKenzie, *Immunospecific ferromagnetic iron-dextran reagents for the labeling and magnetic separation of cells*. J Immunol Methods, 1982. **52**(3): p. 353-67.

37. Heyn, C., et al., *Detection threshold of single SPIO-labeled cells with FIESTA*. Magn Reson Med, 2005. **53**(2): p. 312-20.
38. Bulte, J.W.M., *Magnetic nanoparticles as markers for cellular MR imaging*. Journal of Magnetism and Magnetic Materials, 2005. **289**: p. 423-427.
39. Walczak, P., et al., *Applicability and limitations of MR tracking of neural stem cells with asymmetric cell division and rapid turnover: the case of the shiverer dysmyelinated mouse brain*. Magn Reson Med, 2007. **58**(2): p. 261-9.
40. Arbab, A.S., W. Liu, and J.A. Frank, *Cellular magnetic resonance imaging: current status and future prospects*. Expert Rev Med Devices, 2006. **3**(4): p. 427-39.
41. Magnitsky, S., et al., *In vivo and ex vivo MRI detection of localized and disseminated neural stem cell grafts in the mouse brain*. Neuroimage, 2005. **26**(3): p. 744-54.
42. Dahnke, H. and T. Schaeffter, *Limits of detection of SPIO at 3.0 T using T2 relaxometry*. Magn Reson Med, 2005. **53**(5): p. 1202-6.
43. Hoehn, M., et al., *Monitoring of implanted stem cell migration in vivo: a highly resolved in vivo magnetic resonance imaging investigation of experimental stroke in rat*. Proc Natl Acad Sci U S A, 2002. **99**(25): p. 16267-72.
44. Kircher, M.F., et al., *In vivo high resolution three-dimensional imaging of antigen-specific cytotoxic T-lymphocyte trafficking to tumors*. Cancer Res, 2003. **63**(20): p. 6838-46.
45. Foster-Gareau, P., et al., *Imaging single mammalian cells with a 1.5 T clinical MRI scanner*. Magn Reson Med, 2003. **49**(5): p. 968-71.
46. Bulte, J.W., et al., *Hepatic hemosiderosis in non-human primates: quantification of liver iron using different field strengths*. Magn Reson Med, 1997. **37**(4): p. 530-6.
47. Bos, C., et al., *In vivo MR imaging of intravascularly injected magnetically labeled mesenchymal stem cells in rat kidney and liver*. Radiology, 2004. **233**(3): p. 781-9.
48. Rad, A.M., et al., *Quantification of superparamagnetic iron oxide (SPIO)-labeled cells using MRI*. J Magn Reson Imaging, 2007. **26**(2): p. 366-74.
49. Terrovitis, J., et al., *Magnetic resonance imaging overestimates ferumoxide-labeled stem cell survival after transplantation in the heart*. Circulation, 2008. **117**(12): p. 1555-62.
50. Kuhlper, R., et al., *R2 and R2\* mapping for sensing cell-bound superparamagnetic nanoparticles: in vitro and murine in vivo testing*. Radiology, 2007. **245**(2): p. 449-57.
51. Pawelczyk, E., et al., *In vitro model of bromodeoxyuridine or iron oxide nanoparticle uptake by activated macrophages from labeled stem cells: implications for cellular therapy*. Stem Cells, 2008. **26**(5): p. 1366-75.
52. Cunningham, C.H., et al., *Positive contrast magnetic resonance imaging of cells labeled with magnetic nanoparticles*. Magn Reson Med, 2005. **53**(5): p. 999-1005.
53. Mani, V., et al., *Gradient echo acquisition for superparamagnetic particles with positive contrast (GRASP): sequence characterization in membrane and glass superparamagnetic iron oxide phantoms at 1.5T and 3T*. Magn Reson Med, 2006. **55**(1): p. 126-35.
54. Seppenwoolde, J.H., M.A. Viergever, and C.J. Bakker, *Passive tracking exploiting local signal conservation: the white marker phenomenon*. Magn Reson Med, 2003. **50**(4): p. 784-90.
55. Patil, S., O. Bieri, and K. Scheffler, *Echo-dephased steady state free precession*. MAGMA, 2009.
56. Farrar, C.T., et al., *Impact of field strength and iron oxide nanoparticle concentration on the linearity and diagnostic accuracy of off-resonance imaging*. NMR Biomed, 2008. **21**(5): p. 453-63.



**Appendix 1. Proof of ethics approval for animal use.** A copy of the official document from the University Council on Animal Care permitting the use of mice for these studies.





07.01.09

\*This is the 2<sup>nd</sup> Renewal of this protocol  
\*A Full Protocol submission will be required in 2011

Dear Dr. Dekaban

Your Animal Use Protocol form entitled:

**In Vivo MR Imaging to Assess Delivery and Efficacy of Dendritic Cell Vaccines**

has had its yearly renewal approved by the Animal Use Subcommittee.

This approval is valid from **07.01.09 to 06.30.10**

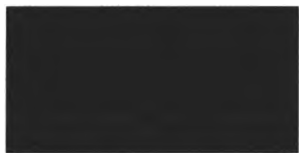
The protocol number for this project remains as [REDACTED]

1. This number must be indicated when ordering animals for this project.
2. Animals for other projects may not be ordered under this number.
3. If no number appears please contact this office when grant approval is received.  
If the application for funding is not successful and you wish to proceed with the project, request that an internal scientific peer review be performed by the Animal Use Subcommittee office.
4. Purchases of animals other than through this system must be cleared through the ACVS office. Health certificates will be required.

**REQUIREMENTS/COMMENTS**

Please ensure that individual(s) performing procedures on live animals, as described in this protocol, are familiar with the contents of this document.

The holder of this *Animal Use Protocol* is responsible to ensure that all associated safety components (biosafety, radiation safety, general laboratory safety) comply with institutional safety standards and have received all necessary approvals. Please consult directly with your institutional safety officers.

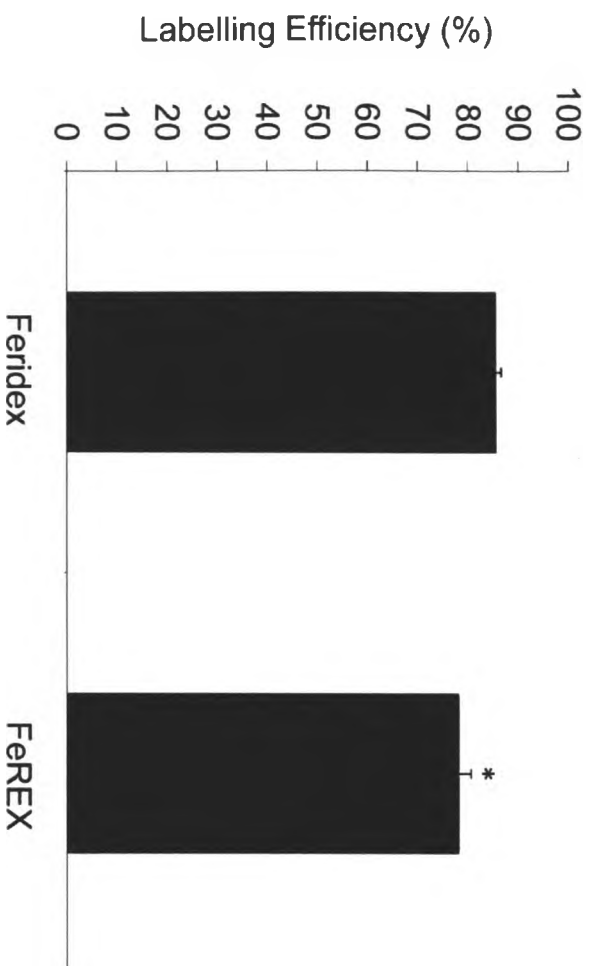


c.c. C Willert, M Pickering

**The University of Western Ontario**  
Animal Use Subcommittee / University Council on Animal Care  
Health Sciences Centre, • London, Ontario • CANADA – N6A 5C1



**Appendix 2. Labelling efficiency of DCs achieved following overnight incubation with SPIO.** Mouse DCs were incubated overnight (20 hours) in the presence of SPIO (Feridex or FeREX) at a concentration of 200 µg of Fe/mL. Cells were left untreated to serve as a control. On day 5, DCs were collected, washed, and magnetically separated into SPIO<sup>+</sup> and SPIO<sup>-</sup> populations, and each population was counted to determine the efficiency of SPIO labelling. Data are means ± SE and are taken from 5 independent experiments. Differences are significant if  $p < 0.05$  (\*).





**Appendix 3. Magnetically labelling DCs *in vitro* on magnetic plates increases the amount of iron taken up per cell.** DCs were given SPIO (Feridex; 200 µg of Fe/mL) overnight. Cells were incubated on magnetic plates (Invitrogen) for either 10, 12, 16, or 18 hours to enhance iron uptake. Cells labelled with iron but not put on a magnetic plate and cells left untreated (UT) served as controls. Following overnight incubation, cells were washed to remove free SPIO and characterized using flow cytometry. Supernatants were collected and analyzed using a Luminex detection assay to determine if magnetic plate incubation altered cytokine secretion. DCs were also saved and analyzed for their intracellular iron content using ICP-mass spectroscopy. **(A)** Histograms are gated on viable CD11c<sup>+</sup> cells. Magnetic plate incubation does not have apparent effects on DC maturation (as assessed by CD86 expression). **(B)** Analysis of cytokine profiles of DCs indicate no significant effects ( $p > 0.05$ ). **(C)** Red dashed line indicates the threshold of iron per cell required for detection by cellular MRI (5.4 pg of Fe/cel). Data are representative of triplicate data. Data are means  $\pm$  SE. Differences are significant if  $p < 0.05$  (\*, \*\*, \*\*\*).

